PHD THESIS

Aastha Jindal

MARCH 27, 2015

UNIVERSITY OF PIEMONTE ORIENTALE
Via Solaroli 17 Novara-28100 ITALY

PhD in Molecular Medicine

UNIVERSITÀ DEGLI STUDI DEL PIEMONTE ORIENTALE "AMEDEO AVOGADRO"

Dipartimento di Scienze della Salute

Corso di Dottorato di Ricerca in Medicina Molecolare

ciclo **XXVII**

Titolo tesi

MECHANISMS THAT INFLUENCE HEPATIC INFLAMMATION IN NONALCOHOLIC STEATO-HEPATITIS (NASH)

SSD: MED/04

Coordinatore

Prof. Emanuele Albano

Tutor

Prof. Emanuele Albano

Dottorando

Aastha Jindal

Contents

1. Epidemiology

Non-alcoholic fatty liver disease (NAFLD) is characterized by an increase in the hepatic content of triglycerides also known as steatosis variably associated with the development of parenchymal damage and inflammation a condition known as non-alcoholic steatohepatitis (NASH) (Vuppalanchi and Chalasani 2009). At present NAFLD/NASH represents the hepatic manifestation of the so called Metabolic Syndrome (MS) (Yki-Jarvinen 2014). The term metabolic syndrome defines a complex of clinical manifestations associated to obesity and over-weight that includes diabetes, hypertension, hypertriglyceridemia, and low high-density lipoprotein (HDL) cholesterol. It is estimated that about 47 million U.S. individuals suffer of metabolic syndrome and more than 80% of such subjects develop NAFLD (Younossi and others 2012). On the other hand, more than 90% of NAFLD patients have obesity associated with some features of metabolic syndrome. The prevalence of NAFLD increases as the severity and number of metabolic syndrome parameters increase (Yu and others 2013; Zelber-Sagi and others 2011).

The epidemiological significance of NAFLD streams from the data published by the United States Center for Disease Control and Prevention that estimates that about 66% of US adults in are overweight, and half of those are obese (Yu and others 2013; Zelber-Sagi and others 2011). The prevalence of obesity is projected to increase in the United States up to 45% by 2025. Similarly, by 2030 the projected percent increase in type 2 diabetes mellitus is 32% in Europe, 72% in the United States, and 150% or greater in sub-Saharan Africa, India, and the Middle East (Bambha and others 2012; Wong 2013; Yoshiike and Lwin 2005; Younossi and others 2012). As obesity and diabetes are important risk factors for NAFLD, it is likely that the prevalence of NAFLD will rise in the near future to epidemic proportions.

At present, the prevalence of NAFLD in the general population is estimated to range from 2.8% to 46% and this large variability depends on the methodology used, the population investigated, and the type of screening test applied for the detection of liver fat (Bellentani and others 2010). Although hospital-based studies are flawed because of ascertainment bias, population-based studies using non-invasive imaging studies (e.g., sonography) suffer the poor specificity of sonography for the diagnosis of NAFLD. Recently, magnetic resonance imaging has been used to quantify the extension of hepatic steatosis (Bhala and others 2013; Hashimoto and others 2013; Rinella and others 2014) and using this technique, it is estimated that 31% of the U.S. population has NAFLD. In contrast, depending on the definition used, between 2.8%

and 24% of U.S. adults have NAFLD according to a comprehensive National Health and Nutrition Examination Survey III (NHANES III) data set–based analysis. The prevalence of NAFLD in the Dionysos study was noted to be 94% in obese patients (body mass index BMI≥ 30), 67% in overweight patients (BMI between 25 and 30), and 25% in patients with normal weight (Bellentani and others 2010). Assessment of NAFLD is further confounded by the fact that approximately 70% to 80% of subjects with NAFLD have normal ALT levels. Among type 2 diabetics, 40% to 70% have associated NAFLD. This observation has been confirmed by a recent case-control study based on evaluation of hepatic steatosis that has shown that patients with type 2 diabetes had up to 200% more fat in their liver than did matched controls (Ali and Cusi 2009; Ducluzeau and others 2013; Williamson and others 2011). In an autopsy series in which liver histology was used to define the presence of a fatty liver, hepatic steatosis was found in approximately 2.7% of lean individuals and 18.5% of obese individuals. Similar data have been reported from autopsies of air crash victims. A relationship between BMI and the presence of a fatty liver has also been established in otherwise apparently healthy individuals being considered as donors for living donor liver transplantation. Clearly, no single marker or test has sufficient positive or negative predictive power for diagnosing NAFLD.

Regardless of the methodology used, several aspects of the epidemiology of NAFLD are consistently observed. Fatty liver, as well as NASH, occurs in all age groups, including children. Although studies published before 1990 emphasized that NASH occurs mostly in women (53% to 85% of all patients), more recent studies have shown that NASH is equally frequent in both genders (Sheth and others 1997). The prevalence of NAFLD is directly related to BMI, with more than 80% of subjects with a BMI higher than 35 kg/m2 having steatosis. Waist circumference may be an even better predictor of underlying IR and NAFLD than the BMI (Rocha and others 2005).

Epidemiological studies have also evidenced that the prevalence of NAFLD show large inter-ethnical variations with Hispanic subjects showing prevalence around 45%, whereas African Americans have a lower prevalence (24%) (Kallwitz and others 2009; Lomonaco and others 2011). Furthermore, the phenotype of NAFLD is highly likely to reflect complex interactions between environmental and lifestyle-related factors and genetic predisposition. Obesity and diabetes often cluster within families. The causes of such familial clustering include both genetic and environmental factors (Carulli and others 2009; Merriman and others 2006).

2. Histopathology

The characteristic histopathologic features of adult NAFLD include mainly zone 3 macrovesicular steatosis variably associated with lobular inflammation, cellular injury represented by cytologic ballooning, Mallory-Denk bodies (MDBs), or both and pericellular fibrosis. Based on these characteristics, NAFLD has two broad histologic patterns: hepatic steatosis, or NAFL, and Steatohepatitis (NASH) (Brunt and others 2011; Brunt and others 2003). At difference to its literal meaning, Steatohepatitis does not simply represent the presence of steatosis and inflammation. Steatohepatitis is defined by the presence of hepatic steatosis with varying degrees of inflammation along with evidence of cell injury, usually in the form of cytologic ballooning (**Figure 1**) (Charlton and others 2011; Cotrim and others 2004). Fibrosis is not required for the diagnosis of steatohepatitis (Bahrami and others 2003; Brunt and others 2011; Burt and others 1998). The inflammation associated with steatohepatitis is generally modest and has mainly lobular distribution. However, variable degree of portal inflammation can be detected in specific individuals. Portal fibrosis may be associated with NAFLD, particularly in pediatric subjects and in those who are morbidly obese (Gramlich and others 2004).

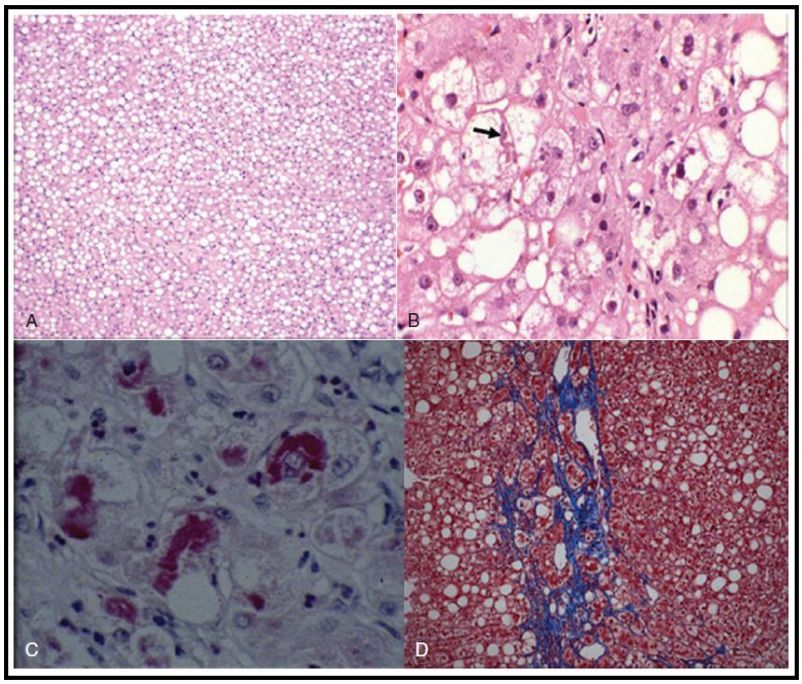

Figure 1: Histologic features of nonalcoholic steatohepatitis. **(A)** Macrovesicular steatosis. (Low power, hematoxylin and eosin [H & E] stain). **(B)** Cytologic ballooning with eosinophilic Mallory-Denk bodies *(arrow)*. **(C)** "Ropy" Mallory-Denk bodies stained with antibodies to ubiquitin. **(D)** Pericellular fibrosis in centrilobular location. (Masson trichrome stain.)

2.1 Grading and Staging

To improve the prognostic assessement of NAFLD/NASH several systems for grading and staging NAFLD have been proposed, but only two systems have been validated to any

degree. A landmark study by Brunt and colleagues examined 10 separate histologic parameters. Based on these parameters, a three-grade, four-stage system of classifying NAFLD was developed. Significant histologic lesions included steatosis, ballooning, and inflammation. The necro-inflammatory grade correlated with alanine aminotransferase (ALT) activity. The staging score reflected both location and the extent of fibrosis. More recently, using the Brunt classification as a starting point, the NIH-sponsored NASH CRN proposed and validated a scoring system. Although 14 separate parameters were evaluated, 4 were scored semi-quantitatively, including steatosis (0 to 3), cytologic ballooning (0 to 2), lobular inflammation (0 to 2), and fibrosis (0 to 4). A NAFLD activity score (NAS) was then developed that included the un-weighted scores for steatosis, inflammation, and cytologic ballooning (**Table 1**). The NAS correlated well with the presence of steatohepatitis during a blinded validation process and was typically associated with a score of 5 or higher. Those with a score of 3 or less were not usually found to have steatohepatitis, whereas a score of 4 was associated with some divergence of opinion (**Figure 2**). It is, however, important to note that the NAS cannot be used to diagnose the presence of steatohepatitis, which is identified by the presence of steatosis, inflammation, and cytologic ballooning in a typical pattern. The NASH CRN staging system divides stage 1 into several subsets (**Table 2**), thereby improving its sensitivity to change in earlier stages of the disease. This system is highly valuable as a research tool for the design and analysis of clinical trials related to NASH. However, its role in routine clinical practice remains to be established.

A major limitation of any histologic scoring system is sampling variability. In one study, two biopsy specimens were obtained from the same site at the same time. About 20% of subjects had at least a one-stage variability between specimens, whereas 12% had a two-stage variation. Similar data have been obtained from studies in which biopsy specimens from the left and right lobes were compared.

Table 1: NASH Clinical Research Network Scoring System: NAFLD Activity Score							
Steatosis Grade			Lobular Inflammation			Hepatocellular Balloning	
Degree	Description		Degree	Description		Degree	Description
0	<5%		0	None		0	None
1	5%-33%		1	<2 foci/20x optical field		1	Mild; Few
2	34%-66%		2	2-4 foci/20x optical field		2	Moderate to marked; many
3	>66%		3	>4 foci/20x optical field			

Table 2: NASH Clinical Research Network Scoring System: Fibrosis Score	
Degree	**Description**
0	None
1a	Mild (delicate) zone 3 perisinusoidal fibrosis
1b	Moderate (dense) zone 3 perisinusoidal fibrosis
1c	Portal/periportal fibrosis only
2	Zone 3 perisinusoidal fibrosis with portal/ periportal fibrosis
3	Bridging fibrosis
4	Cirrhosis

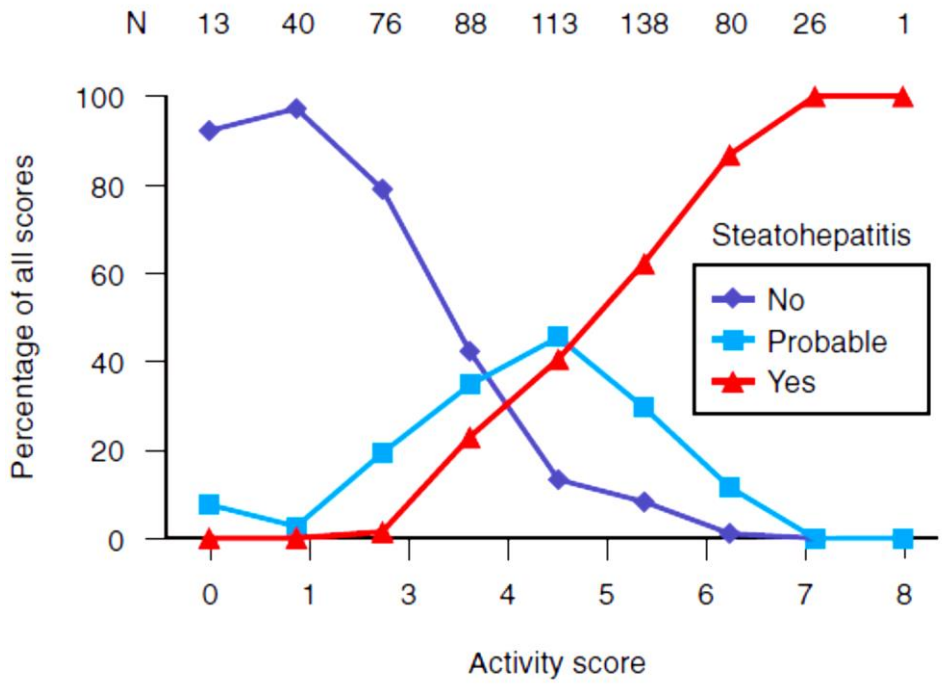

Figure 2: Relationship between the nonalcoholic fatty liver disease activity score (NAS) and the probability of having steatohepatitis.

A group of experienced pathologists diagnosed steatohepatitis to be present, absent, or probable and also independently scored the same biopsy specimens while unaware of their own interpretation to determine the NAS. A score higher than 4 was associated with a high probability of being considered to have steatohepatitis. *(Adapted from Kleiner DE, et al. Design and validation of a histological scoring system for nonalcoholic fatty liver disease. Hepatology 2005;41:1313–1321.)*

3. Clinical Features

Most subjects with NAFLD are asymptomatic and in these individuals the diagnosis is often made incidentally because of either abnormal liver enzyme levels or features of a fatty liver on an imaging study when such tests are performed for unrelated reasons. In others, NAFLD may be diagnosed either as a result of an unusual appearance of the liver during abdominal surgery or because of persistent hepatomegaly. It is important to recognize that in only a minority of subjects has NAFLD been diagnosed and that it currently remains undiagnosed in the great majority of afflicted individuals.

3.1 Symptoms and Signs

Most patients have vague complaints of fatigue or malaise and a sensation of fullness or discomfort on the right side of the upper part of the abdomen without signs of chronic liver disease at the time of diagnosis. Such symptoms often antedate the diagnosis of NAFLD in a third of patients. Abdominal obesity and hepatomegaly are the most common physical findings. Obesity is present in 50% to 90% of subjects. About two thirds of subjects with NAFLD also have other features of metabolic syndrome. We recently confirmed abdominal obesity as a marker of both steatosis and grade of the disease. In addition, about 28% of subjects had increased dorso-cervical fat, which correlated strongly with histologic severity. Acanthosis nigricans may be found in individuals with NAFLD and is suggestive of an underlying insulin-resistant state.

Hepatomegaly is the most common liver-related physical finding in subjects with NAFLD. A minority of people have stigmata of chronic liver disease such as spider angiomas or palmar erythema. Jaundice and features of portal hypertension, such as ascites and variceal hemorrhage, are the initial findings in a small minority of subjects with advanced liver disease.

3.2 Laboratory Abnormalities

Suspicion for NAFLD is triggered by abnormal results on liver chemistry tests that are usually performed for non–liver related reasons. Approximately 7.9% of the U.S. population has persistently abnormal liver enzymes with negative tests for viral hepatitis and other common causes of liver diseases. The majority of these subjects could have NAFLD if they have risk factors associated with NAFLD, such as the presence of features of metabolic syndrome. It is also important to note that a large number of subjects with NAFLD have persistently normal liver enzyme levels, and the entire histologic spectrum of NAFLD can be

seen in such individuals. Mild to moderate elevation in serum aminotransferases (ALT) and aspartate aminotransferase (AST) is the most common and often the only laboratory abnormality found in patients with NAFLD. When these values exceed 300 IU/L, alternative causes of liver disease should be sought carefully. The AST/ALT ratio is usually less than 1 but can be reversed in those with advanced fibrosis or cirrhosis. A mild to modest increase in serum alkaline phosphatase and γ-glutamyltransferase (GGT) can be seen in patients with NAFLD, but the degree of elevation is less than that seen in those with alcoholic hepatitis, as is the case with an increased AST/ALT ratio.

Findings of chronic liver disease together with the presence of hypoalbuminemia, coagulopathy, hyperbilirubinemia, and thrombocytopenia suggest advanced liver disease with probable cirrhosis. Serum albumin and the prothrombin time become abnormal before bilirubin becomes elevated. In diabetic subjects, isolated hypoalbuminemia can result from diabetic nephropathy. Hematologic parameters are usually normal unless cirrhosis and portal hypertension lead to hypersplenism. In fact, a large proportion of patients with cryptogenic cirrhosis share many of the clinical and demographic features of patients with NAFLD, thus suggesting that cryptogenic cirrhosis is unrecognized NAFLD in an advanced stage.

About 30% to 50% of subjects with NAFLD have elevated blood glucose and about 60% also have associated hypertriglyceridemia, low HDL cholesterol, or both. An elevated ferritin level is also often seen in subjects with NAFLD. It is, however, not associated with iron overload in most cases and usually reflects an acute phase response. From a practical point of view, the laboratory evaluation of a subject with suspected NAFLD involves excluding alternative causes of liver enzyme abnormalities, documenting hepatic steatosis, making the distinction between hepatic steatosis and steatohepatitis, assessing the stage of the disease, and evaluating for the presence and severity of IR and other complications of metabolic syndrome. Each of these factors must be considered carefully when making a decision about the aggressiveness with which the answer to each of these is sought. It is important to remember that liver enzymes are notably poor predictors of steatosis and significant fibrosis. Therefore liver biopsy remains the gold standard for diagnosing steatohepatitis and for staging the liver disease, unless clinically evident cirrhosis is present.

4. Pathogenesis

Non-alcoholic fatty liver disease is a complex chronic condition caused by the occurrence of step-wise out of control metabolic, inflammatory and cellular activity. Different

factors contributing towards the development of NAFLD/NASH basically involves the influx of free fatty acids (FFA), formation of triglycerides, accumulation of fatty lipids or steatosis, onset of inflammation, mitochondrial dysfunction, oxidative stress and death of mature hepatocytes (Day 2006; Day and James 1998).

4.1 Mechanism of Steatosis

The accumulation of triglycerides originating from the esterification of free fatty acids (FFAs) and glycerol within the hepatocyte is an important aspect of NAFLD/NASH. The contributing factors for the accumulation of FFAs within the liver include enhanced lipolysis in the adipose tissue, dietary sources, and de novo lipogenesis (DNL) (Postic and Girard 2008). Liver has a central role in FFAs metabolisms as hepatocyte utilize FFAs as energy source degrading them in β-oxidation, but a large amount is re-esterificated to triglycerides and exported as very low density lipoprotein (VLDL). Liver VLDL particles are formed through the incorporation of triglyceride into apolipoprotein B (apoB) mediated by microsomal transfer protein (MTP) (Adams and others 2005). Alterations of MTP/apoB synthesis and secretion have been proposed as potential mechanisms underpinning the pathogenesis of NAFLD leading to a decreased capacity for lipid export (Lonardo and Loria 2002). Hence hepatic fat accumulation can occur as a result of increased fat synthesis, increased fat delivery, decreased fat export, and/or decreased fat oxidation (Postic and Girard 2008).

Lipid metabolism in the liver and adipose tissue is controlled by insulin-mediated signals. In healthy individuals, the binding of insulin to its receptor leads to phosphorylation of several substrates including insulin receptor substrates (IRS)-1, -2, -3 and -4, which propagate the insulin signal. Insulin stimulation of IRS-1 and -2 leads to activation of intracellular PI3K (phosphoinositide 3-kinase) and AKT/PKB (protein kinase B) pathways, which are intimately involved in mediating the metabolic effects of insulin (Bugianesi and others 2010). Ultimately, AKT/PKB activation results in translocation of glucose transporter, GLUT4 to the plasma membrane, thus facilitating glucose uptake. In addition, the expression of key lipogenic genes is increased, with a concomitant decrease in gluconeogenic gene expression via its regulation of forkhead (FOXO) transcription factor activity. Insulin has also a potent action in suppressing adipose tissue lipolysis.

Obesity and metabolic syndrome are characterized by an impaired transduction of insulin signals in peripheral tissues leading to a situation known as insulin resistance (IR). In situations of IR insulin-mediated suppression of lipolysis is impaired resulting in an increased

efflux of FFA from the adipose tissue. Hyper-insulinaemia associated with IR leads also to an up-regulation of the transcription factor sterol regulatory element binding protein-1c (SREBP-1c), which is a key transcriptional regulator of genes involved in DNL as well as to the inhibition of β-oxidation of FFA thus further promoting hepatic lipid accumulation (Chitturi and others 2002; Choudhury and Sanyal 2004). Furthermore, in NAFLD additional factors can interfere with insulin signalling cascade, and thus contribute to hepatic IR. These factors include tumour necrosis factor-alpha (TNF-a) signals and jun N-terminal kinase 1 (JNK1) and SOCS (suppressors of cytokine signalling) activation. Increased lipid metabolites such as diacylglycerol (DAG) have also been implicated in interfering with insulin signalling through the modulation of IRS-2 phosphorylation mediated by a protein kinase Ce (PKCe) (Capeau 2008; Choudhury and Sanyal 2005; Cusi 2009).

During the progression of NAFLD the worsening of steatosis is tightly associated with chronic hepatic inflammation, an effect in part mediated by activation of the Ikk-b/NF-kB signalling pathway. In murine models of high-fat diet (HFD)-induced steatosis, increased NF-kB activity is associated with elevated hepatic expression of inflammatory cytokines such as TNF-a, interleukin-6 (IL-6) and interleukin 1-beta (IL-1b), as well as with the activation of Kupffer cells. Accordingly, both serum and hepatic levels of TNF-α are elevated in patients with NASH, and levels correlate with histological severity. In addition to its proinflammatory effects, TNF-α promotes IR. Conversely, inhibition of TNF-α signalling improves IR and histological parameters of NASH. Similarly, serum IL-6 levels are also elevated in both animal and human models of IR and NAFLD, and levels correlate with increasing liver inflammation and fibrosis. Liver-specific NF-kB inhibition prevents HFD-induced inflammatory gene expression, whereas HFD-induced hyperglycaemia and IR can be reproduced by selective over-expression of constitutively active Ikk-b in hepatocytes. The Ikk-b/NF-kB pathway in hepatocytes can also be activated directly by FFA, providing a further mechanism by which central obesity with consequent increased hepatic FFA supply can contribute to inflammation. (Armutcu and others 2013; Baeck and others 2012; Hui and others 2004).

A further aspect in the mechanisms leading to hepatic steatosis directly involves the changes occurring in the adipose tissue. Adipose tissue is not just an inert site of energy storage, but an actively secreting endocrine organ. The functional role of adipocyte-derived cytokines (adipokines), is now increasingly recognized, with leptin and adiponectin amongst the best described. Leptin is a 16 kDa hormone produced mainly by mature adipocytes whose actions

include the regulation of energy intake and expenditure, regulation of the immune system, and promotion of inflammation and fibrogenesis. Conversely, adiponectin has anti-inflammatory activity and increases insulin sensitivity. In obesity adipocytes that accumulate triglycerides modify their pattern of adipokine secretion leading to higher leptin secretion at the expensed of adiponectin production (Marra and others 2005; Musso and others 2005). In fact, the circulating levels of adiponectin are inversely proportional to body fat content and are reduced in patients with NAFLD. Adiponectin antagonises the effects of TNF-α, which itself suppresses adiponectin production (Takei and Sato 2006). The importance of adiponectin in NAFLD is supported by studies showing that serum adiponectin levels can help to distinguish NASH from simple steatosis. Other adipose tissue derived factors found in excess in NAFLD include TNF-α, IL-6, angiotensinogen and resistin, all of which antagonise the lipogenic effects of insulin, but their precise role in the pathogenesis of NAFLD remains to be determined (Mirza 2011; Orlik and others 2010; Polyzos and others 2013).

4.2 Mechanism of Hepatocyte Injury

As previously mentioned, nonalcoholic steatohepatitis (NASH) is characterized by parenchymal injury involving hepatocyte ballooning, presence of Mallory-Denk bodies and extensive liver cell apoptosis (Duwaerts and Maher 2014). Accordingly, serum levels of of caspase-cleaved cytokeratins (CK) 8 and 18 have been recently proposed as specific markers of hepatocyte death in NASH (Eguchi and others 2014). Several mechanisms have been invoked to explain the proapoptotic state in NASH. Triglyceride accumulation itself increases apoptosis by the interaction of unoxidized palmitoyl CoA with serine to form dihydro-sphingosine, a precursor of ceramide. Ceramide is a potent inducer of apoptosis via an inducible nitric oxide synthetase (iNOS)-mediated pathway that requires the transcriptional factor NF-κB (Harbrecht and others 2012) (Alexander 1998; Harbrecht and others 2012; Ou and others 1997; Pinto and others 2000). It has also been shown that hepatocyte incapability to esterify the excess of FFAs secondary to increased peripheral lipolysis in the insulin-resistant state triggers apoptosis through a process known as produce lipotoxicity. Several mechanisms account for lipotoxicity. FFAs can directly induce translocation of Bax to lysosomes, where it causes the release of cathepsin. Cathepsin, acting via NF-κB, induces TNF-α and activation of TNF receptor–associated death pathways. Recently, the potential role of ER stress in the development of hepatocyte lipotoxicity in NASH has gained interest. The ER is the principal site for synthetic activity within cells. Such activity requires not only appropriate synthesis but

also local mechanisms to ensure that the proteins are correctly folded because this is essential for their recognition by appropriate receptors and trafficking to their final destination. Under conditions in which there is increased protein or lipid synthetic activity in the ER, depletion of ATP, depletion of calcium, or altered glucose homeostasis, the regulatory function of the ER in maintaining normal synthetic function is disrupted. This leads to the activation of an intracellular program called the unfolded protein response (UPR) (Henkel and Green 2013; Kapoor and Sanyal 2009; Malhi and Kaufman 2011; Zhang and others 2012a; Zheng and others 2011). Activation of the UPR initially leads to an adaptive response in which protein synthesis decreases and allows restoration of normal ER function. However, if the initiating factors are not corrected, alarm pathways are activated, including activation of a number of stress kinases, which eventually results in activation of homologous protein (CHOP), a potent apoptosis-inducing factor. Recent studies have reported that patients with NAFLD have a variable degree of UPR activation. Inositol requiring enzyme-1 (IRE-1) activation appears to play an important role in the genesis of cell injury in NASH via activation of JNK phosphorylation. Interestingly, there seems to be a close association of IRE-1 activation with the histologic activity of the disease. Failure to generate ER degradation-enhancing α-mannosidase like protein (EDEM) in response to spliced X box–binding protein (sXBP) in some subjects raises the possibility that patients with the lowest EDEM levels are at particular risk of progressing to cirrhosis because of insufficient degradation of unfolded proteins, thus perpetuating the ER stress. Despite increased phosphorylated eIF-2a, patients with NASH are apparently unable to up-regulate activating transcription factor 4 (ATF4), CHOP, and growth arrest and DNA damage- 34 (GADD34), which contributes to the failure to recover from ER stress (Cao and others 2012; Fang and others 2013; Lee and others 2012; Pagliassotti 2012; Zhang and others 2012b). Thus NASH is specifically associated with failure to generate sXBP1 and activation of c-jun N-terminal kinase (JNK) (Malhi and others 2006). Accordingly, JNK activation is evident in liver biopsies from NASH patients and pharmacological or genetic JNK inhibition prevents lipotoxicity “in vitro” and ameliorates steatohepatitis in rodent models of NASH (Cazanave and Gores 2010; Czaja 2010). Interestingly, the antiapoptotic B-cell lymphoma-2 (BCL2) protein appears to be strongly expressed in human steatohepatitis, probably representing an adaptive response. Thus, on the basis of the recognized significance of hepatocyte apoptosis in the pathogenesis of NAFLD, it has been proposed that the development of progressive NAFLD in some patients but not in others may be the result of increased susceptibility of steatotic hepatocytes to apoptosis arising from abnormal regulation of BCL2 proteins, alteration in JNK

activation, or preferential activation of ER stress (Li and others 2014; Malhi and others 2006; Panasiuk and others 2006).

Additional mechanisms of hepatocyte injury in NAFLD/NASH involve the effect of inflammatory cytokines and particularly TNF-α and oxidative stress. The key role of cytokine production in the progression of steatosis to NASH is supported by studies demonstrating that cytokines can replicate all of the histological features associated with NASH, including hepatocyte apoptosis/necrosis and Mallory body formation (Marra and others 2008).

4.3 Oxidative Stress

Oxidative stress is a result of an imbalance between prooxidant and antioxidant species. This could be due to either increased production of prooxidants reactive oxygen species (ROS) or reactive nitrogen species (RNS) or decreased antioxidant defenses Potential sources of ROS in the liver include the mitochondria, the peroxisomes, the microsomal oxidative system, and iron overload. (Alkhouri and McCullough 2012; Basaranoglu and others 2013; Baskol and others 2007). The mechanisms responsible for oxidative stress in NAFLD/NASH have been characterized to some extent showing that FFA and cholesterol accumulation within the mitochondria along with TNF-α cause mitochondrial dysfunction. These mitochondrial structural defects associated with impaired mitochondrial respiratory chain activity produce a state of uncoupled oxidation and phosphorylation that leads to increased ROS production. This concept is further supported by evidence of decreased ATP formation in the liver of subjects with NASH (Begriche and others 2006; Gambino and others 2011). Another possible source of ROS can be the cytochrome P-450 system. This system, particularly CYP2E1, is over-expressed in subjects with NAFLD along with cytochrome P4502E1 activity (Lieber 2004). CYP2E1 can be induced as a result of insulin-resistance as well as to cope with the increase in FFAs (Lieber 2004). In line with these findings, CYP2E1 deletion in mice results in less susceptibility to high fat diet induced NAFLD/NASH as well as in lower hepatic oxidative stress (Abdelmegeed and others 2012).

A growing body of evidence from the experimental models of NAFLD/NASH suggests that oxidative stress plays a key role in the mechanisms causing the death of fat-laden hepatocytes as well as contributes to the activation of hepatic stellate cells to matrix-producing myofibroblasts (Gambino and others 2011). Accordingly, antioxidant supplementation reduces liver injury in experimental rodent models of NASH (Laurent and other 2004). The relevance of these observations to humans is supported by several studies showing an increase in

oxidative stress markers, in the liver and in the serum of both adult paediatric patients with NAFLD/NASH (Chalasani and others 2004; Ikura and others 2006; Seki and others 2002). Furthermore, as compared to normal livers, liver biopsies from NASH patients display a lower mRNAs expression of different antioxidant enzymes (Sreekumar and others 2003). On the same vein, recent evidences indicates that antioxidant treatments might be effective in improving hepatic damage in NASH (Pacana and Sanyal 2012).

4.4 Mechanisms of Inflammation

Inflammation, along with hepatocyte damage, is the main feature of the progression from simple steatosis to NASH. In fact, the molecular mechanisms able to promote inflammation cross-talk with those responsible for hepatocellular damage and fibrosis. The precise mechanisms of inflammation in NASH have not yet been completely elucidated, but current evidence indicates both the innate and adaptive immunity have a role in the initiation and maintenance of lobular inflammation. The innate immune system is an important factor in the promotion and progression NASH. Hepatic infiltration of innate immune cells such as macrophages, granulocytes and natural killer (NK) has been commonly observed in early stages of the disease and they are considered as driving force of NASH progression.

The hepatic macrophage population is named after the scientist Karl Wilhelm von Kupffer. Kupffer cells are located predominantly in the periportal area. They originate from bone marrow and in healthy livers Kupffer cells are responsible for the phagocytosis of particulate matters, presentation of antigen accompanied by immune regulation, and the release of soluble mediators. Alike other macrophages, Kupffer cells and hepatic monocyte-derived macrophages are a highly plastic populations that may adopt various phenotypes ranging between the extreme states known as M1 and M2. Inflammation driven by M1 Kupffer cells is counterbalanced by alternatively-polarized M2 macrophages that produce anti-inflammatory cytokines such as IL-10, and promote resolution of inflammation (Murray and Wynn 2011; Sica and Mantovani 2012). Macrophage polarization into an M2 phenotype is promoted by Th2-derived cytokines (IL-4, IL-13) (Murray and Wynn 2011; Sica and Mantovani 2012), that may also originate from hepatocytes (Kang and others 2008), while such factors promoting M2 Kupffer cell polarization are poorly characterized.

Increasing evidence suggests that Kupffer cells critically contribute to the progression of NAFLD. In fact at the onset of NASH lipid accumulation in Kupffer cells significantly contribute to the production of pro-inflammatory cyto/chemochines, which, in turn, stimulate

the liver infiltration by circulating monocytes (Tosello-Trampont and others 2012; Leroux and others 2012). Hepatic monocyte infiltration is primarily promoted by CCL2, a chemokine up-regulated in the serum and in the liver of patients with NASH (Haukeland and others 2006), that drives the recruitment of inflammatory Ly6C-positive monocytes through the interaction with C–C chemokine receptor 2 (CCR2). According, pharmacological inhibition of genetic deficiency of CCL2/CCR2 dyad reduces macrophage infiltration and ameliorated steatohepatitis in experimental mice model of NASH (Baeck and others 2012; Miura and others 2012). However, variable results have been obtained in mice with different genetic backgrounds (Galastri and others 2012). Other chemokines contributing to monocyte recruitment include CCL5 (RANTES) as interference with CCL5 functions ameliorates experimental NASH (Berres and others 2010).

Upon liver infiltration monocytes rapidly differentiates to M1 polarized macrophages and the extent of macrophage M1 responses appears to modulate NASH severity among different mice strains (Maina and others 2012). Furthermore, macrophage release of IL-15 and CXCL16 is important for stimulating the recruitment and the survival of T-lymphocytes and NKT cells (Locatelli and others 2013; Wehr and other 2013). Pro-inflammatory cytokines released from activated Kupffer cells also activate hepatic sinusoidal endothelial cells to upregulate adhesion molecules (ICAM1, VCAM-1) and in combination with the chemokines secreted from macrophages stimulate the recruitment of neutrophils to the liver (Tosello-Trampont and others 2012). Neutrophils, in turn secrete reactive oxygen species (ROS), oxidants, defensins, as well as chemokines to attract more neutrophils and monocytes (Rensen and others 2012). Following their recruitment to the liver macrophages release not only pro-inflammatory cytokines but also growth factors as G-CSF, and GM-CSF that can extend the lifespan of neutrophils thus sustaining their presence at the site of inflammation (Rensen and others 2012). The production of ROS, NO and cytokines by neutrophils and macrophages significantly contribute to promote hepatocyte cytotoxicity.

Lymphocytes are commonly found throughout the parenchyma and in the portal tracts of healthy livers and include T and B cells subpopulations as well as other subsets belonging to innate immunity as natural killer (NK) and natural killer T-cells (NKT) that shares features in common with both NK and T cells. NKT cells are particularly frequent in the liver because these cells express a specific chemokine receptor (CXCR6) that interacts with the chemokine CXCL16 abundantly produced by hepatic sinusoidal endothelia (Geissmann and others 2005; Swain 2010). Although the total number of hepatic CD3+ T lymphocytes is not appreciably

modified in NASH, an imbalance between CD8+/CD4+ CD3+ T-cell subtypes has been observed (Ferreyra Solari and coworkers 2012). CD4+ T helper cells are a sub-group of lymphocytes that are capable of switching B cell to antibody production, activating cytotoxic T cells and contributing to the phagocyte functions. Recent reports have shown that an increase in circulating IFN-γ-producing CD4+ T-cells characterizes NASH in both paediatric and adult patients in conjunction with an enhanced liver IFN-γ expression (Ferreyra Solari and coworkers 2012; Inzaugarat and others 2011), suggesting the possible relevance of Th-1 responses to the human disease. Furthermore, a higher number of Th-17 cells has been observed in mice with steatosis induced by feeding a high fat diet and in liver biopsies of NASH patients. Accordingly, the Th-17 related genes (ROR-γT, IL-17, IL-21, IL-23) are up-regulated in NASH patients as compared to healthy controls and neutralization of IL-17 in high fat diet fed mice ameliorates liver injury and inflammation (Tank and other 2011). In spite IL-17 has been involved in the pathogenesis of hepatic fibrosis (Meng and others 2012), the actual role of DC4+ Th-17 T cells in the pathogenesis of NASH is still poorly characterized.

Conversely, recent studies have pointed out a possible involvement of natural killer T (NKT) cells in the progression of NASH. NKT cells account for 20-35% of mouse and 10-15% of rat and human liver lymphocytes. They recognize lipid antigens presented by the non-classical MHC class I-like molecule CD1 and can be directly cytotoxic by Fas ligand (FasL), or perforin/granzyme-dependent mechanisms in addition to regulate innate and adaptive immunity through the production of IFN-γ and IL-4 (Seino and Taniguchi 2005; Exley and Koziel 2004). Beside classical cytokines, NKT cells also secrete osteopontin (OPN) (Syn and others 2012), a cytokine with both pro-inflammatory and pro-fibrogenic capacities and the fetal morphogen, sonic hedgehog (Shh), which activates hepatic stellate cells (HSC) into collagen secreting myofibroblasts and amplifies the repair-associated inflammatory response (Uede 2011; Gao and Radaeva 2013; Syn and others 2012). The role of NKT cells during the progression from NAFLD to NASH is complex as the development of steatosis in mice receiving a high fat diet is associated with a reduction of hepatic NKT cells. This reduction is due to a lowering of hepatic CD1d expression and an increase of NKT apoptosis due to an impaired production of IL-15 in a combination with an up-regulation in hepatic expression of IL-12 (Li and other 2005; Yang and other 2007). Indeed, Kupffer cell depletion lowers IL-12 expression and blocks the impairment of NKT cells (Li and other 2005; Kremer and others 2010). On the contrary, in mice with advanced NASH there is an increase in the number of NKT cells, which parallels the progression of the disease to fibrosis. NKT cell expansion

involves IL-15 production and is associated with an increase in liver IFN-γ and OPN production (Locatelli and others 2012). Accordingly, induction of NASH in NKT cell deficient mice is characterized by a blunted OPN expression and by an improvement in liver injury and collagen deposition (Syn and others 2010). In the setting of human NASH, advanced fibrosis is correlated with increased hepatic levels of OPN and Hh and elevated plasma OPN levels in comparison with early fibrosis (Syn and others 2012; Tajiri and other 2009).

4.5 Mechanisms of Fibrosis.

In many chronic liver diseases unresolved inflammation promotes pathologic repair leading to progressive fibrosis and cirrhosis (Friedman 2008). As mentioned above hepatic cirrhosis represent the final outcomes of NASH. In fact, within 8 years, 15% of NASH patients develop clinically and histologically evident cirrhosis. Death rate ascribed to NASH-related cirrhosis accounts for 12-25%, while end-stage NASH is responsible for about 4-10% of liver transplants (Neuschwander-Tetri and Cadwell 2003). This makes NASH an increasingly important cause of liver cirrhosis. NASH-related fibrosis develops primarily in the pericentral areas, where thin bundles of fibrotic tissue surround groups of hepatocytes and thicken the space of Disse, in a "chicken wire" fashion (Brunt 2010). The main cell type responsible for extracellular matrix deposition are hepatic stellate cells (HSCs), These cells respond to the production of transforming growth factor β1 (TGF-β1), platelet-derived growth factor (PDGF) and fibroblast-derived growth factors produced by macrophages trans-differentiating into myofibroblast-like cells (HSC/MSs) that are responsible for the secretion of collagen and extracellular matrix components (Friedman 2008). Furthermore, decreased hepatic matrix degradation due to a reduced production of matrix metalloproteases (MMPs) and/or an increased production of matrix metalloprotease inhibitors might also contribute to collagen accumulation (Friedman 2008). Macrophage activation in response to chronic inflammatory stimuli is mostly responsible for the secretion of pro-fibrogenic cytokines (Friedman 2008). In addition, HSC proliferation and transformation to collagen-producing myofibroblasts is influenced by lymphocyte-derived cytokines and oxidative stress (Novo and others 2008). Although the development of fibrosis in NASH does not appears to be appreciably different from those in other liver diseases, alterations in adipokine secretion consequent to obesity might have a specific role for the induction of fibrogenesis in this condition. Activated HSCs selectively express leptin receptors and leptin stimulates HSC survival, the expression of pro-inflammatory and angiogenic cytokines (Wang and others 2008). The pro-fibrogenic action of

leptin might be enhanced by the combined lowering of adiponectin as adiponectin reduces proliferation and increases apoptosis of cultured HSC (Wang and others 2008).

5. Aims of the work

In spite of the growing number of studies investigating the pathogenesis of NAFLD/NASH, a number of issues concerning the mechanisms involved in promoting lobular inflammation and the evolution of NASH to fibrosis/cirrhosis are still unresolved. In particular, it is still unclear why only some NAFLD patients develop steatohepatitis. Furthermore, among the subjects with NASH there is a large inter-individual variability in the evolution to fibrosis. The factors responsible for such an inter-individual variability represent a particular challenge as multiple interaction occur between hepatocytes, inflammatory cells and hepatic stellate cells in the different phases of the disease progression.

In my doctoral project, I have addressed some of these issues by investigating the possible involvement of adaptive immune mechanisms in the evolution of NASH and characterizing morphological and functional modifications occurring in monocyte-derived cells during the disease progression.

6. Paper 1

Adaptive Immune Responses Triggered by Oxidative Stress Contribute to Hepatic Inflammation in NASH

Published on Hepatology 2014;59:886-897.

Background and Aims: The mechanisms responsible for the progression of simple steatosis to steatohepatitis (NASH) are still incompletely characterized. Oxidative stress is one of the features of NAFLD/NASH and hepatic oxidative stress markers, such as 4-hydroxynonenal (4-HNE) and 8-hydroxydeoxyguanosine, correlate with the severity of necro-inflammation and fibrosis, suggesting that oxidative injury might be involved in triggering steatohepatitis. Studies in atherosclerosis have evidenced that lipid peroxidation products originating from oxidized LDL generate a variety of neo-antigens able to stimulate the innate immune system, which in turn promotes inflammation in atheroma. As previous data indicate that both adult and children with NAFLD/NASH have increased titres of IgG against oxidative stress derived antigens, in in the present study we have used the methionine-choline deficient (MCD) diet model of steatohepatitis to get insides in the involvement of immune responses in promoting hepatic inflammation in NASH.

Key results: In MCD diet fed mice, the development of liver injury and lobular inflammation paralleled with the presence IgG against malonildialdehyde (MDA) and 4-HNE-derived antigens. Moreover, the hepatic recruitment of CD4+ and CD8+ T-lymphocytes responsive to the same antigens was also observed. Mice immunization with MDA-adducted bovine serum albumin (MDA-BSA) before feeding the MCD diet stimulated transaminase release, lobular inflammation, and the hepatic expression of proinflammatory cytokines. Hepatic inflammation was accompanied by a stimulation in the liver recruitment and Th-1 activation of CD4+ T cells that further stimulated macrophage M1 responses. In this setting, depleting $CD4^+$ T-cells in MCD-fed immunized mice by using an anti-CD4 monoclonal IgG significantly lowered lobular inflammation and focal necrosis.

Conclusions: These results indicate that adaptive immune responses triggered by oxidative stress-derived antigens contribute to hepatic inflammation in experimental NASH by promoting Th-1 responses by CD4+ T-lymphocytes.

ADAPTIVE IMMUNE RESPONSES TRIGGERED BY OXIDATIVE STRESS CONTRIBUTE TO HEPATIC INFLAMMATION IN NASH

Salvatore Sutti, Aastha Jindal, Irene Locatelli, Marco Vacchiano, Luca Gigliotti, Cristina Bozzola, Emanuele Albano.

Dept. of Health Sciences and Interdisciplinary Research Centre for Autoimmune Diseases, University "Amedeo Avogadro" of East Piedmont,

Via Solaroli 17, 28100 Novara.

Running title: Adaptive immunity in mice NASH.

Keywords: Nonalcoholic fatty liver disease, lipid peroxidation, NKT cells, Th-1 responses, antibodies.

Words: 4723

References: 49

Note: The authors have no conflict of interest

Corresponding Author:

Prof. Emanuele Albano, Department of Health Science, University "Amedeo Avogadro" of East Piedmont, Via Solaroli 17, 28100 Novara, Italy.

Tel. +39 0321 660642 Fax +39 0321 620421 E-mail: albano@med.unipmn.it

Abstract

Previous studies have shown that human non-alcoholic steatohepatitis (NASH) is often associated with the presence of circulating antibodies against proteins adducted by lipid peroxidation products. Here we used the methionine-choline deficient (MCD) model of NASH to characterize the possible involvement of adaptive immunity in NASH.

In mice fed with the MCD diet up to 8 weeks liver injury and lobular inflammation worsen in a time-dependent manner in parallel with the development of IgG against malonyldialdehyde (MDA) and 4-hydroxynonenal (4-HNE)-derived antigens and the hepatic recruitment of $CD4^+$ and $CD8^+$ T-lymphocytes that were responsive to the same antigens. Moreover, in these animals the individual IgG reactivity against MDA-adducts positively correlated with transaminase release and TNF-α expression. To substantiate the role of immune responses triggered by oxidative stress in the progression of NASH, mice were immunized with MDA-adducted bovine serum albumin (MDA-BSA) before feeding the MCD diet. MDA-BSA immunization did not affect the livers of control mice, but further stimulated transaminase release, lobular inflammation and the hepatic expression of pro-inflammatory cytokine in MCD-fed mice. The increased severity of NASH in immunized MCD-fed mice was associated with the liver recruitment and the Th-1 activation of $CD4^+$ T-cells that accounted for an increased M1 activation of hepatic macrophages. Moreover, hepatic fibrosis was also evident in these animals in concomitance with an IL-15-mediated increase of hepatic natural killer T-cells (NKT) and the up-regulation in liver osteopontin production by NKT cells and hepatic macrophage.

Conclusions: These results indicate that oxidative stress can contribute to the progression of NASH by stimulating both humoral and cellular responses, pointing to the possible contribution of adaptive immunity to the pathogenesis of the disease.

Abbeviations:

4-HNE 4-hydroxynonenal; MCD methionine-choline deficient; MDA malonildialdehyde; NAFLD NonAlcoholic Fatty Liver Disease; NASH NonAlcoholic SteatoHepatitis; NK natural killer; NKT natural killer T cells:OPN osteopontin

Introduction

A key issue in understanding the pathogenesis non-alcoholic fatty liver disease (NAFLD) concerns the identification of the mechanisms responsible for switching from simple steatosis to steatohepatitis (NASH). This aspect is clinically relevant because steatosis does not appear to adversely affect the long-term outcome of NAFLD [1], whereas parenchimal injury and inflammation are the driving forces for the disease evolution to fibrosis/cirrhosis [2,3]. Oxidative stress is one of the features of NAFLD/NASH [4] and oxidative stress markers, such as the hepatic content of 4-hydroxynonenal (4-HNE) and 8-hydroxydeoxyguanosine, correlate with the severity of necro-inflammation and fibrosis [5,6], suggesting that oxidative injury might be involved in triggering steatohepatitis. In this scenario, recent evidence indicates that lipid peroxidation products originating from phospholipid oxidation can act as damage-associated molecular patterns (DAMPs) and promote inflammation through the interaction with both soluble and cell-associated pattern recognition receptors [7,8]. A further mechanism by which oxidative stress can stimulate inflammation involves adaptive immunity. Indeed, in atherosclerosis as well as in several auto-immune diseases the interaction of lipid peroxidation products with cellular proteins leads to the formation of immunogenic adducts that induce both humoral and cellular immune responses [9,10].

Previous studies from our laboratory have shown that high titres of IgG against some of the antigens originating from oxidative stress, namely malondialdehyde- (MDA) derived adducts, are detectable in about 40% of adult NAFLD/NASH patients and in 60% of children with NASH [11,12]. In these latter, high antibody titres associated with more severe lobular inflammation and 13 fold increased risk of a NAFLD Activity Score ≥5 [12], while in adults anti-MDA IgG are an independent predictor of fibrosis [11]. From this background, we sought to investigate the possible contribution of immune reactions triggered by oxidative stress in modulating hepatic inflammation in NASH. For the experiments we relayed on a rodent model of NASH based on mice feeding with a methionine-choline deficient (MCD) diet that, despite it does not reproduce key features of human NAFLD/NASH such as obesity and insulin resistance, causes well evident oxidative stress and a rapidly progressing steato-hepatitis [13].

Material and Methods

Animal and Experimental protocol. Eight weeks old male C57BL/6 mice were purchased from Harlan-Nossan (Corezzana, Italy) and fed for 4 or 8 weeks with either methionine-choline deficient (MCD) or control diets (Laboratorio Dottori Piccioni, Gessate, Italy). For

immunization experiments mice were injected subcutaneously with 100μg of MDA-adducted bovine serum albumin (MDA-BSA) in incomplete Freud's adjuvant and re-boosted after one week with the same antigen. The control groups received either saline or incomplete Freud's adjuvant injections. MCD diet feeding was started 2 weeks after the second injection. In some experiments immunized mice were treated with 400μg of the anti-CD4 monoclonal antibody GK1.5 (BioXCell, West Lebanon, NH, USA) while receiving the MCD diet (See supplementary materials for further details) to deplete hepatic $CD4^+$ T cells. The efficiency of cell depletion was preliminary evaluated by flow cytometry and was >97% in both the liver and the spleen. All the experiments were approved by the Italian Ministry of Health and by the University Commission for Animal Care following the criteria of the Italian National Research Council.

Antigen preparation and antibody measurement. Protein adducts with lipid peroxidation products were prepared as in [12,14] and used to coat polystyrene microwell ELISA plates (Nunc, S/A, Roskilde, Denmark). Mouse sera (0.20 ml, 1:50 dilution) were added in duplicate and the antibody binding was revealed using peroxidase-linked goat anti-mouse IgG or IgM sera as previously described [12,14]. The results were expressed as optical density following the subtraction of background reactivity.

mRNA extraction and Real time PCR. Liver RNA was retro-transcripted with High Capacity cDNA Reverse Transcription Kit (Applied Biosystems Italia, Monza, Italy). RT-PCR was performed in a Techne TC-312 termalcycler (TecneInc, Burlington NJ, USA) using TaqMan Gene Expression Master Mix and TaqMan Gene Expression probes for mouse TNF-α, IL-12p40, IL-17a, IFN-γ CCL2, iNOS, CD40, CD40L, osteopontin, α1-procollagen, T-bet, RORγT and beta-actin (Applied Biosystems Italia, Monza, Italy). All samples were run in duplicate and the relative gene expression calculated as $2^{-\Delta Ct}$ was expressed as fold increase over control samples.

Histology and immunohistochemistry. Steatosis and lobular inflammation were scored blind according to Kleiner et al. [15] in hematoxilin/eosin stained sections. Hepatocyte apoptosis was detected by terminal deoxyribonucleotide transferase (TdT)-mediated dUTP nick-end labeling (TUNEL) using Apoptags Kit (Intergen Company, New York, USA). Liver infiltrating T- and B-cells were evidenced in frozen sections using, respectively, anti-mouse CD3, anti-mouse B220 rat monoclonal antibodies (R&D System Europe Ltd, Abingdon, UK) and a horse-radish peroxidase polymer kit (Biocare Medical, Concord, CA, USA). Polyclonal

antibodies against α-smooth muscle actin (□-SMA) (Labvision, Bio-Optica, Milan, Italy) were used to detect activated hepatic stellate cells in formalin-fixed sections.

Intrahepatic lymphocyte isolation and flow cytometry analysis. Hepatic mononucleated cells were isolated and purified on a density gradient as in [16]. The cells were stained with fluorochrome-conjugated antibodies for CD45, CD3, CD4, CD8, NK1.1, F4/80, CD69, CD107a, IL-2 and IFN-γ (eBiosciences, San Diego CA, USA) and analyzed with a FACScalibur (Becton Dikinson) flow cytometer. De-complemented mouse serum was used to block unspecific immunoglobulin binding. A polyclonal anti-osteopontin rabbit antiserum (Millipore, Temecula, CA, USA) and phycoerythrin-conjugated anti-rabbit IgG (Sigma-Aldrich, Milan, Italy) were used for detecting ostepontin producing cells. Intrahepatic lymphocyte response to MDA adducts was investigated by flow cytometry analysis of IL-2 production following overnight incubation with 10μg/mL MDA adducted or native murine albumin in the presence of brefeldin A (3μg/ml), anti-CD3e and CD28 antibodies (1μg/ml) according to [17].

Additional methods are described in the supplementary materials.

Data analysis and statistical calculations. Statistical analyses were performed by SPSS statistical software (SPSS Inc. Chicago IL, USA) using one-way ANOVA test with Tukey's correction for multiple comparisons or Kruskal-Wallis test for non-parametric values. Significance was taken at the 5% level. Normality distribution was preliminary assessed by the Kolmogorov-Smirnov.

Results

Immune responses against oxidative stress related-antigens associates with NASH progression.

NASH induced by feeding mice with a methionine/choline deficient (MCD) diet is characterized by a time-dependent progression of liver injury (13). Accordingly, in C57BL/6 mice receiving the MCD diet for up to eight weeks we observed a progressive increase in hepatic triglyceride content, transaminase release and circulating TNF-α levels that paralleled with the histological severity of hepatic inflammation (Supplementary figure 1). Liver oxidative stress, as measured by thiobarbituric acid reactive compounds (TBARs) was also well evident at an early time point in the animals with NASH (Fig.1). As observed in humans, oxidative stress in the mice with NASH associated with the development of IgG against adducts originating from lipid peroxidation products such as malonyldialdehyde (MDA) and

4-hydroxynonenal (4-HNE) and the IgG titres increased in parallel with the disease progression (Fig. 1). Moreover, in these animals the individual IgG reactivity against MDA-adducts, but not liver TBARs, positively correlated with ALT and TNF-α mRNA values (r=0.61, p=0.04; r=0.66, p=0.03, respectively). Immunohistochemistry revealed that the hepatic inflammatory infiltrates were also enriched by T- and B-lymphocytes (Supplementary figure 1), the number of which positively correlated with the individual IgG reactivity against MDA-adducts (r=0.68, p=0.02; r=0.75, p=0.006, respectively). Flow cytometry analysis of hepatic mononucleated cells from control and NASH livers confirmed a progressive recruitment of T-lymphocytes that involved both effector $CD8^+$ T-cells and $CD4^+$ helper T-cells (Fig. 1). Furthermore, the proportion of $CD3^+$ T-cells expressing the CD69 activation marker was increased in the livers MCD-fed mice as compared to controls (Fig. 1). Intra-hepatic $CD4^+$ T-cells from mice with NASH also showed an enhanced interferon-γ (IFN-γ) expression (Fig.1), suggesting that lipid peroxidation-derived antigens might contribute to the development of cell-mediated immune responses. Supporting this view, we observed that $CD8^+$ and $CD4^+$ T-cells obtained from NASH, but not from healthy livers, produce IL-2 when incubated "in vitro" with MDA-modified murine albumin (Fig. 1).

The induction of immunity against MDA-adducts enhances NASH severity in mice.

To substantiate the possible role of adaptive immunity triggered by lipid peroxidation-derived antigens in promoting hepatic inflammation in NASH, we induced immune reactions against MDA adducts by immunizing C57BL/6 mice with MDA-modified bovine serum albumin (MDA-BSA) in incomplete Freund's adjuvant before the administration of the MCD diet. In preliminary experiments, this immunization protocol led to appreciable humoral and cellular reactivity against MDA adducts (not shown). In the animals receiving the control diet MDA-BSA immunization did not affect liver histology and ALT release neither significantly modified the hepatic expression of pro-inflammatory markers (Supplementary Fig. 2). However, following four weeks on the MCD diet ALT release and the hepatic mRNA expression of the inflammatory mediators, TNF-α and CCL2, were higher in MDA-BSA-immunized than in naïve mice (Fig. 2). No appreciable changes in liver injury and inflammation were observed in mice injected with incomplete Freund's adjuvant before receiving the MCD diet (Fig 2). The enhanced severity of NASH was further supported by histology that showed higher scores for lobular inflammation and increased frequency of necro-inflammatory foci and apoptotic cells in MCD-fed immunized mice (Fig. 3).

Furthermore, circulating TNF-α levels were three fold higher in these latters as compared to similarly treated naïve mice (Fig. 2). In a recent report, Bieghs and co-workers demonstrated that the induction of IgM antibodies cross-reacting with oxidized phosphatidylcholine ameliorated NASH caused by feeding a high-fat/cholesterol diet to LDL receptor-deficient C57BL/6 mice [19]. In our hands, the immunization with MDA-BSA adducts did not influence the IgM reactivity towards MDA-derived antigens and moderately stimulated that against oxidized phosphatidylcholine (Supplementary Fig. 3), indicating that different mechanisms were involved. Thus, we sought to investigate further the role of oxidative stress-driven immunity in promoting liver inflammation in NASH.

Characterization of immune response associated with the development of NASH in immunized mice.

Flow cytometry of intrahepatic lymphocytes showed that MDA-BSA immunization did not modify liver T-cells profile in mice fed the control diet (Supplementary Fig. 3). However, immunization further promoted $CD3^+$ T-cell recruitment in MCD-fed mice increasing both the $CD8^+$ and $CD4^+$ pools (Fig. 4). However, the proportion of $CD8^+$ T-cells expressing the CD107a activation marker was unchanged (Fig. 4). Th-1 and Th-17 activation of $CD4^+$ T-lymphocytes are important pro-inflammatory stimuli. We observed that the expression of the Th-1 transcription factor T-cell T-box transcription factor (T-bet) as well as liver IFN-γ content were selectively increased in MCD-fed immunized animals (Fig. 4), in parallel with a stimulation of macrophages M1 activation markers IL-12p40 and inducible NO synthase (iNOS) (Fig. 2). Among immunized MCD-fed mice there was also a positive correlation between the individual IFN-γ expression and that of TNF-α, IL-12p40 and iNOS ($r=0.82$, 0.75 and 0.88 respectively; $p<0.02$). No changes were instead evident in the hepatic mRNAs for the Th-17 transcription factor retinoic acid-related orphan receptor-γt (ROR-γt) and of IL-17a (not shown). Furthermore, MCD-fed immunized mice also showed an up-regulation in the mRNAs of CD40 ligand (CD40L; CD154) and of its receptor CD40, a pair of co-stimulatory receptor-ligand molecules involved in macrophage activation by $CD4^+$ T-cells [19]. Consistently, depleting $CD4^+$ T-cells in MCD-fed immunized mice by using an anti-CD4 monoclonal IgG significantly lowered the hepatic mRNA expression of IFN-γ and CD40L as well as that of macrophage M1 markers iNOS and IL-12p40 (Fig. 5). In these animals, histology also showed that $CD4^+$ T-cell depletion ameliorated lobular inflammation and focal necrosis (Fig. 5).

The progression of NASH in immunized mice also involves NKT cells.

Unexpectedly, changes in liver natural killer T (NKT) cells associated with the worsening of NASH occurring in immunized mice. According to previous observations [20,21], the development of NASH in naïve mice was characterized by the lowering of liver natural killer (NK) ($CD3^-$, $NK1.1^+$) and NKT ($CD3^+$, $NK1.1^+$) pools. On the contrary, MCD-fed immunized animals did not show NK cell depletion, while the NKT fraction was significantly higher than in controls (Fig. 6). Recent findings in animal models of NAFLD/NASH have implicated macrophages production of IL-15 in controlling liver NKT cell differentiation and survival [22]. In turn, NKT cells have been proposed to contribute to the progression of NASH to fibrosis through the production of osteopontin (OPN) [16,23]. In hour hands, the expansion of NKT cells observed in MCD-fed immunized mice paralleled with an increase of hepatic IL-15 content (Fig. 6). Such an effect was likely mediated by $CD4^+$ T-cell activation, as depleting immunized mice of $CD4^+$ T-cells significantly lowered the intrahepatic IL-15 mRNA (Fig. 5). We also observed that, while the development of NASH in naïve mice did not affect liver OPN, OPN levels were significantly up-regulated in MCD-feed immunized animals and such an increase involved an expansion of OPN-expressing NKT cells and F4/80-positive hepatic macrophages (Fig. 6). Furthermore, in line with OPN capacity to stimulate hepatic stellate cell (HSC) activation, Sirius Red staining for collagen and α-smooth muscle actin (□-SMA) positive HSCs were more evident in the livers of immunized as compare to naïve MCD-fed mice (Fig. 2).

Discussion

Recent studies have implicated the contribution of adaptive immunity to fat inflammation in obesity, as $CD4^+$/$CD8^+$ T-cells are recruited to the adipose tissue and provide stimulation for the macrophage production of pro-inflammatory mediators [24,25]. Lymphocytes are often detected in the lobular infiltrates of NASH [26], but the actual role of adaptive immunity in the disease pathogenesis is still poorly understood. We previously reported that sub-sets of adults and paediatric NAFLD/NASH patients show antibody responses against oxidative stress-related antigens, such as MDA-derived adducts, that associate with an increased severity of lobular inflammation or fibrosis [10,11]. Similar antibodies are also detected along with hepatic injury and inflammation in rats with NASH induced by the enteral nutrition with a high fat diet, while preventing oxidative stress with N-acetylcysteine attenuates both IgG formation and the severity of steatohepatitis [27]. In the present study, IgG against lipid peroxidation-derived

adducts are evident during the progression of NASH caused a methionine/choline deficient (MCD) diet in parallel with the liver recruitment of both $CD4^+$ and $CD8^+$ T-lymphocytes recognizing the same antigens and positively correlate with the severity liver injury. The possible contribution of such immune responses to the progression of experimental NASH is further substantiated by the observation that stimulating immune responses against MDA-protein adducts, one of the antigens recognized by the antibodies associated with both human and rodent NASH, promotes parenchymal injury and inflammation in mice fed with the MCD diet. Our data are not in contrast with a recent report Bieghs and co-workers showing that IgM targeting oxidized low density lipoproteins (LDLs) reduces NASH in LDL receptor-deficient mice receiving a high-fat/cholesterol diet [18]. These discrepancies, in fact, can be explained considering that in the two experimental settings the immune responses involved and the mechanisms leading to NASH are quite different. In Bieghs's work mice were immunized with heat-inactivated pneumococci that lead to the production of natural IgM against bacterial antigens and cross-react with oxidized phosphatidylcholine in LDLs [18]. Feeding a high-fat/cholesterol diet to LDL receptor-deficient mice causes Kupffer cell engulfment by oxidized LDLs that, in turn, promotes Kupffer cell activation and hepatic inflammation [28]. In this scenario, IgM interaction with oxidized LDLs reduces their uptake by Kupffer cells, lowering the pro-inflammatory stimuli [19]. These conditions are quite different from those occurring in MCD-induced NASH, where parenchymal injury, oxidative stress and inflammation result from the impairment of hepatocyte lipid secretion [13]. Furthermore, our data indicate that the immunization with MDA-adducts mainly stimulates IgG production and T-cell responses and that these latter are responsible for stimulating inflammation.

Concerning the mechanisms by which adaptive immunity promotes the evolution of NASH, we have observed that a stimulation in liver IFN-γ production and CD40L (CD154) expression parallels with the increase of hepatic $CD4^+$ T-cells in MCD-fed immunized mice. CD40L is a co-stimulatory molecule predominantly expressed by $CD4^+$ T-cells and activated platelets that, by the interacting with its receptor CD40 on macrophages and lymphocytes, has a key role in orchestrating inflammation and immunity in several diseases, including atherosclerosis and obesity [29,30]. Conversely, $CD4^+$ T-cell depletion prevents the up-regulation of IFN-γ and ameliorates lobular inflammation, indicating that a Th-1 activation of $CD4^+$ T-lymphocytes plays a major role in promoting NASH. A Th-1 activation is also a feature of $CD4^+$ T-cell responses to LDL oxidation antigens in atherosclerotic plaques [29]. Interestingly, an increase in circulating IFN-γ-producing $CD4^+$ T-cells has been observed in both paediatric and adult

NASH patients in conjunction with an enhanced liver IFN-γ expression [31,32], suggesting the possible relevance of these mechanisms to the human disease. A recent report indicates that an increase in hepatic $CD8^+$ T-cells characterizes paediatric NASH [31]. In our hands, $CD8^+$ T-cell recruitment is also evident in NASH livers and is further promoted by pre-immunization. However, pre-immunization does no affect the expression $CD8^+$ T-cell activation markers, suggesting that in this experimental setting effector T-cells do not significantly contribute to hepatic inflammation. Nonetheless, the involvement of $CD8^+$ T-cells in NASH requires further investigations. In a similar manner, more studies are needed to clarify the role of B-cell responses. The presence of circulating IgG might just be a hallmark of immune activation against oxidative stress derived epitopes, as 35% of the patients with alcoholic liver disease showing anti-MDA antibodies also have circulating $CD4^+$ T-lymphocytes responsive to the same antigens [33]. However, it can be excluded that B-cell responses can influence the disease evolution, since growing evidence indicates that they can either stimulate or prevent the progression of liver injury to fibrosis [34,35].

Accumulating evidence indicates that NKT cells can orchestrate inflammation in autoimmune liver diseases and modulate hepatic fibrogenesis [36,37]. In line with these observations, recent data point to an involvement of NKT cells in NASH. Indeed, steatosis and the early phases of steatohepatitis are characterized by the lowering of liver NKT pool as consequence of IL-12 production and Tim-3/galectin-9 signaling [20-22]. Conversely, NKT expansion is a feature of advanced NASH in both humans and rodents [23,38,39]. In these latter, NKT depletion prevents hepatic inflammation and fibrosis [23,38]. We observed that an increase in NKT cells characterizes the enhanced severity of NASH in immunized MCD-fed mice, as opposed to NKT cell depletion present in similarly treated naïve animals, further supporting the contribution of NKT cells to NASH progression. Changes in the hepatic levels of IL-15 have been proposed to modulate NKT pool in NASH [20,22]. IL-15 is a pleiotropic cytokine responsible for macrophage, T, NK and NKT cell survival and maturation [40]. In healthy livers, IL-15 is constitutively produced by hepatocytes to create a T-cell favorable environment [41], while an increased IL-15 expression by both hepatocytes and macrophages in response to injury is critical for driving both innate and adaptive immunity [22,42]. We observed that IL-15 is selectively up-regulated in immunized, but not in naïve MCD-fed mice concomitantly with NKT cell recruitment, suggesting that parenchymal damage and inflammation resulting from Th-1 responses, might promote an IL-15-mediated expansion of NKT cells, which, in turn, can participate to the evolution of NASH.

According to Syn and co-workers, osteopontin (OPN) generated by NKT cells can contribute to fibrosis in NASH [23]. OPN is a Th-1 cytokine produced by both immune and parenchymal cells that modulates both inflammation and tissue healing [43]. Indeed, OPN production by NKT cells drives concanavalin A-induced hepatitis [44], but OPN can also stimulate collagen synthesis by hepatic stellate cells (HSCs) through a TGF-β1-indipendent pathway [45]. An up-regulation in liver OPN is evident in either humans and rodents with advanced NASH [16,23,46], while OPN-deficient A/J mice are protected against steatohepatitis and fibrosis induced by MCD diet feeding [46,47]. In our hands, hepatic OPN content is specifically up-regulated in MCD-fed immunized mice in concomitance with NKT cell recruitment and OPN-expressing NKT cells are increased in the livers of these animals. Moreover, we observed that hepatic macrophages also contribute to OPN production. This is consistent with the capacity of Th-1 cytokines to stimulate OPN synthesis in macrophages [48]. However, we can not exclude that in this setting other liver cells, such as cholangiocytes, might also generate OPN [46]. Differently from that reported by Sahai and co-workers [47] using A/J mice, we did not observe changes in hepatic OPN expression in naïve C57BL/6 mice receiving the MCD diet for 4 weeks. This discrepancy might reflect strain differences in mice susceptibility to steatohepatitis [49] and further support importance of OPN in NASH evolutions. Considering OPN action in stimulating HSC [45], the elevated OPN levels observed in MCD-fed immunized mice might account for the stimulation in collagen deposition that is evident in these animals in spite a high IFN-γ production that should antagonize fibrogenesis.

In conclusion, the results presented indicate that immune responses triggered by oxidative stress-derived antigens contribute to hepatic inflammation in experimental NASH by promoting the Th-1 activation of $CD4^+$ T-lymphocytes. NASH in immunized animals is also associated with an increase in liver NKT cells that likely participate to the disease evolution by generating osteopontin. Altogether, these data support the observations in humans about the possible contribution of adaptive immunity in the mechanisms leading to NAFLD evolution.

Financial support

This work has been supported by grants from the Fondazione Cariplo, Milan (Grant N° 2011-0470) and Italian Ministry of Education (PRIN Grant 2009ARYX4T).

References

1. Lazo M, Clark JM. The epidemiology of nonalcoholic fatty liver disease: a global perspective. Semin Liver Dis. 2008;28:339-350.

2. Marra F, Gastaldelli A, Svegliati-Baroni G, Tell G, Tiribelli C. Molecular basis and mechanisms of progression of non-alcoholic steatohepatitis. Trends Mol Med 2008;14:72-81.

3. Tilg H, Mochen AR. Evolution of inflammation in non-alcoholic fatty liver disease: the multiple parallel hits hypothesis. Hepatol 2010;52:1836-1846.

4. Gambino R, Musso G, Cassader M. Redox balance in the pathogenesis of nonalcoholic fatty liver disease: mechanisms and therapeutic opportunities. Antioxid Redox Signal. 2011;15:1325-1365.

5. Seki S, Kitada T, Yamada T, Sakaguchi H, Nakatani K, Wakasa K. In situ detection of lipid peroxidation and oxidative DNA damage in non-alcoholic fatty liver disease. J Hepatol 2002;37:56-62.

6. Chalasani N, Deeg MA Crabb DW. Systemic lipid peroxidation and its metabolic and dietary correlates in patients with non-alcoholic steatohepatitis. Am J Gastroenterol 2004;99:1497-14502.

7. Miller YI, Choi SH, Weisner P, Fang L, Harkewicz R, Hartvigsen K, Boillier A, et al. Oxidation-specific epitopes are danger-associated molecular patterns recognized by pattern recognition receptors of innate immunity. Circ Res 2011;108:235-248.

8. Weismann D, Binder CJ. The innate immune response to products of phospholipid peroxidation. Biochim Biophys acta 2012;1818:2465-2475.

9. Palinski W, Witztum JL. Immune response to oxidative neoepitopes on LDL and phospholipids modulate the development of atherosclerosis. J Int Med 2000;247:171-180.

10. Kurien BT, Scofield RH. Autoimmunity and oxidatively modified antigens. Autoimmun Rev 2008;7:567-573.

11. Nobili V, Parola M, Alisi A, Marra F, Piemonte F, Mombello C, Sutti S, et al. Oxidative stress parameters in paediatric non-alcoholic fatty liver disease. Int J Molec Med 2010;26:471-476.

12. Albano E, Mottaran E, Vidali M, Reale E, Saksena S, Occhino D, Burt AD, et al. Immune response toward lipid peroxidation products as a predictor of the progression of non-alcoholic fatty liver disease (NAFLD) to advanced fibrosis. Gut 2005;54:987-993.

13. Larter CZ, Yeh MM. Animal model of NASH: getting both pathology and metabolic contest right. J. Gastroenterol. Hepatol. 2008;23:1635-1648.

14. Rolla R, Vidali M, Serino R, Pergolini P, Albano E, Bellomo G. Antibodies against oxidized phospholipids in laboratory tests exploring lupus anti-coagulant activity. Clin Exp Immunol. 2007;149:63-69,

15. Kleiner DE, Brunt EM, Van Natta M, Behling C, Contos MJ, Cummings OW, Ferrell LD, et al. Nonalcoholic Steatohepatitis Clinical Research Network. Design and validation of a histological scoring system for nonalcoholic fatty liver disease. Hepatol. 2005;41:1313-1321.

16. Locatelli I, Sutti S, Vacchiano M, Bozzola C, Albano E. NF-kB1 deficiency stimulates the progression of nonalcoholic steatohepatitis (NASH) in mice by promoting NKT-mediated responses. Clin Sci (Lond). 2013;124:279-287.

17. Nomura LE, Walker JM, Maecker HT. Optimization of whole blood antigen specific cytokine assay for $CD4^+$ T cells. Cytometry 2000;40:60-68.

18. Bieghs V, van Gorp PJ, Walenbergh SM, Gijbels MJ, Verheyen F, Buurman WA, Briles DE, et al. Specific immunization strategies against oxidized low-density lipoprotein: a novel way to reduce nonalcoholic steatohepatitis in mice. Hepatol. 2012;56:894-903.

19. Suttles J, Stout RD. Macrophage CD40 signaling: A pivotal regulator of disease protection and pathogenesis. Sem Immunol 2009;21:257-264.

20. Li Z, Soloski MK, Diehl AM. Dietary factors alter hepatic innate immune system in mice with nonalcoholic fatty liver disease. Hepatol. 2005;42:880-885.

21. Kremer M, Thomas E, Milton RJ, Perry AW, van Rooijen N, Wheeler MD, Zacks S, et al. Kupffer cell and interleukin-12-dependent loss of natural killer T cells in hepatosteatosis. Hepatol. 2010;51,130-141.

22. Tang ZH, Liang S, Potter J, Jiang X, Mao HQ, Li Z. Tim-3/galectin-9 regulate the homeostasis of hepatic NKT cells in a murine model of nonalcoholic Fatty liver disease. J Immunol. 2013;190:1788-1796.

23. Syn WK, Agboola KM, Swiderska M, Michelotti GA, Liaskou E, Pang H, Xie G, et al. NKT-associated hedgehog and osteopontin drive fibrogenesis in non-alcoholic fatty liver disease. Gut 2012;61:1323-1329.

24. Kaminski D, Randall TD. Adaptive immunity and adipose tissue biology. Trends Immunol 2010;31:384-390.

25. Chatzigeorgiou A, Karalis KP, Bornstein SR, Chavakis T. Lymphocytes in obesity-related adipose tissue inflammation. Diabetol 2012;55:2583-2592.

26. Brunt EM, Pathology of non-alcoholic fatty liver disease. Nat Rev Gastroenterol Hepatol 2010; 7:195-203.

27. Baumgardner JN, Shankar K, Hennings L, Albano E, Badger TM, Ronis MJJ. N-acethylcysteine attenuates progression of liver pathology in a rat model of non-alcoholic steatohepatitis. J Nutr 2008;138:1872-1879.

28. Walenbergh SM, Koek GH, Bieghs V, Shiri-Sverdlov R. Non-alcoholic steatohepatitis: The role of oxidized low-density lipoproteins. J Hepatol. 2013;58:801-810. doi:10.1016/j.jhep.2012.11.014.

29. Hansson GK, Libby P. The immune response in atherosclerosis: a double-edged sword. Nature Rev Immunol 2006;6:508-519.

30. Poggi M, Engel D, Christ A, Beckers L, Wijnands E, Boon L, Driessen A, et al. CD40L deficiency ameliorates adipose tissue inflammation and metabolic manifestations of obesity in mice. Arterioscler Thromb Vasc Biol. 2011;31:2251-2260.

31. Inzaugarat ME, Ferreyra Solari NE, Billordo LA, Abecasis R, Gadano AC, Cherñavsky AC. Altered phenotype and functionality of circulating immune cells characterize adult patients with nonalcoholic steatohepatitis. J Clin Immunol. 2011;31:1120-1130.

32. Ferreyra Solari NE, Inzaugarat ME, Baz P, De Matteo E, Lezama C, Galoppo M, Galoppo C, et al. The role of innate cells is coupled to a Th1-polarized immune response in pediatric nonalcoholic steatohepatitis. J Clin Immunol. 2012;32:611-621.

33. Stewart SF, Vidali M, Day CP, Albano E, Jones DEJ. Oxidative stress as a trigger for cellular immune response in patients with alcoholic liver disease. Hepatol. 2004;39:197-203.

34. Novobrantseva TI, Majeau GR, Amatucci A, Kogan S, Brenner I, Casola S, Shlomchik MJ, et al. Attenuated liver fibrosis in the absence of B cells. J Clin Invest. 2005;115:3072-3082.

35. Dhirapong A, Lleo A, Yang GX, Tsuneyama K, Dunn R, Kehry M, Packard TA, et al. B cell depletion therapy exacerbates murine primary biliary cirrhosis. Hepatol. 2011;53:527-535.

36. Santodomingo-Garzon T, Swain MG. Role of NKT cells in autoimmune liver disease Autoimmunity Rev 2011;10:793-800.

37. Gao B, Radaeva S. Natural killer and natural killer T cells in liver fibrosis. Biochim Biophys Acta 2012 doi 10.1016/j.bbadis.2012.09.008

38. Syn WK, Oo YH, Pereira TA, Karaca GF, Jung Y, Omenetti A, Witek RP, et al. Accumulation of natural killer T cells in progressive non-alcoholic fatty liver disease. Hepatol. 2010;51:1998-2007.

39. Tajiri K, Shimizu Y, Tsuneyama K, Sugiyama T. Role of liver-infiltrating $CD3^{+}CD56^{+}$ natural killer T cells in the pathogenesis of nonalcoholic fatty liver disease. Eur J Gastroenterol. Hepatol. 2009;21:673-680.

40. Di Sabatino A, Calarota SA, Vidali F, MacDonald TT, Corazza GR. Role of IL-15 in immune and infectious diseases. Cytokine Growth Factor Rev 2011;22:19-33

41. Correia MP, Cardoso EM, Pereira CF, Neves R, Uhrberg M, Arosa FA. Hepatocytes and IL-15: a favorable microenvironment for T cell survival and $CD8^{+}$ T cell differentiation. J. Immunol. 2009;182:6149-6159.

42. Suzuki A, McCall S, Choi SS, Sicklick JK, Huang J, Qi Y, Zdanowicz M, et al. Interleukin-15 increases hepatic regenerative activity. J Hepatol. 2006;45:410-418.

43. Uede T. Osteopontin intrinsic tissue regulator of intractable inflammatory disease. Pathol Int 2011;61:265-280.

44. Diao H, Kon S, Iwabuchi K, Kimura C, Morimoto J, Ito D, Segawa T, et al. Osteopontin as a mediator of NKT cell function in T cell-mediated liver diseases. Immunity 2004;21:539-550

45. Urtasun R, Lopategi A, George J, Leung TM, Lu Y, Wang X, Ge X, Fiel MI, Nieto N. Osteopontin, an oxidant stress-sensitive cytokine, up-regulates collagen-I via integrin α(V)β(3) engagement and PI3K-pAkt-NFκB signaling. Hepatol. 2012;55:594-608.

46. Syn WK, Choi SS, Liaskou E, Karaca GF, Agboola KM, Oo YH, Mi Z, et al. Osteopontin is induced by hedgehog pathway activation and promotes fibrosis progression in nonalcoholic steatohepatitis. Hepatol. 2011;53:106-115.

47. Sahai A, Malladi P, Melin-Aldana H, Green RM, Whitington PF. Upregulation of osteopontin expression is involved in the development of nonalcoholic steatohepatitis in a dietary murine model. Am. J. Physiol. Gastrointest. Liver Physiol. 2004;287:G264-G273.

48. Ritting SR. Osteopontin in macrophage functions. Exp Rev Mol Med 2011;13:e15 doi:10.1017/S1462399411001839.

49. Rangnekar AS, Lammert F, Igolnikov A, Green RM. Quantitative trait loci analysis of mice administered the methionine-choline deficient dietary model of experimental steatohepatitis. Liver Internat. 2006;26:1000-1005.

Figures

Figure 1: Adaptive immune responses against oxidative stress-derived antigens during the progression of NASH induced by a methionine-choline deficient (MCD) diet.

Panels A-C: Liver oxidative stress, as evaluated by thiobarbituric acid reactive compounds (TBARs), and circulating IgG against malondialdehyde- (MDA) or 4-hydroxynonenal (4-HNE) modified bovine serum albumin were measured in control mice (empty bars) or mice fed with the MCD diet for 4 (light grey bars) and 8 (dark grey bars) weeks. The IgG values are expresses as optical density at 490 nm. The results refer to 8-10 animals in each group and the boxes include the values within 25th and 75th percentile, while the horizontal bars represent the medians. The extremities of the vertical bars (10th-90th percentile) comprise the eighty percent of the values. Panels D,E: Flow cytometry analysis of liver monucleated cells isolated from controls (Cont) or MCD-fed mice: representative dot blots of T-lymphocyte staining for CD45 and CD3 and percent distribution of total CD3$^+$, CD8$^+$ or CD4$^+$ T-cells. The values refer to 4-5 animals in each group and the bars represent medians ± S.D. Panels F,G: T-lymphocyte activation in NASH was assessed in intrahepatic CD3$^+$ T-cells isolated from mice receiving the MCD diet for 8 weeks by evaluating the expression of CD69 as well as in CD4$^+$ T-cells by interferon-γ (IFN-γ) production. Panel H: The contribution of oxidative stress-derived antigens in promoting T-cell responses in NASH was evaluated in intrahepatic CD4$^+$ and CD8$^+$ T-cells obtained from control and MCD-fed (8 weeks) mice by measuring intracellular IL-2 production following in vitro incubation with 10µg/mL of MDA-modified murine albumin.

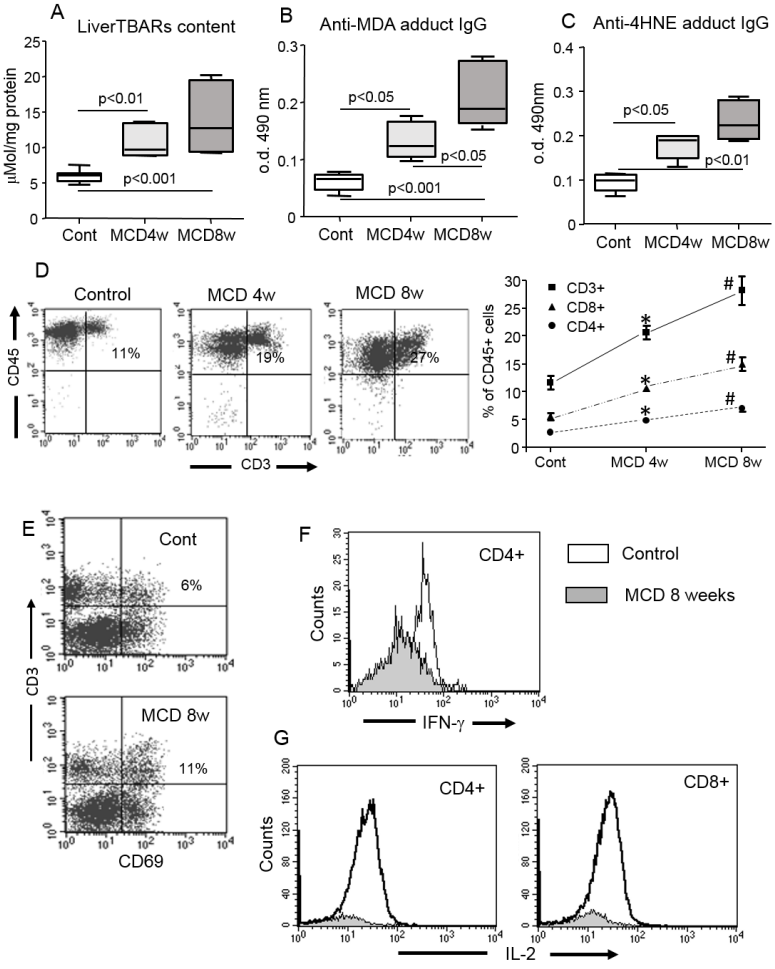

Figure 1

Figure 2: The induction of immune responses against oxidative stress-derived antigens worsens liver injury and inflammation in C57BL/6 mice with NASH induced by feeding a methionine-choline deficient (MCD) diet.

C57BL/6 mice were immunized with MDA-modified bovine serum albumin (MDA-BSA) in incomplete Freund's adjuvant before 4 weeks feeding with the MCD diet. Panels A-D: The differences in NASH severity were assessed by alanine aminotransferase (ALT) release, hepatic triglyceride content and liver mRNA levels for TNF-α, CCL2. The experimental groups were: naïve controls (Cont), naïve MCD-fed mice (MCD), mice pretreated with the incomplete Freund's adjuvant and receiving the MCD diet (Ad+MCD), mice receiving the complete immunization protocol plus the MCD diet (Imm-MCD). Panel E: Circulating TNF-α levels were determined in the same animals. Panels F,G: Effect of the stimulation of immune responses on liver mRNA levels for macrophage M1 activation markers IL-12p40 and iNOS in MCD-fed mice. Hepatic mRNAs were measured by RT-PCR and expressed as fold increase over control values after normalization to the β-actin gene expression. The values refer to 8-12 animals in each group and the boxes include the values within 25th and 75th percentile, while the horizontal bars represent the medians. The extremities of the vertical bars (10th-90th percentile) comprise the eighty percent of the values.

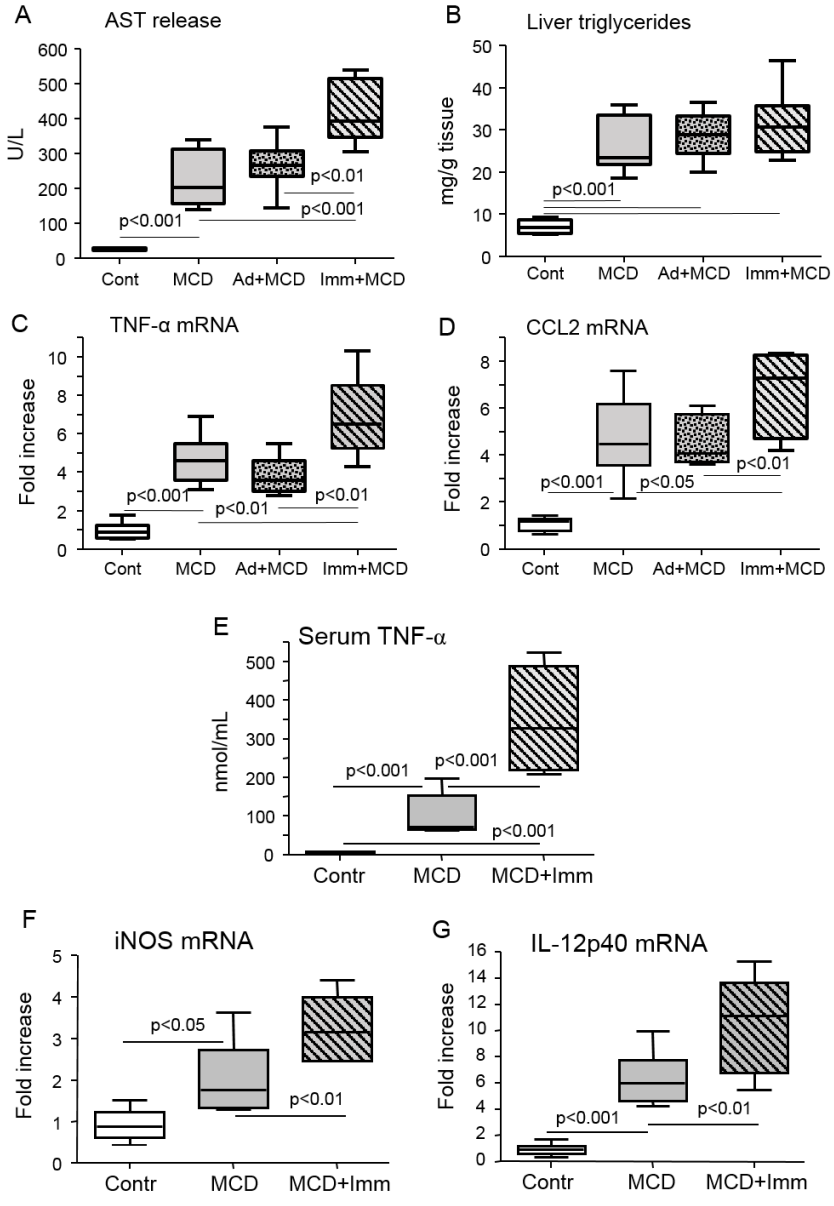

Figure 2

Figure 3: The induction of immune responses against oxidative stress-derived antigens promotes steato-hepatitis and fibrosis in mice fed a methionine-choline deficient (MCD) diet.

C57BL/6 mice were immunized with MDA-modified bovine serum albumin (MDA-BSA) in incomplete Freund's adjuvant before 4 weeks feeding with the MCD diet. Panels A-E: Liver histology was evaluated in hematoxilin/eosin stained sections from naïve (MCD) or pre-immunized (Imm-MCD) MCD-fed animals (magnification 400x). Lobular inflammation was scored according to Kleiner et al. [15] while the number of necro-inflammatory foci and apoptotic hepatocytes were counted in ten different high magnification microscopic fields. Panels F-I: Collagen deposition (Panels F,G) and activated hepatic stellated cells expressing α-smooth muscle actin (α-SMA) (Panels H,I) were evidenced by, respectively, Sirius Red staining or immunohistochemistry.

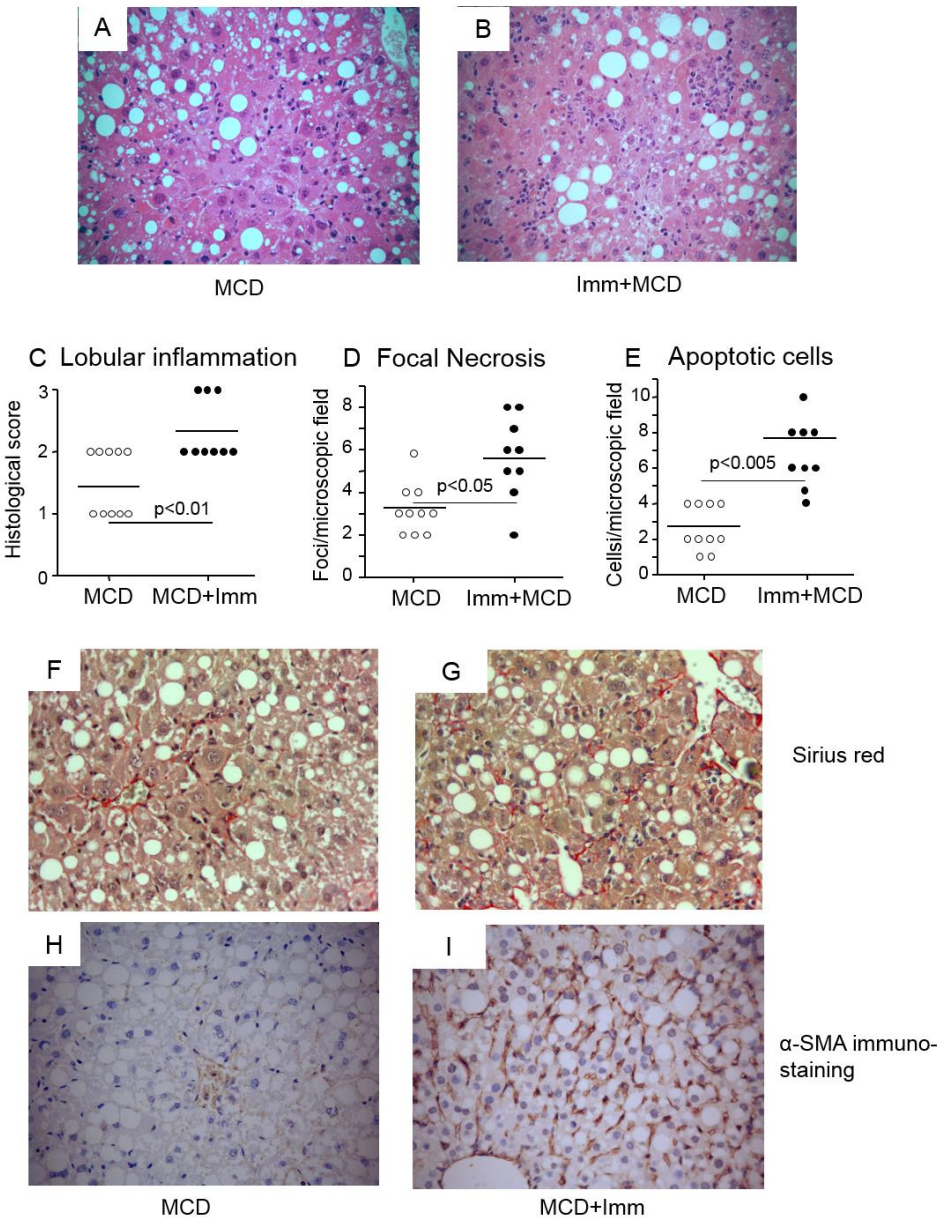

Figure 3

Figure 4: The immune responses against oxidative stress-derived antigens promote the liver recruitment of T-lymphocytes and Th-1 responses.

Liver monucleated cells were isolated from the livers of either naive controls (Cont), naïve mice fed 4 weeks a methionine-choline deficient (MCD) diet or mice pre-immunized with MDA-modified bovine serum albumin before the administration of the MCD diet (Imm-MCD). Panels A-D show representative dot blots of T-lymphocytes staining for CD45 and CD3 and the percent distribution of total $CD3^+$ and $CD8^+$ or $CD4^+$ T-cells sub-sets. The values refer to 5-6 animals in each group and the bars represent medians ± S.D. Panel E: Representative dot blots of $CD8^+$ T-cells displaying the CD107b activation marker. Panels F-J: Th-1 activation of $CD4^+$ T-cells was evidenced by the intrahepatic production of interferon-γ (IFN-γ) and the mRNA expression of the Th-1 trascription factor T-bet, CD40 and CD40 ligand (CD154). The RT-PCR values were normalized to those of the β-actin gene and presented as fold increase over control values. The data refer to 8-12 animals in each group and the boxes include the values within 25^{th} and 75^{th} percentile, while the horizontal bars represent the medians. The extremities of the vertical bars (10^{th}-90^{th} percentile) comprise the eighty percent of the values.

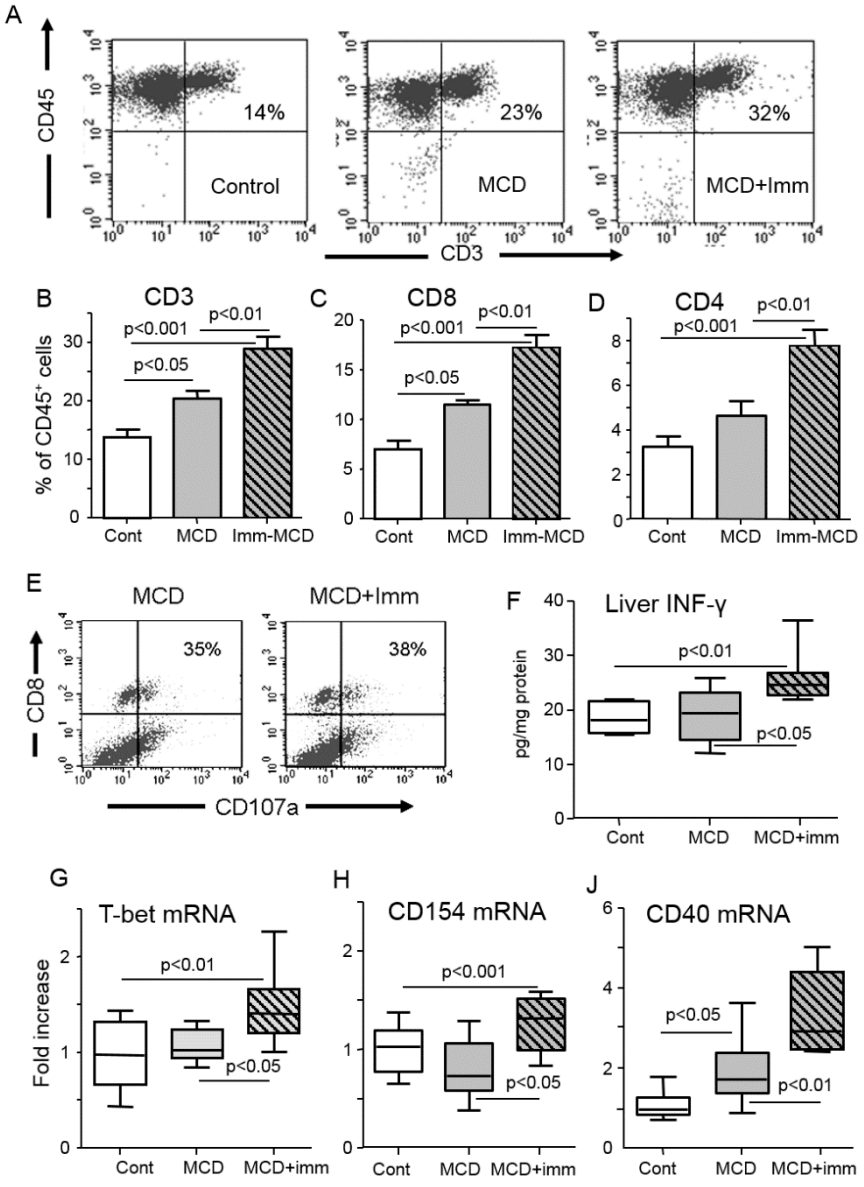

Figure 4

Figure 5: CD4⁺ T-lymphocyte depletion improves hepatic inflammation in MDA-BSA immunized mice receiving the MCD diet.

After immunization with MDA-modified bovine serum albumin (MDA-BSA) C57BL/6 mice were depleted of $CD4^+$ T-cells by repeated injection of an anti-CD4 monoclonal antibody during 4 weeks feeding with the MCD diet. Panels A-D: Liver histology was evaluated in hematoxilin/eosin stained sections from mice receiving anti-CD4 IgG or vehicle (magnification 400x). Lobular inflammation was scored according to Kleiner et al. [15] while the number of necro-inflammatory foci were counted in ten different high magnification microscopic fields. Panels E-I: Effect of $CD4^+$ T-cell depletion on the hepatic expression of interferon-γ (IFN-γ), CD40 ligand (CD154), IL-15 and macrophage M1 activation markers (IL-12p40, iNOS). The mRNA levels were measured by RT-PCR and expressed as fold increase over control values after normalization to the β-actin gene expression. The values refer to 6 animals in each group and the boxes include the values within 25^{th} and 75^{th} percentile, while the horizontal bars represent the medians. The extremities of the vertical bars (10^{th}-90^{th} percentile) comprise the eighty percent of the values.

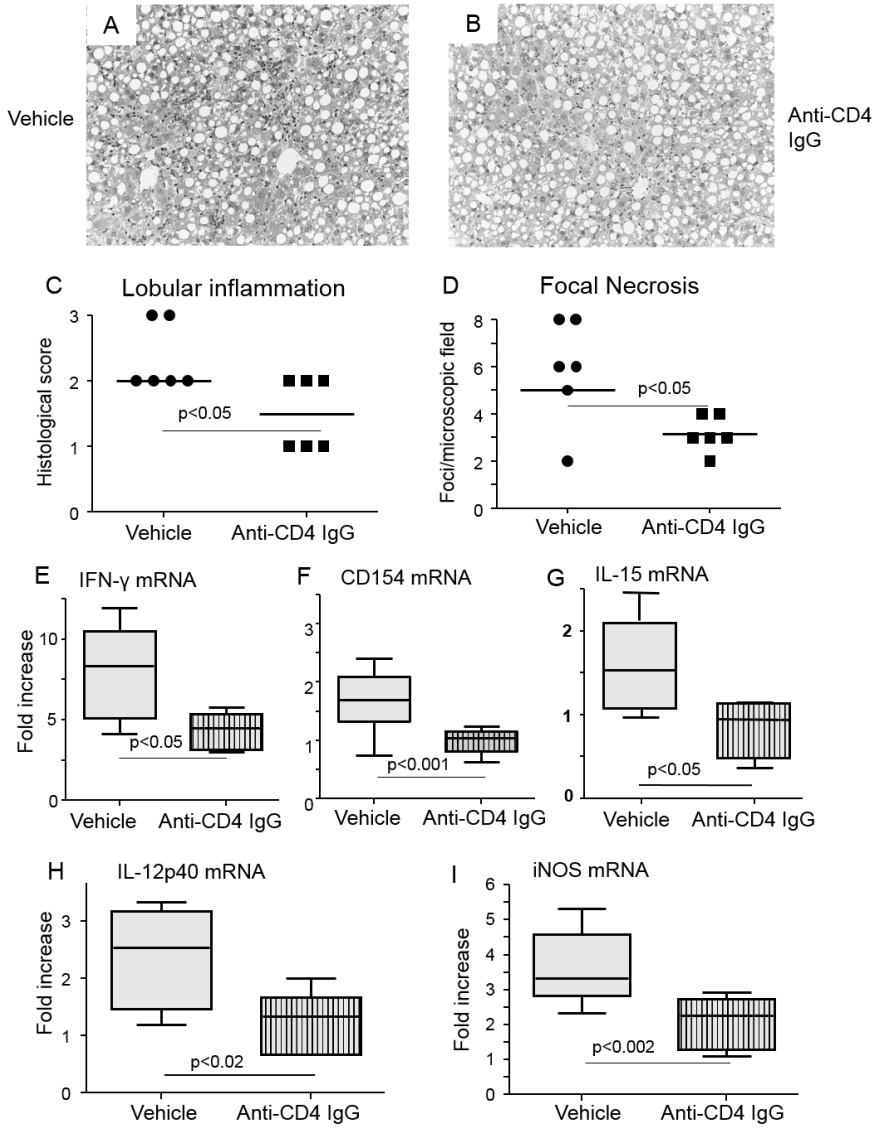

Figure 5

Figure 6: Increased severity of NASH in immunized mice associates with the recruitment and activation of hepatic NKT cells.

Liver monucleated cells were isolated from the livers of either naive controls (Cont), naïve mice fed 4 weeks a methionine-choline deficient (MCD) diet or mice pre-immunized with MDA-modified bovine serum albumin before the administration of the MCD diet (Imm-MCD). Panels A-C show representative dot blots of CD3 and NK1.1 staining and the percent distribution of total $CD3^-$ $NK1.1^+$ NK and $CD3^+$ or $NK1.1^+$ NKT-cells sub-sets. The values refer to 5-6 animals in each group and the bars represent medians ± S.D. Panels D,E: The intrahepatic content of IL-15 and osteopontin were determined by ELISA assays. The data refer to 6-8 animals in each group and the boxes include the values within 25^{th} and 75^{th} percentile, while the horizontal bars represent the medians. The extremities of the vertical bars (10^{th}-90^{th} percentile) comprise the eighty percent of the values. Panels G and F show a representative dot blots of the osteopontin (OPN) expression by $F4/80^+$ hepatic macrophages or $NK1.1^+$ NK/NKT cells.

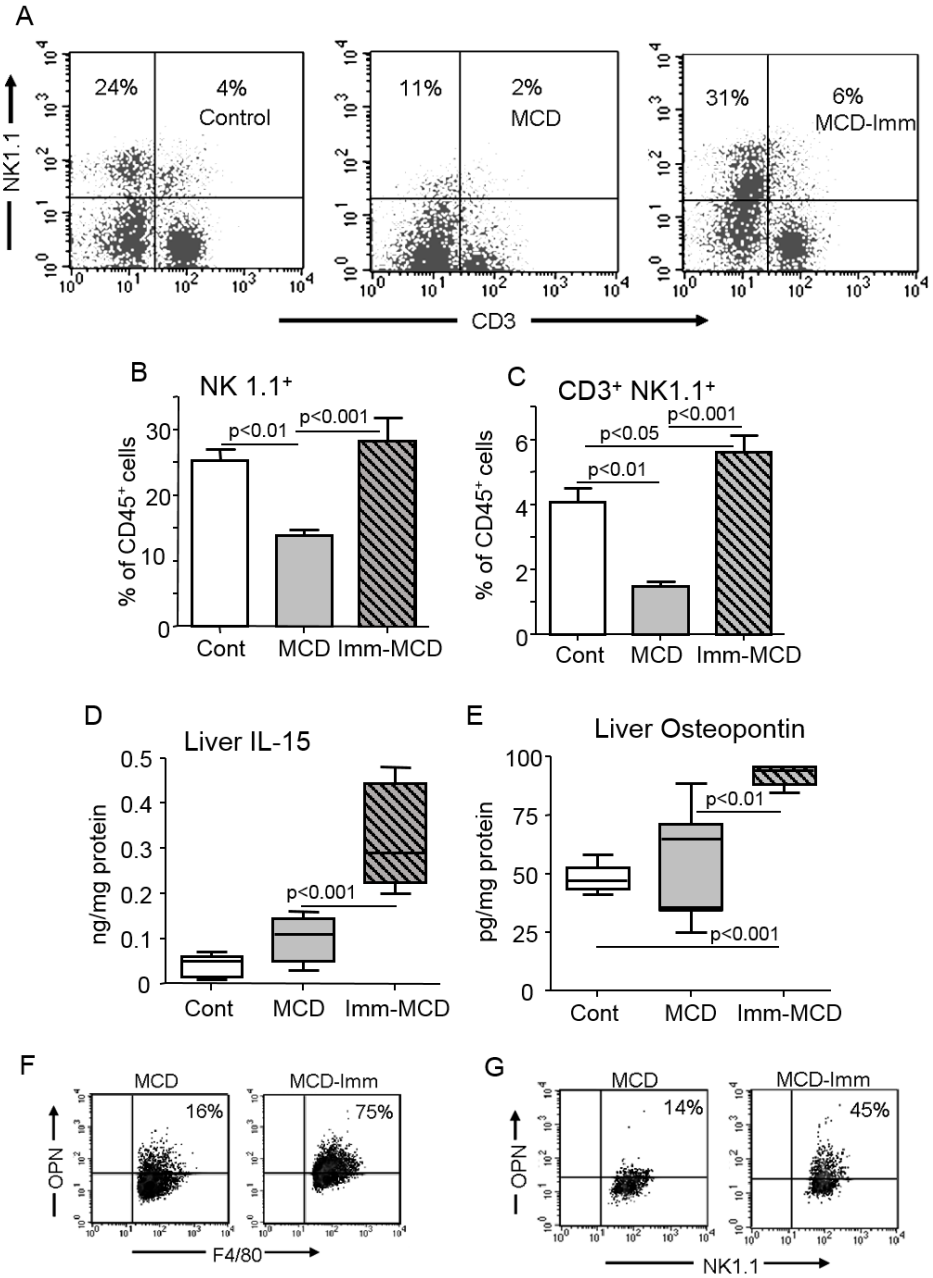

Figure 6

ADAPTIVE IMMUNE RESPONSES TRIGGERED BY OXIDATIVE STRESS CONTRIBUTE TO HEPATIC INFLAMMATION IN NASH

Salvatore Sutti, Aastha Jindal, Irene Locatelli, Marco Vacchiano, Luca Giliotti, Cristina Bozzola,
Emanuele Albano.

Supplementary Materials

Addendum to Materials and Methods

Composition of the methionine-choline deficient (MCD) diet used in the experiments
The MCD diet composition (mg/kg) was as follows: sucrose 455, corn starch 200, corn oil 100, cellulose 30, mineral mix 35, calcium phosphate 3, vitamin mix 5, Vit A 40, Vit D3 5, Vit E 121, aminoacid mix 171.

Induction of hepatic $CD4^+$ T cell depletion: For CD4 T-cell depletion mice were injected IP daily 3 times with 400μg of rat anti-$CD4^+$ monoclonal antibody GK1.5 at the start of MDC feeding and further treated twice a week during the following 3 weeks. According to Arora et al. (Infect Immun 2006:74:4339-4348), by depleting $CD4^+$ T cells, the monoclonal GK1.5 antibody would make the mice tolerant against the immunization versus rat IgG. Thus, the use as a control of isotype-matched rat IgG is inappropriate, because it would lead to a mouse anti-rat IgG response resulting in immunocomplexe formation and stimulation of inflammation. Therefore, control mice received saline injection.
Biochemical analysis. Plasma ALT and liver triglyceride were determined by spectrometric kits supplied by Radim S.p.A. (Pomezia, Italy) and Sigma Diagnostics (Milano, Italy), respectively. Oxidative stress was evaluated in liver homogenates by thiobarbituric acid-reactive substances according to Ohkawa et al. (Anal Biochem 1979;95:351-358) and protein carbonyl determination (Oxyblot kit, Merck-Millipore, Milano, Italy). Circulating TNF-α and liver IFN-γ, IL-15 and osteopontin levels were evaluated by commercial ELISA kits supplied by Peprotech (Milano, Italy) and R&D Systems (Abingdon, UK).

Supplementary figures

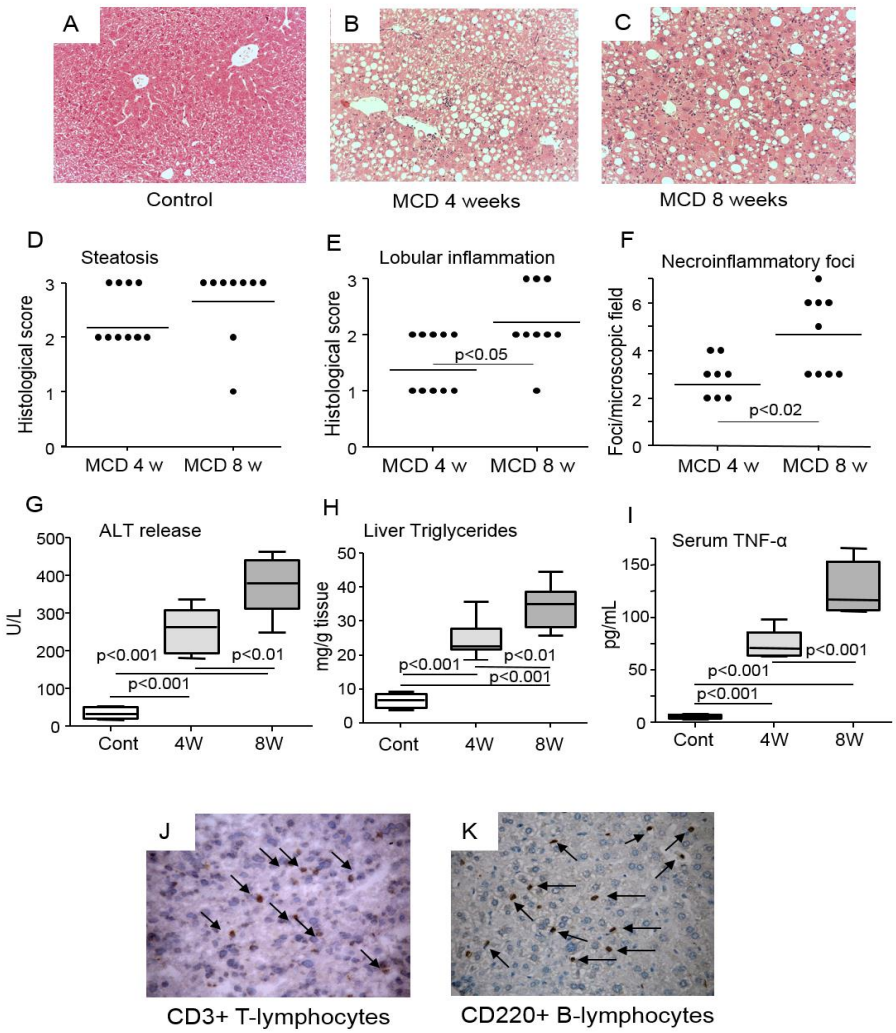

Supplementary Fig 1

Supplementary Figure 1: Time-dependent increase in the severity of steatohepatitis in C57BL/6 mice fed a methionine-choline deficient (MCD) diet.

Panels A-E: Liver histology was evaluated in hematoxilin/eosin stained sections from naïve (MCD) or pre-immunized (Imm-MCD) MCD-fed animals (magnification 400x). Hepatic steatosis and lobular inflammation were scored according to Kleiner et al. [15], while the number of necro-inflammatory foci were counted in ten different high magnification microscopic fields.

Panels F-H: Alanine aminotransferase (ALT) release, liver triglyceride content and circulating TNF-α levels were evaluated in control (Cont) or MCD-fed (MCD) mice receiving the diet for 4 and 8 weeks. The data refer to 8-10 animals in each group and the boxes include the values within 25th and 75th percentile, while the horizontal bars represent the medians. Eighty percent of the values are comprised between the extremes of the vertical bars (10th-90th percentile).

Panels I,J show liver T- and B-lymphocytes (arrows) as evidenced by immunohistochemistry using antibodies against mouse CD3 and B220, respectively.

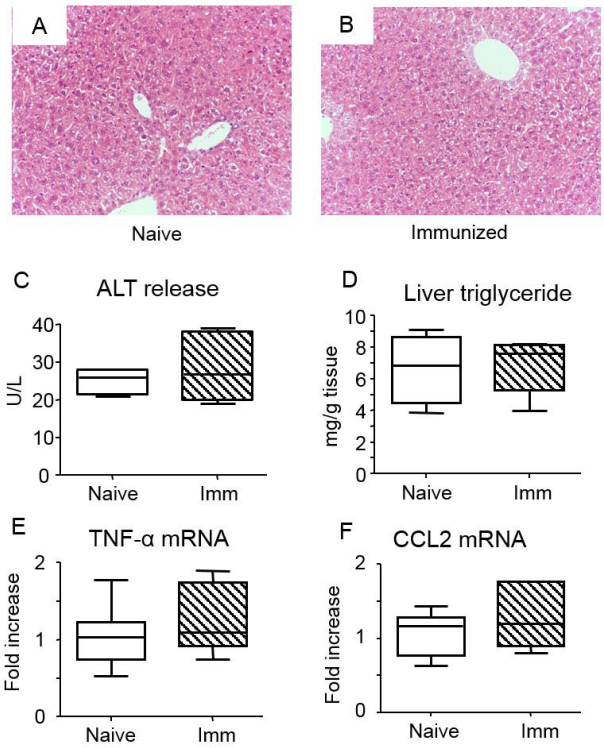

Supplementary Fig 2

Supplementary Figure 2: Induction of immune responses against oxidative stress-derived antigens does not cause liver injury in mice receiving a control diet.

C57BL/6 mice were immunized with MDA-modified bovine serum albumin (MDA-BSA) in incomplete Freund's adjuvant before the administration of a control diet for 4 weeks. Panels A,B shows liver histology (hematoxilin/eosin stained sections magnification 200x). Alanine aminotransferase (ALT) release (Panel C), liver triglyceride content (Panel D) and the hepatic mRNA expression of TNF-α and CCL2 (Panels E,F) were evaluated in naïve (Cont) or pre-immunized (Imm) animals. The RT-PCR values were normalized to those of the β-actin gene and presented as fold increase over control values. The data refer to 6-8 animals in each group and the boxes include the values within 25th and 75th percentile, while the horizontal bars represent the medians. Eighty percent of the values are comprised between the extremes of the vertical bars (10th-90th percentile).

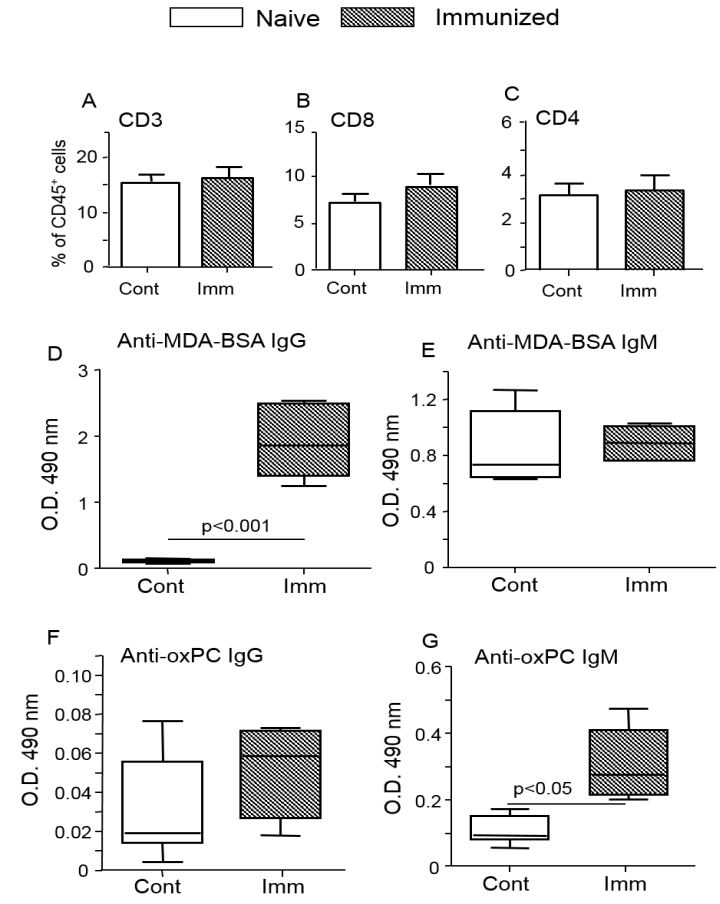

Supplementary Fig 3

Supplementary Figure 3: Effects of mice immunization against MDA-derived antigens on liver lymphocytes and humoral immune responses.

C57BL/6 mice were immunized with MDA-modified bovine serum albumin (MDA-BSA) in incomplete Freund's adjuvant. Liver monucleated cells were isolated from either naive (Cont) or pre-immunized (Imm) mice fed a control diet and the percentage distribution of total $CD3^+$, $CD8^+$ or $CD4^+$ T-cells was evaluated by flow cytometry (Panels A-C). The values refer to 4 animals in each group and the bars represent medians ± S.D. Circulating IgG and IgM against malondialdehyde-modified bovine serum albumin (MDA-BSA) or oxidized phosphatidylcholine (ox-PC) were measured by ELISA in the serum of control (empty bars) or immunized animals (hatched bars) and the values are expresses as optical density at 490 nm. (Panels D-G). The values refer to 5-6 animals the boxes include the values within 25^{th} and 75^{th} percentile, while the horizontal bars represent the medians. Eighty percent of the values are comprised between the extremes of the vertical bars (10^{th}-90^{th} percentile).

7. Paper 2

CX3CR1-expressing inflammatory dendritic cells contribute to the progression of non-alcoholic steatohepatitis (NASH) in mice

Submitted to Clinical Sciences (January 2015)

Background & Aims: Liver dendritic cells (DCs) are a heterogeneous population of specialized bone marrow-derived cells involved in antigen presentation to lymphocytes. In healthy livers DCs have a predominant tolerogenic phenotype, but recent evidence suggests their possible contribution in the evolution of chronic liver diseases. In this study, we have investigated the role of monocyte-derived inflammatory dendritic cells (moDCs) in experimental NASH induced by feeding mice with a methionine-choline deficient (MCD) diet.

Results: The progression of steatohepatitis was characterized by an increase in hepatic mononuclear cells displaying the monocyte/macrophage markers F4-80, Ly6C and CD11b in combination with the fractalkine receptor (CX_3CR1). These cells were characterized by the expression of dendritic cell (CD11c, MHCII) markers as well as by a sustained TNF-α production, suggesting monocyte differentiation to inflammatory moDCs. Treating 4 weeks MCD-fed mice with the H_2S donor NaHS that interferes with CX_3CL1/CX_3CR1 up-regulation in monocyte-derived cells, blocked the increase in liver CX_3CL1 and CX_3CR1 and selectively prevented the accumulation of TNF-α-producing CX_3CR1^+-moDCs without interfering with macrophage functions. Furthermore, NaHS reduced hepatic and circulating TNF-α levels and ameliorated transaminase release and parenchymal injury.

Conclusions: Altogether, these results show that inflammatory CX_3CR1^+-moDCs contributed in sustaining inflammation and liver injury by TNF-α production during NASH progression. Inhibition of CX_3CR1 through H_2S interference prevents differentiation of moDCs and related inflammation, suggesting CX_3CR1^+ interference as possible approach to NASH therapy.

CX_3CR1-EXPRESSING INFLAMMATORY DENDRITIC CELLS CONTRIBUTE TO THE PROGRESSION OF STEATOHEPATITIS

Salvatore Sutti[§], Irene Locatelli[§], Stefania Bruzzì, Aastha Jindal, Marco Vacchiano, Cristina Bozzola, Emanuele Albano

Dept. of Health Sciences and Interdisciplinary Research Centre for Autoimmune Diseases, University "Amedeo Avogadro" of East Piedmont, Novara, Italy.

[§] These two authors equally contributed to the work

Running title: Inflammatory dendritic cells in steatohepatitis.

Keywords: Nonalcoholic fatty liver disease, macrophages, dendritic cells, liver fibrosis, chronic inflammation, CX_3CR1.

Words: 2645
Figure 6
Tables 0
References: 40

Corresponding Author:
Prof. Emanuele Albano, Department of Health Science, University "Amedeo Avogadro" of East Piedmont, Via Solaroli 17, 28100 Novara, Italy. Tel. +39 0321 660642 Fax +39 0321 620421; E-mail: emanuele.albano@med.unipmn.it

Abstract

Objectives: Liver monocyte recruitment plays a major role in the development of non-alcoholic steatohepatitis (NASH). However, little is known about the phenotypic changes occurring in monocyte-derived cells during disease evolution. In this study, we have investigated the possible role of monocyte-derived inflammatory dendritic cells (moDCs) in experimental steatohepatitis.

Design: MoDCs were analysed by flow cytometry in the livers of C57BL/6 mice with steatohepatitis induced by feeding a methionine-choline deficient (MCD) diet for up to 8 weeks.

Results: The progression of steatohepatitis was characterized by an increase in hepatic mononuclear cells displaying the monocyte/macrophage marker F4-80$^+$. In the early phases (4 weeks on the MCD diet) Ly6C^{high}/CD11b$^+$/F4-80$^+$ cells were prevalent. However, their frequency did not further grow with the disease progression, when a tenfold expansion of F4-80$^+$/CD11b$^+$ cells expressing the fractalkine receptor (CX_3CR1) was evident. These cells were characterized by the combined expression of monocyte (F4-80, Ly6C) and of dendritic cell (CD11c, MHCII) markers as well as by a sustained TNF-α production, suggesting monocyte differentiation to inflammatory moDCs. Hydrogen sulfide (H_2S) is known to interfere with CX_3CL1/CX_3CR1 up-regulation in monocyte-derived cells. Treating 4 weeks MCD-fed mice with the H_2S donor NaHS while continuing on the same diet, blocked the increase in liver CX_3CL1 and CX_3CR1 and selectively prevented the accumulation of TNF-α-producing CX_3CR1^+-moDCs without interfering with macrophage functions. Furthermore, NaHS reduced hepatic and circulating TNF-α levels and ameliorated transaminase release and parenchymal injury.

Conclusions: Altogether, these results show that inflammatory CX_3CR1^+-moDCs contributed in sustaining inflammation and liver injury during steatohepatitis progression.

Abbreviations:

α-SMA; α-Smooth Muscle Actin, DCs; Dendritic Cells, moDCs; monocyte-derived Dentritic Cells, MCD; Methionine-Choline Deficient diet, NAFLD; NonAlcoholic Fatty Liver Disease, NASH; NonAlcoholic SteatoHepatitis

Introduction

The development of lobular inflammation and parenchymal injury represents the key feature in the transition from non-alcoholic fatty liver disease (NAFLD) to steatohepatitis (NASH) and is clinically relevant because inflammatory mechanisms are the driving forces for the disease evolution to fibrosis/cirrhosis [1]. Circulating free fatty acids, oxidative damages, endoplasmic reticulum stress and adipokine unbalances have been proposed to trigger hepatic inflammation by stimulating Kupffer cell activation [2,3]. Indeed, at the onset of NASH Kupffer cells significantly contribute to the production of pro-inflammatory cyto/chemochines, which, in turn, stimulate the liver infiltration by circulating monocytes [4,5]. These latter rapidly differentiates to M1 polarized macrophages further contributing to the release of pro-inflammatory mediators [6]. Accordingly, Kupffer cell depletion or interference with monocyte recruitment through CCL2/CCR2 signaling prevent hepatic injury and inflammation in experimental models of NASH [4,6,7]. Furthermore, the extent of macrophage M1 responses appears to modulate NASH severity among different mice strains [6]. Recent studies have revealed the existence of at least two distinct monocyte subsets. Inflammatory monocytes are characterized as $Ly6C^{high}/CCR2^{+}/CX3CR1^{-}$ in mice and $CD14^{+}/CD16^{-}$ in humans and migrate to tissues in early phase of the response to injury producing pro-inflammatory mediators [9,10]. A second population defined as $Ly6C^{-}/CCR2^{-}/CX3CR1^{+}$ in mice and $CD14^{-}/CD16^{+}$ in humans has less characterized functions and appears involved in tissue healing [9,10]. Studies using different mice models of chronic liver injury have shown that infiltrating macrophages in injured livers derive from Ly6C/CD11b-expressing circulating monocytes [12,13]. However, the phenotype of the monocyte-derived cells responsible for the evolution of chronic liver diseases, including NASH, are still incompletely characterized [14]. In this study, we have investigated the features of liver infiltrating monocyte-derived cells during the progression of experimental steatohepatitis. To this aim, we used steatohepatitis induced in mice by feeding a methionine-choline deficient (MCD) diet that, in spite differing in its pathogenesis from the human NASH, it allows to follow hepatic chronic inflammation up to the development of overt fibrosis [15].

Material and Methods

Animal and Experimental protocol. Eight weeks old male C57BL/6 mice were purchased from Harlan-Nossan (Corezzana, Italy) and fed for 4 or 8 weeks with either methionine-choline deficient (MCD) or control diets (Laboratorio Dottori Piccioni, Gessate, Italy). In some experiments, 4 weeks MCD-fed mice received NaHS (1mg/kg body wt) daily for further 4 weeks while continuing on their deficient diet. The experimental protocols were approved by the Italian Ministry of Health and by the University Commission for Animal Care following the criteria of the Italian National Research Council.

Biochemical analysis. Plasma ALT and liver triglycerides were determined by spectrometric kits supplied by Radim S.p.A. (Pomezia, Italy) and Sigma Diagnostics (Milano, Italy), respectively. Circulating TNF-α were evaluated by commercial ELISA kits supplied by Peprotech (Milano, Italy).

Histology and immunohistochemistry. Steatosis and lobular inflammation were scored blind according to Kleiner et al. [16] in hematoxilin/eosin stained liver sections. Hepatocyte apoptosis was detected by terminal deoxyribonucleotide transferase-mediated dUTP nick-end labeling (TUNEL) as reported in [17]. Collagen deposition was evidenced by Picro-Sirius Red staining. Liver macrophages and activated hepatic stellate cells were evidenced in formalin-fixed sections using, respectively, anti-mouse F4-80 (eBioscience, San Diego CA, USA) and α-smooth muscle actin (α-SMA) polyclonal antibodies (Labvision, Bio-Optica, Milan, Italy) in combination with horse-radish peroxidase polymer kit (Biocare Medical, Concord, CA, USA).

mRNA extraction and Real time PCR. Liver RNA was retro-transcripted with High Capacity cDNA Reverse Transcription Kit (Applied Biosystems Italia, Monza, Italy). RT-PCR was performed in a Techne TC-312 termalcycler (TecneInc, Burlington NJ, USA) using TaqMan Gene Expression Master Mix and TaqMan Gene Expression probes for mouse TNF-α, IL-12p40, CD11b, iNOS, CX_3CL1, CX_3CR1 α1-procollagen, TGF-β1, α-SMA and beta-actin (Applied Biosystems Italia, Monza, Italy). All samples were run in duplicate and the relative gene expression calculated as $2^{-\Delta Ct}$ was expressed as fold increase over control samples.

Intrahepatic mononucleated cell isolation and flow cytometry analysis. Liver mononucleated cells were isolated from the livers of naive and MCD-fed mice and purified on a density gradient (Lympholyte®-M, Cedarlane Laboratoires Ltd. Burlington, Canada) as described in [18]. Cells were washed with Hank's medium and incubated 30 min with de-complemented mouse serum to block unspecific immunoglobulin binding. The cells were then stained with fluorochrome-conjugated antibodies for CD45, CD11b, Ly6C, CD11c, MHCII (eBiosciences,

San Diego CA, USA), F4-80 (Invitrogen, Abingdon, UK) or CX_3CR1 (R&D System, Minneapolis, MN, USA) and analyzed with a FACScalibur (Becton Dikinson, Franklin Lakes, NJ, USA) flow cytometer following prior gating for CD45 and the absence of cell aggregates. Intracellular staining for TNF-α was performed using a specific fluorochrome-conjugated antibody (eBiosciences, San Diego CA, USA).

Data analysis and statistical calculations. Statistical analyses were performed by SPSS statistical software (SPSS Inc. Chicago IL, USA) using one-way ANOVA test with Tukey's correction for multiple comparisons or Kruskal-Wallis test for non-parametric values. Significance was taken at the 5% level. Normality distribution was preliminary assessed by the Kolmogorov-Smirnov.

Results.

Feeding mice with a methionine-choline deficient (MCD) diet for up to 8 weeks resulted a progressive worsening of steatohepatitis as evaluated by a time dependent increase in liver triglyceride accumulation, transaminase release and hepatic inflammation (Supplementary Fig. 1). Although the hepatic mRNAs for α-1 procollagen was significantly up-regulated already after 4 weeks on the MCD diet, appreciable fibrosis, as evidenced by collagen staining with Picro-Sirius Red and α-SMA-positive activated hepatic stellate cells (HSCs), was evident in more advanced disease after 8 weeks of treatment (Supplementary Fig. 1). In parallel with the progression of NASH, flow cytometry showed a time-dependent expansion of intra-hepatic mononuclear cells expressing the mice monocyte/macrophage marker F4-80 (Fig. 1). Consistently, F4-80-positive cells in liver sections increased from 71.8±23 cell/mm^2 in controls up to 146.8±10.2 cells/mm^2 ($p<0.01$) in 8 weeks MCD-fed mice. Previous studies have reported that in injured livers inflammatory macrophages derive from $Ly6C^+/CD11b^+$ blood monocytes [12-14]. Accordingly, we observed that in the early phases of steatohepatitis (4 weeks on the MCD diet) $Ly6C^{high}/CD11b^+/F4\text{-}80^+$ cells were prevalent. However, their frequency did not further increased in advanced disease (Fig. 1) and this paralleled with a decline in the mRNAs of inflammatory M1 activation markers inducible NO synthase (iNOs) and IL-12p40 (Supplementary Fig. 1). At this stage, an elevation in the liver expression of both fractalkine (CX_3CL1) and the fractalkine receptor CX_3CR1 become evident (Supplementary Fig. 2). CX_3CR1 up-regulation largely involved monocyte-derived $F4\text{-}80^+$ cells (Supplementary Fig. 2) and led to a tenfold expansion of a pool of $F4\text{-}80^+/CD11b^+/CX_3CR1^{high}$ myeloid cells (Fig. 1). Further characterization of these cells showed

that they co-expressed CD11b and Ly6C (Fig. 2), suggesting their origin from liver infiltrating $Ly6C^{high}$ inflammatory monocytes rather than from the $Ly6C^{-}/CCR2^{-}/CX3CR1^{+}$ monocyte sub-set. Moreover, these cells showed an increased expression of the dendritic cell (DC) markers CD11c and major histocompatibility class II (MHCII) complex (Fig. 2).

Henning and co-workers [19] recently reported that the development of steatohepatitis in MCD-fed mice is associated with an expansion in hepatic mature myeloid DCs and a concomitant reduction in $B220^{+}$ phasmocytoid and $Cd8a^{+}$ lymphocytoid DCs. We confirmed that the progression of steatohepatitis was characterized by an appreciable increase in the fraction of hepatic $CD11c^{high}/MHCII^{+}$ DCs (Fig. 2). Such an expansion involved a pool of cells that were $F4\text{-}80^{high}$ and $Ly6C^{high}$ (Fig. 3), while the pools of $CD11c^{high}/MHCII^{+}/B220^{+}$ phasmocytoid DCs and $CD11c^{high}/MHCII^{+}/CD8a^{+}$ lymphocytoid DCs were significantly decreased (Supplementary Fig. 3). Interestingly, the expanding DC sub-set also expressed CX_3CR1 and CX_3CR1^{high} cells were particularly evident within the pool $CD11c^{high}/F4\text{-}80^{+}$ cells (Fig. 3). Altogether, these data suggested that DC expansion occurring in during the progression of steatohepatitis involved a sub-set of CX_3CR1^{high} monocyte-derived dendritic cells (moDCs) [20]. M1 activation of hepatic macrophages has been shown to be an important factor in driving hepatic inflammation in NASH through the production of TNF-α and other pro-inflammatory mediators [4,6]. However, according to a previous report [20] in our hands advanced steatohepatitis was characterized by a down-modulation of M1 activation markers (Supplementary Fig. 1). Yet a steadily elevation in both the hepatic mRNA and serum levels of TNF-α were evident during the disease progression (Fig. 4) and individual level of circulating TNF-α positively correlated with transaminase release ($r=0.82$; $p=0.035$). An elevated production of inflammatory mediators, including TNF-α, is a feature of moDCs [21,22]. In line with this, we observed that $CD11c^{high}/F4\text{-}80^{+}$ moDCs had an enhanced expression of TNF-α which specifically involved cells that were CX_3CR1^{+} (Fig. 4). Furthermore, $CX_3CR1^{+}/TNF\text{-}\alpha^{+}$ cells accumulated in the livers of 8 weeks MCD-fed mice, suggesting that CX_3CR1^{+} moDCs might sustain hepatic TNF-α production during the progression of steatohepatitis.

Recent studies have shown that genetic and pharmacological interference with CX_3CR1 ameliorates the evolution of atherosclerotic plaques [23-25]. In this context, hydrogen sulfide (H_2S) has been reported to improve atherosclerosis by preventing the up-regulation of CX_3CL1/CX_3CR1 in monocyte/macrophages exposed to pro-inflammatory stimuli [25]. As CX_3CR1-expressing DCs are already present in healthy livers (Fig. 3), in subsequent

experiments we sought to investigate whether mice treatment with the H_2S donor NaHS might selectively influence the development of CX_3CR1^{high} moDCs in MCD-induced steatohepatitis. Preliminary analysis showed that chronic administration of NaHS (1mg/kg body wt) did not influence transaminase release and hepatic inflammation markers in control mice (not shown). In subsequent experiments, mice fed for 4 weeks with the MCD diet received daily NaHS while continuing on the diet up to the eighth week. In these animals we observed that NaHS ameliorated CX_3CL1 and CX_3CR1 mRNA up-regulation (Fig. 5), without interfering with those of CCL2, CCR2 or CD11b (Supplementary Fig. 4). NaHS supplementation did not modify the hepatic pools of inflammatory macrophages and of DCs (Supplementary Fig. 4), but halved CX_3CR1 expression in F4-80$^+$ or $CD11c^{high}$ cells (Fig. 5). In particular, NaHS-treatment selectively reduced the fraction of CX_3CR1^{high}/F4-80$^+$/$CD11c^{high}$ moDCs (Fig. 5). Furthermore, NaHS decreased intracellular TNF-α levels as well as the fraction of TNF-α-producing cells (Fig. 6). In line with that, hepatic TNF-α mRNA and circulating TNF-α levels were lowered in NaHS-supplemented mice (Fig. 6). Despite NaHS treatment did not significantly influence the histopathological scores of steatosis (2.3±0.8 vs 1.8±0.4; p=0.1) and lobular inflammation (1.7±0.6 vs 1.6±0.5; p=0.8), it appreciably reduced the number of necrotic foci and apoptotic cells (Fig. 6). NaHS also prevented further elevation of transaminase release in the animals maintained on the MCD diet (Fig. 6), indicating that the sustained production of TNF-α by CX_3CR1^+ moDCs contributed to hepatocellular injury in advanced NASH. Although TNF-α-producing DCs have also been implicated in promoting hepatic fibrosis [23], in our hands, mice treatment with NaHS did not appreciably affected pro-collagen-1α, α-SMA and TGF-β1 mRNAs as well as collagen staining with Picro-Sirius Red (Supplementary Fig. 5).

Discussion

Growing evidence indicates that Ly6C$^+$ monocyte-derived macrophages are central players in NASH as they are important sources of inflammatory mediators [6-8] and, by interacting with activated CD4 helper T-lymphocytes and NKT cells, drive lobular inflammation and fibrogenesis [17,26]. Here we show for the first time that a sub-set Ly6C$^+$ cells expressing CX_3CR1 and showing features of inflammatory dendritic cells also contribute to the evolution of steatohepatitis.

Liver dendritic cells (DCs) are a heterogeneous population of specialized bone marrow-derived cells mainly involved in antigen presentation to lymphocytes [27]. In healthy livers, DCs

represent a small fraction of non-parenchymal cells and have a predominant tolerogenic phenotype [28], but a dramatic DC expansion occurs in chronic liver disease in combination with a stimulation in their antigen presenting activity and the release of pro-inflammatory cytokines [29]. In particular, experiments in a mice model of NASH have evidenced that hepatic DCs expand and mature in the early phases of the disease and acquire the capacity to specifically stimulate $CD4^+$ T-cells [19]. Such an activation likely relates to the stimulation of both humoral and cellular immune responses that also characterizes the evolution of NASH [17]. However, the specific features of NASH-associated DCs have not been investigated in detail.

Although most of dendritic cells derive from common bone marrow precursors, growing evidence indicates that under inflammatory conditions infiltrating monocytes can differentiate into a special sub-set of dendritic cells, called monocyte-derived inflammatory dendritic cells (moDCs) [21]. These cells co-express both dendritic and monocyte/macrophage surface markers and show a high production of inflammatory mediators combined to an efficient antigen presenting activity [21]. Our present data add on the involvement of DCs in NASH by showing that, with the progression of steatohepatitis, DC expansion involves a sub-set of cells featuring monocyte markers (F4-80^{high}/Ly6C^{high}) along with CX_3CR1 expression and TNF-α production. On these bases, we propose that during the evolution of NASH a sub-set of Ly6C^{high} monocytes/macrophages might acquire CX_3CR1 and differentiate to TNF-α-producing moDCs. Supporting this view, Barlic and co-workers have observed that during the development of atherosclerosis oxidized lipids stimulate human monocytes to switch from CCR2 to CX_3CR1 expression [30]. Furthermore, recent studies have shown that Ly6C^{high} monocytes differentiate to Ly6C^+/$CD11b^+$/CX_3CR1^+ moDCs in the intestinal *lamina propria.* This process in greatly enhanced during gut inflammation and CX_3CR1^+ moDCs exacerbate colitis by secreting TNF-α [31,32].

Hydrogen sulphide (H_2S) is increasingly recognized to act as an endogenous mediator exerting anti-inflammatory and cytoprotective activity in several tissue including the gastrointestinal tract [33,34]. Zhang and co-workers [25] have recently shown that in either RAW 246.7 cells or mice peritoneal macrophages H_2S selectively antagonizes CX_3CR1 expression induced by LPS or interferon-γ acting through signals mediated by the transcription factor NFkB and peroxisome proliferator activated receptor-γ (PPAR-γ). They also demonstrate that by interfering with the CX_3CL1/CX_3CR1 dyad mice NaHS supplementation reduces the development of atherosclerotic plaques [25]. Mice feed with a high fat diet show a reduced

hepatic H_2S production [35], while H_2S supplementation ameliorates oxidative stress and hepatic inflammation in mice with MCD-induced NASH [36]. In our hands, the H_2S donor NaHS has not a generalized anti-inflammatory action, but interferes with the up-regulation of CX_3CL1/CX_3CR1 dyad associated with the progression of steatohepatitis and selectively blocks the development of TNF-α-producing CX_3CR1^{high} moDCs, indicating that CX_3CL1/CX_3CR1 signaling might have an important role in the differentiation of $Ly6c^{high}$ inflammatory monocytes to moDCs. NaHS treatment also prevents further elevation of transaminase release in the animals maintained on the MCD diet, indicating that CX_3CR1^+ moDCs can contribute to the evolution of steatohepatitis not only through the stimulation of immune responses [17], but also by directly sustaining hepatic TNF-α production. This is in line with the observation that TNF-α-producing DCs sustain hepatic inflammation in mice with tioacetamide-induced fibrosis [22].

Two recent papers have reported that CX_3CR1 genetic deficiency exacerbates hepatic injury and fibrosis induced by chronic CCl_4 treatment and bile duct ligation [37,38]. In particular, Karlmark and co-workers [38] have shown that CX_3CR1 is required for the survival and the differentiation of liver infiltrating macrophages and can limit their M1 polarization. On the same vein, unspecific hepatic DC destruction exacerbates acetaminophen hepatotoxicity [39] and unexpectedly worsens the evolution of experimental NASH [19]. At present, there is no explanation for the discrepancies between these findings and our present results. We have observed that in the livers of control animals about 30% of DCs constitutively express CX_3CR1. Liver DCs are known to have a predominant immune-suppressive activity [28] and these properties are shared also by CX_3CR1^+ DCs [40]. Thus, it is possible that genetic CX_3CR1 deficiency or hepatic DC ablation might enhance damage-associated inflammation by affecting a population of tolerogenic DCs and might overcame the protection given by preventing the development of moDCs.

We are well aware that steatohepatitis induced by the MCD diet does not reproduce important features of the human NASH such as obesity and insulin resistance [15]. However, the difficulties to differentiate the role of moDCS in both clinical and experimental settings justify its use as, differently from other experimental protocols, it causes extensive steatohepatitis. Nonetheless, further studies are required to better define the relative contribution of constitutive versus monocyte-derived CX_3CR1-expressing DCs during the evolution of chronic liver diseases.

In conclusion, the data presented indicate that the evolution of steatohepatitis involves the emergence of CX_3CR1-expressing moDCs that can sustain hepatic inflammation in advanced disease through TNF-α production. Our results also show that interference with CX_3CR1 up-regulation prevents the differentiation of moDCs, pointing CX_3CR1 as a possible target for the therapy of NASH.

Acknowledgements

This work has been supported by a grant from the Fondazione Cariplo, Milan, Italy (Grant N°2011-0470).

Conflict of interest

The authors have no competing interests on the matter concerning the present manuscript.

Author contribution

SS and IL designed the study and performed the experiments; AJ, SB and MV performed the experiments; CB evaluated pathology; EA contributed to the study design and supervised the study and the manuscript preparation.

References

1. Lazo M, Clark JM. The epidemiology of nonalcoholic fatty liver disease: a global perspective. Semin Liver Dis. 2008;28:339-350.
2. Marra F, Gastaldelli A, Svegliati-Baroni G, et al. Molecular basis and mechanisms of progression of non-alcoholic steatohepatitis. Trends Mol. Med. 2008;14:72-81.
3. Tilg H, Moschen AR. Evolution of inflammation in non-alcoholic fatty liver disease: the multiple parallel hits hypothesis. Hepatol. 2010;52:1836-1846.
4. Tosello-Trampont AC, Landes SG, Nguyen V, et al. Kuppfer cells trigger nonalcoholic steatohepatitis development in diet-induced mouse model through tumor necrosis factor-α production. J Biol Chem. 2012;287:40161-40172.
5. Leroux A, Ferrere G, Godie V, et al. Toxic lipids stored by Kupffer cells correlates with their pro-inflammatory phenotype at an early stage of steatohepatitis. J Hepatol. 2012;57:141-149.
6. Maina V, Sutti S, Locatelli I, et al. Bias in macrophage activation pattern influences non-alcoholic steatohepatitis (NASH) in mice. Clin Sci (Lond) 2012; 122:545-553.
7. Baeck C, Wehr A, Karlmark KR, et al. Pharmacological inhibition of the chemokine CCL2 (MCP-1) diminishes liver macrophage infiltration and steatohepatitis in chronic hepatic injury. Gut. 2012;61:416-426.

8. Miura K, Yang L, van Rooijen N, et al. Hepatic recruitment of macrophages promotes nonalcoholic steatohepatitis through CCR2. Am J Physiol Gastrointest Liver Physiol. 2012;302:G1310-G1321.
9. Ziegler-Heitbrock L. Cell Immunol. Monocyte subsets in man and other species. 2014;289:135-139. doi: 10.1016/j.cellimm.2014.03.019.
10. Murray PJ, Wynn TA. Protective and pathogenetic functions of macrophage subsets. Nat Rev Immunol. 2011;11:723-737
11. Karlmark KR, Weiskirchen R, Zimmermann HW, et al. Hepatic recruitment of the inflammatory Gr1+ monocyte subset upon liver injury promotes hepatic fibrosis. Hepatol. 2009;50:261-274.
12. Baeck C, Wei X, Bartneck M, et al. Pharmacological inhibition of the chemokine C-C motif chemokine ligand 2 (monocyte chemoattractant protein 1) accelerates liver fibrosis regression by suppressing Ly-6C(+) macrophage infiltration in mice. Hepatol. 2014;59:1060-1072.
13. Ehling J, Bartneck M, Wei X, et al. CCL2-dependent infiltrating macrophages promote angiogenesis in progressive liver fibrosis. Gut. 2014; doi: 10.1136/gutjnl-2013-306294.
14. Tacke F, Zimmermann HW. Macrophage heterogeneity in liver injury and fibrosis. J Hepatol. 2014;60:1090-1096.
15. Larter CZ, Yeh MM. Animal model of NASH: getting both pathology and metabolic contest right. J. Gastroenterol. Hepatol. 2008;23:1635-1648.
16. Kleiner DE, Brunt EM, Van Natta M, et al. Design and validation of a histological scoring system for nonalcoholic fatty liver disease. Hepatol. 2005;41:1313-1321.
17. Sutti S, Jindal A, Locatelli I, al. Adaptive immune responses triggered by oxidative stress contribute to hepatic inflammation in NASH. Hepatol. 2014;59:886-897.
18. Crispe NI. Isolation of mouse intrahepatic lymphocytes. In: Current Protocols in Immunology. 1997;3.21.1-321.8.
19. Henning JR, Graffeo CS, Rehman A, et al. Dendritic cells limit fibroinflammatory injury in nonalcoholic steatohepatitis in mice. Hepatol. 2013;58:589-602.
20. Locatelli I, Sutti S, Jindal A, et al. Endogenous annexin A1 is a novel protective determinant in nonalcoholic steatohepatitis in mice. Hepatol. 2014;60:531-544.
21. Domininguez PM, Ardavin C. Differentiation and function of mouse monocyte-derived dendritic cells in steady state and inflammation. Immunol Rev. 2010;234:90-104.
22. Connolly MK, Bedrosian AS, Mallen-St Clair J, et al. In liver fibrosis, dendritic cells govern hepatic inflammation in mice via TNF-alpha. J Clin Invest. 2009;119:3213-3225.
23. Lesnik PI, Haskell CA, Charo IF. Decreased atherosclerosis in CX3CR1-/- mice reveals a role for fractalkine in atherogenesis. J Clin Invest. 2003;111:333-340.
24. Poupel L, Boissonnas A, Hermand P, et al. Pharmacological inhibition of the chemokine receptor, CX3CR1, reduces atherosclerosis in mice. Arterioscler Thromb Vasc Biol. 2013;33:2297-2305.
25. Zhang H, Guo C, Wu D, et al. Hydrogen sulfide inhibits the development of atherosclerosis with suppressing CX3CR1 and CX3CL1 expression. PLoS One. 2012;7:e41147. doi: 10.1371/journal.pone.0041147

26. Wehr A, Baeck C, Heymann F, et al. Chemokine receptor CXCR6-dependent hepatic NK T Cell accumulation promotes inflammation and liver fibrosis. J Immunol. 2013;190:5226-5236.

27. Hashimoto D, Miller J, Merad M. Dendritic cell and macrophage heterogeneity in vivo. Immunity 2011;35:323-335.

28. Crispe IN. Immune tolerance in liver disease. Hepatol. 2014; doi: 10.1002/hep.27254. [Epub ahead of print]

29. Rahman AH, Aloman C. Dendritic cells and liver fibrosis. Biochim Biophys Acta 2013; 1832:998-1004.

30. Barlic J, Zhang Y, Foley JF, et al. Oxidized lipid-driven chemokine receptor switch, CCR2 to CX3CR1, mediates adhesion of human macrophages to coronary artery smooth muscle cells through a peroxisome proliferator-activated receptor gamma-dependent pathway. Circulation. 2006;114:807-819.

31. Varol C, Vallon-Eberhard A, Elinav E, et al. Intestinal lamina propria dendritic cell subsets have different origin and functions. Immunity. 2009;31:502-512.

32. Rivollier A, He J, Kole A, et al. Inflammation switches the differentiation program of Ly6Chi monocytes from antiinflammatory macrophages to inflammatory dendritic cells in the colon. J Exp Med. 2012;209:139-155.

33. Wallace JL, Ferraz JG, Muscara MN. Hydrogen sulfide: an endogenous mediator of resolution of inflammation and injury. Antioxid Redox Signal. 2012;17:58-67.

34. Chan MV, Wallace JL. Hydrogen sulfide-based therapeutics and gastrointestinal diseases: translating physiology to treatments. Am J Physiol Gastrointest Liver Physiol. 2013;305:G467-G473.

35. Peh MT, Anwar AB, Ng DS, Atan MS, et al. Effect of feeding a high fat diet on hydrogen sulfide (H_2S) metabolism in the mouse. Nitric Oxide. 2014;pii:S1089-8603(14)00022-6. doi: 10.1016/j.niox.2014.03.002.

36. Zhu-Lin L, Tang LJ, Wang T, et al. Effects of treatment with hydrogen sulfide on methionine choline deficient diet-induced non-alcoholic steatohepatitis in rats. J Gastroenterol Hepatol 2014;29:215–222.

37. Aoyama T, Inokuchi S, Brenner DA, et al. CX3CL1-CX3CR1 interaction prevents carbon tetrachloride-induced liver inflammation and fibrosis in mice. Hepatol. 2010;52:1390-1400.

38. Karlmark KR, Zimmermann HW, Roderburg C, et al. The fractalkine receptor CX_3CR1 protects against liver fibrosis by controlling differentiation and survival of infiltrating hepatic monocytes. Hepatol. 2010;52:1769-1782.

39. Connolly MK, Ayo D, Malhotra A, Dendritic cell depletion exacerbates acetaminophen hepatotoxicity. Hepatol. 2011;54:959-968.

40. Liao G, van Driel B, Magelky E, et al. Glucocorticoid-induced TNF receptor family-related protein ligand regulates the migration of monocytes to the inflamed intestine. FASEB J. 2014;28:474-484.

Figure 1. Changes in the hepatic recruitment of Ly6C^{high} and CX3CR1+ monocyte-derived cells during the progression of steatohepatitis.

Mice were fed a control or a methionine-choline deficient (MCD) diet over an 8-week time period.

(Panel A) The time changes of intrahepatic CD45$^+$ cells expressing the monocyte F4-80 marker and (Panel B) the relative prevalence of Ly6C^{high}/CD11b$^+$/F4-80$^+$ and CX$_3$CR1$^+$/CD11b$^+$/F4-80$^+$ cell subsets were evaluated by flow cytometry of liver mononucleated cells isolated at different time points. The percent values refers to the number of cells gated as CD11b$^+$. The data were from 4-6 animals per group.

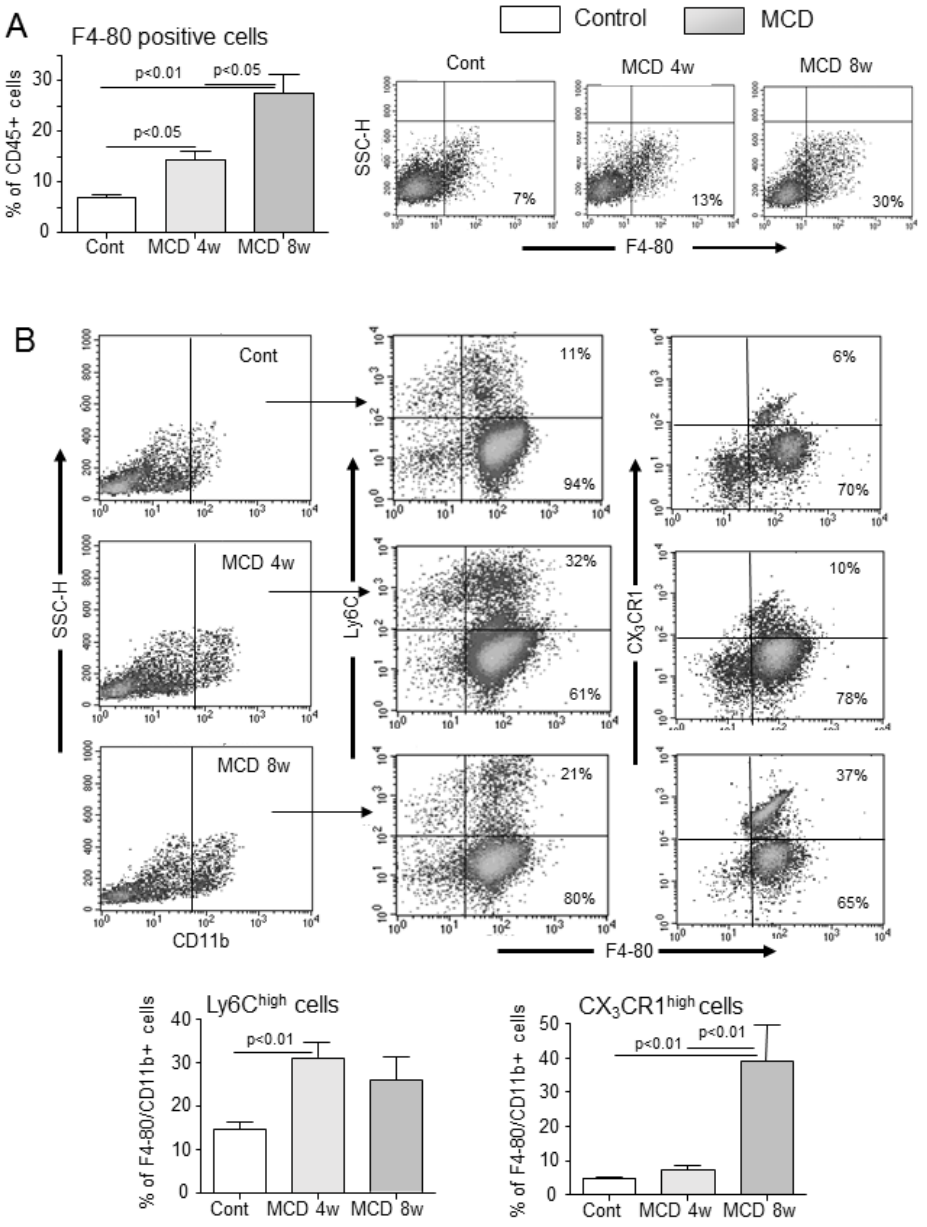

Figure 2. CX_3CR1-positive monocyte-derived cells associated with steatohepatitis show feature of monocyte-derived dendritic cells.

Mice were fed a control or a methionine-choline deficient (MCD) diet for 8-weeks and liver $CD45^+$ mononucleated cells were analyzed by flow cytometry.

(Panel A) $F4\text{-}80^+/CX_3CR1^+$ cells were characterized for the relative distribution of inflammatory monocyte markers CD11b and Ly6C as well as for the expression of dendritic cell markers CD11c and MHCII. Grey lines refers to isotypic controls. One experiment representative of three.

(Panel B) Liver $CD45^+$ mononucleated cells were evaluated for the relative prevalence of $CD11c^{high}/MHCII^+$ dendritic cells. The percent values refers to the number of cells gated as $CD11b^{high}$. Quantitative data represent 4 animals per group.

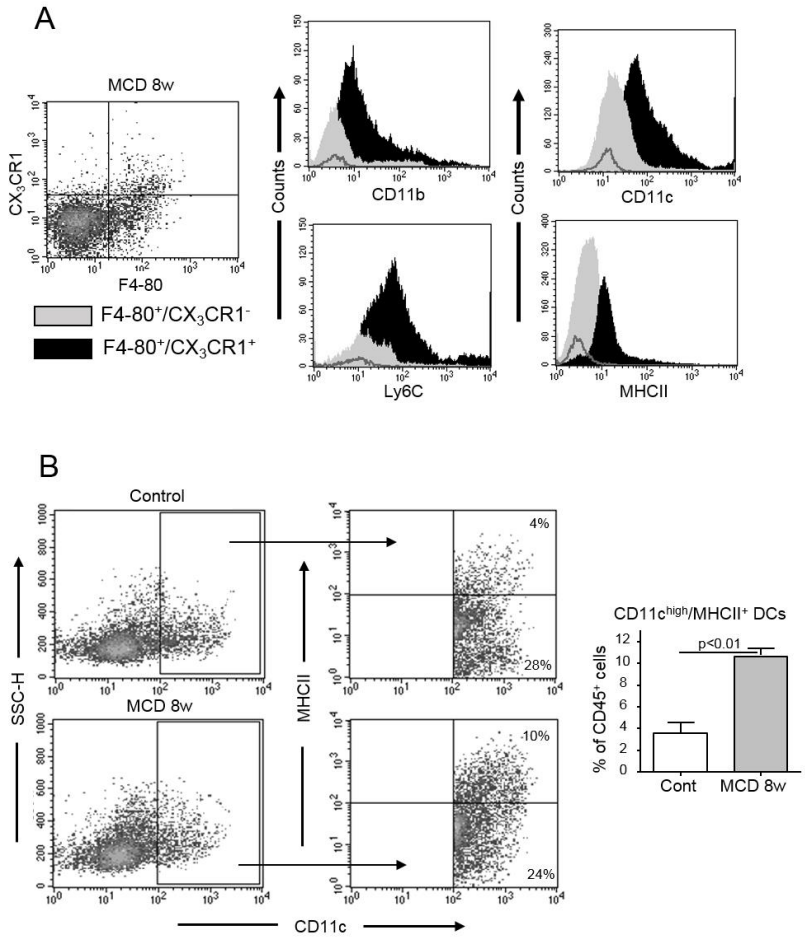

Figure 3. Dentritic cells expansion during the evolution of steatohepatitis involved a pool of CX_3CR1-positive cells with features of monocyte-derived dendritic cells.

Mice were fed a control or a methionine-choline deficient (MCD) diet for 8-weeks and liver $CD45^+$ mononucleated cells were analyzed by flow cytometry.
(Panel A) $CD11c^{high}/MHCII^+$ hepatic dendritic cells were characterized for the expression of inflammatory monocyte markers F4-80 and Ly6C and for that of CX_3CR1. The percent values refers to the number of cells gated as $CD11c^{high}/MHCII^+$. Quantitative evaluation were from 4 animals per group.
(Panel B) Distribution of $CX3CR1^{high}$ expressing cells among $CD11c^{high}/F4\text{-}80^+$ and $CD11c^{low}/F4\text{-}80^+$ cells obtained from the livers of 8 week MCD-fed mice. The percent values refers to the number of cells gated. One experiment representative of three.

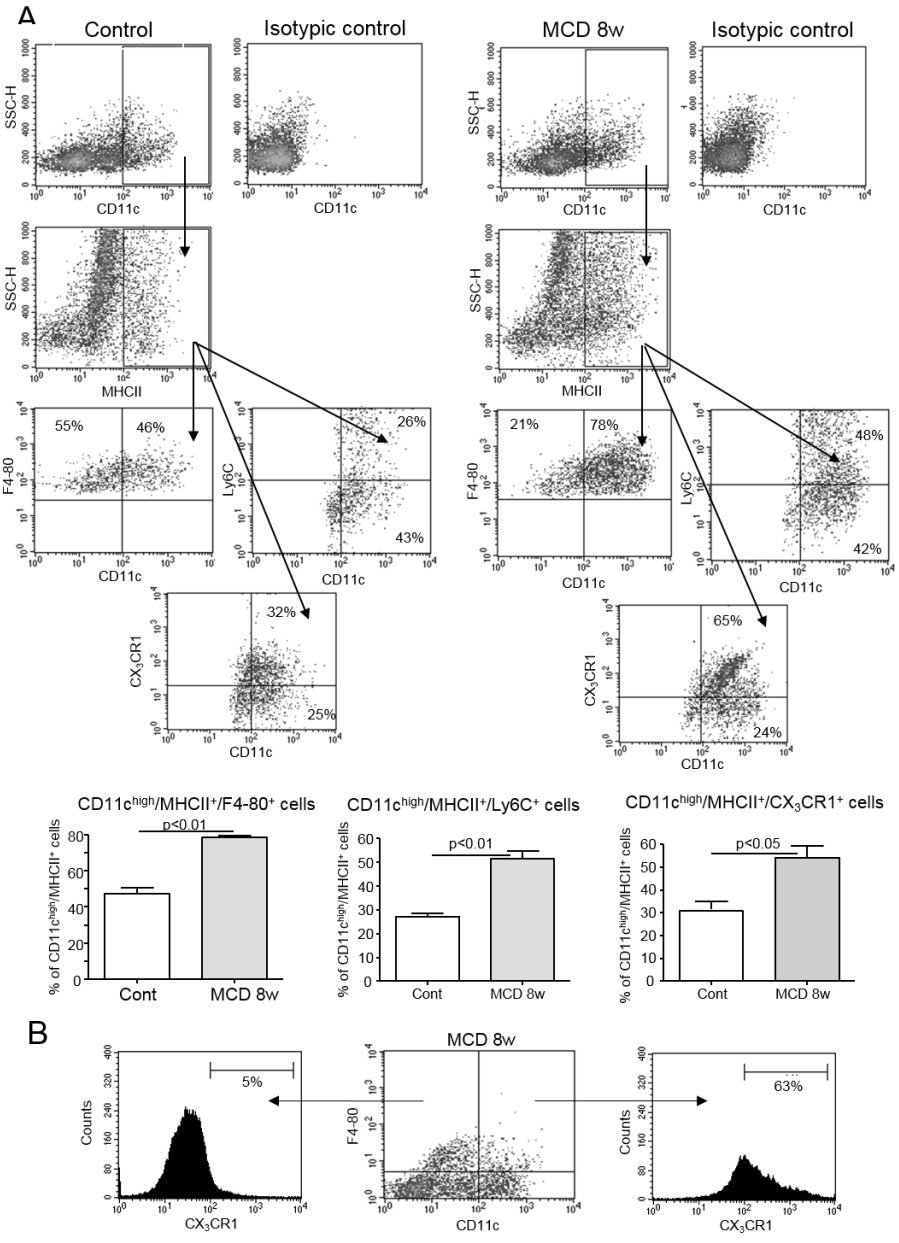

Figure 4. The progression of steatohepatitis is characterized by the increase in CX_3CR1-positive monocyte-derived dendritic cells producing TNF-α.

Mice were fed a control or a methionine-choline deficient (MCD) diet for up to 8-weeks. (Panels A & B) Hepatic mRNA expression and circulating levels of TNF-α were evaluated in control and MCD-fed mice. Boxes include the values within 25th and 75th percentile, while the horizontal bars represent the medians. The extremities of the vertical bars (10th-90th percentile) comprise the eighty percent of the values. Data were from 6-8 animals per group.
(Panel C) TNF-α expression by CD11c^{high}/F4-80^{+} and CD11c^{low}/F4-80^{+} cells was evaluated by flow cytometry along with (Panels D & E) the differential TNF-α expression by F4-80^{+} positive or genitive for CX_3CR1 and the proportion of TNF-α-producing CX_3CR1^{+} cells in control and NASH livers. The percent values refers to the number of cells gated in the areas indicated by the arrows. Grey lines refers to isotypic controls. Quantitative data were from 3-4 animals per group.

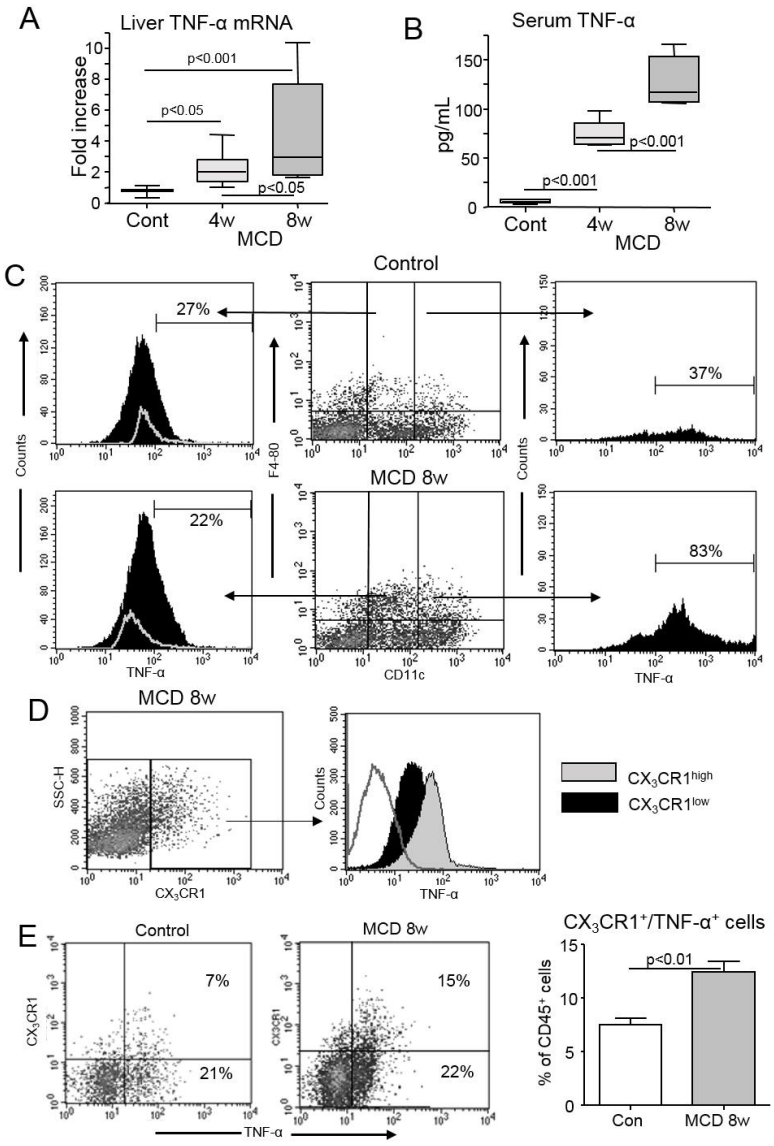

Figure 5. Mice treatment with the H_2S donor NaHS reduces hepatic CX3CL1 expression and CX_3CR1-positive monocyte-derived dendritic cells associated with the progression of steatohepatitis.

Mice were fed a methionine-choline deficient (MCD) diet for 8 weeks. NaHS (1mg/kg body wt) was administered to MCD-fed mice starting from the fourth week of treatment.
(Panel A) The hepatic expression of CX_3CL1 and CX_3CR1 was evaluated by RT-PCR in mRNA extracted from control or MCD-fed mice with or without NaHS supplementation. The values are expressed as fold increase over control values after normalization to the β-actin gene. Data are from 6-9 animals per group; boxes include the values within 25th and 75th percentile, while the horizontal bars represent the medians. The extremities of the vertical bars (10th-90th percentile) comprise the eighty percent of the values.
(Panel B) The effect of NaHS supplementation on CX_3CR1 expression by F4-80$^+$ cells and CD11c^{high} cells was evaluated by flow cytometry. Isotypic controls are shown as dotted lines.
(Panel C) Changes in the distribution of CX_3CR1^{high} moDCs following NaHS supplementation of MCD-fed mice. The percent values refers to the number of cells gated as F4-80$^+$/CD11c^{high}. Data are from 3-4 animals per group.

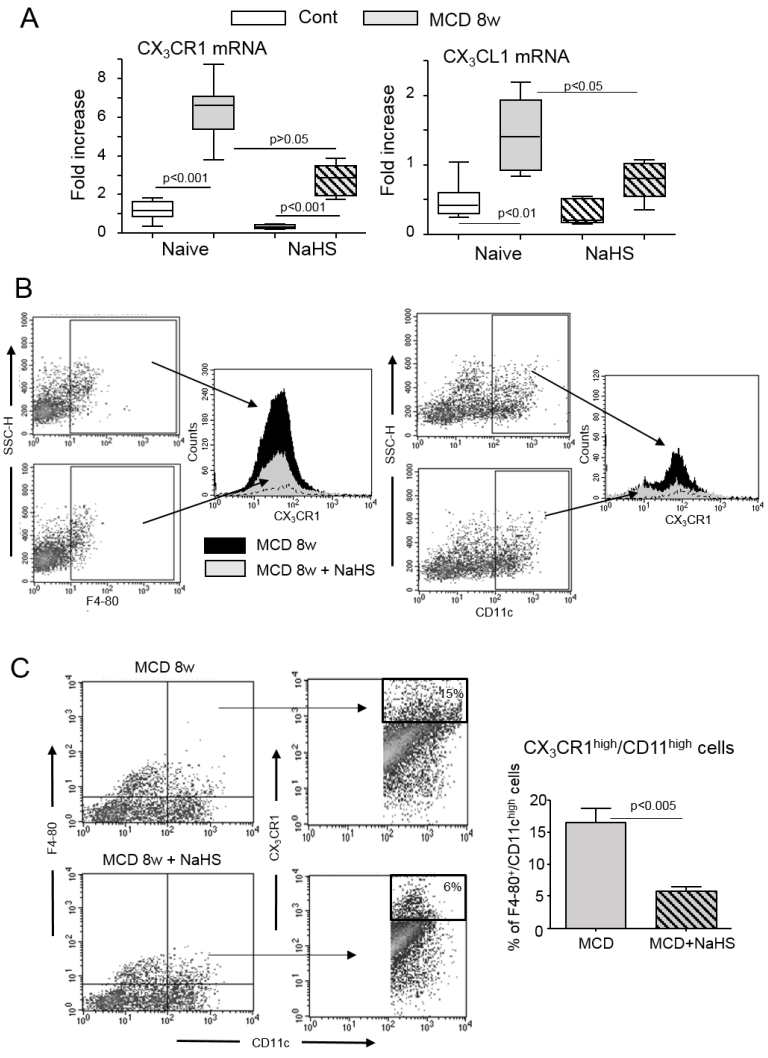

Figure 6. Mice treatment with the H_2S donor NaHS reduces hepatic TNF-α production and improves hepatic injury during the progression of steatohepatitis.

Mice were fed a methionine-choline deficient (MCD) diet for 8 weeks. NaHS (1mg/kg body wt) was administered to MCD-fed mice starting from the fourth week of treatment.
(Panel A) TNF-α expression and the relative prevalence of liver F4-80$^+$/TNF-α$^+$ cells was evaluated by flow cytometry. Data are from 3-4 animals per group. Isotypic controls are shown as dotted lines.
(Panel B) Hepatic TNF-α mRNA and circulating TNF-α levels were evaluated in MCD-fed mice with or without NaHS supplementation. Liver TNF-α mRNA levels were measured by RT-PCR and expressed as fold increase over control values after normalization to the β-actin gene. Circulating TNF-α levels were determined by ELISA in the same animals. Data are from 6-9 animals per group; boxes include the values within 25th and 75th percentile, while the horizontal bars represent the medians. The extremities of the vertical bars (10th-90th percentile) comprise the eighty percent of the values.
(Panels C & D) Liver histology was evaluated in hematoxilin/eosin stained sections from control or MCD-fed animals (magnification 200x). Necro-inflammatory foci and apoptotic cells were counted as reported in [17].
(Panel E) Liver damage was assessed by circulating alanine aminotransferase (ALT) release.

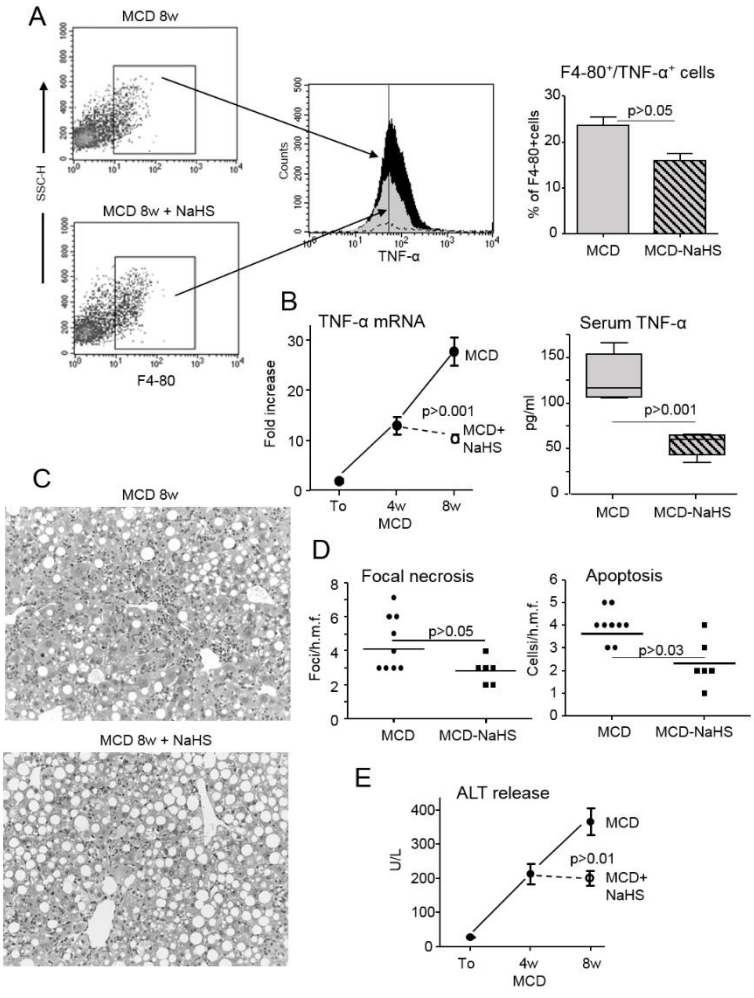

Sutti S, Locatelli I, Bruzzi S, Jindal A, Vacchiano M,
Bozzola C, Albano E

CX$_3$CR1-EXPRESSING INFLAMMATORY DENDRITIC CELLS CONTRIBUTE TO THE PROGRESSION STEATOHEPATITIS

Supplementary Material

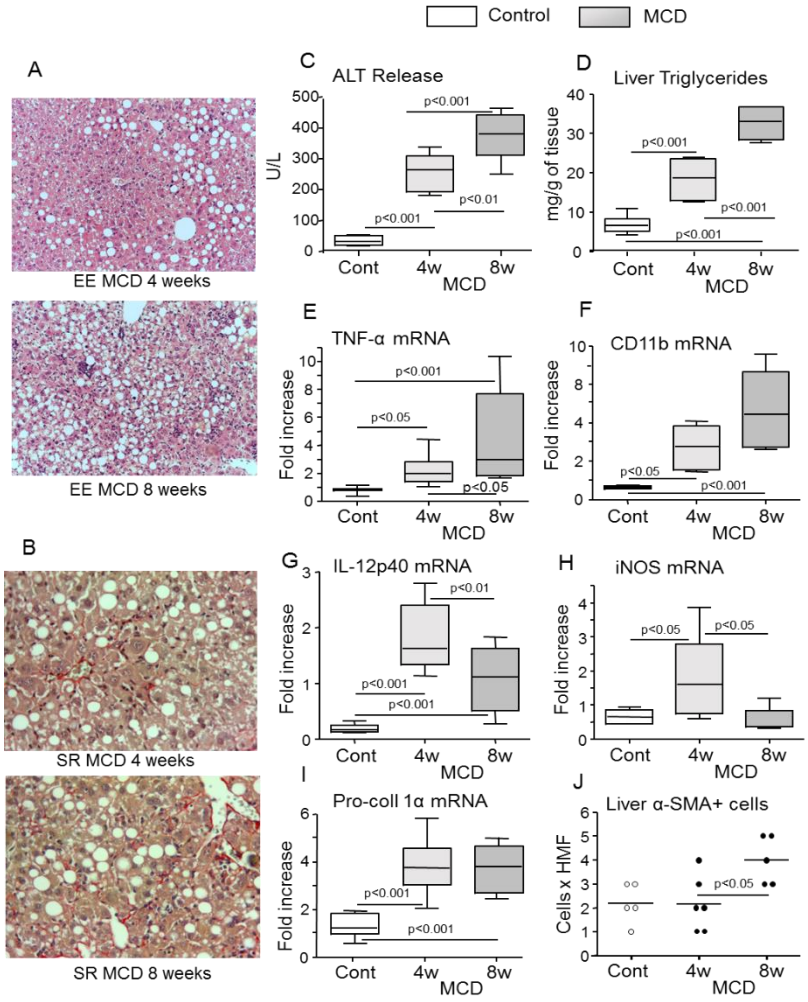

Supplementary Figure 1
Time dependent variations of hepatic injury, inflammation and fibrogenesis during mice feeding with a methionine/choline deficient (MCD) diet.

Wild type C57BL/6 mice received the MCD diet for up to 8 weeks. (A,B) Liver histology was evaluated by hematoxilin/eosin (EE) and collagen Picro-Sirius Red (SR) staining of liver sections from control or MCD-fed animals (magnification 200x). (C,D) Alanine aminotransferase (ALT) release, and hepatic triglyceride content were determined by enzymatic methods. (E-H) CD11b, IL12p40, iNOS, procollagen-1 α, mRNAs were measured by RT-PCR and expressed as fold increase over control values after normalization to the β-actin gene. (I) Activated hepatic stellated cells expressing α-smooth muscle actin (α-SMA) were evidenced by immunohistochemistry. The values refer to 5-6 animals per group and the boxes include the values within 25th and 75th percentile, while the horizontal

bars represent the medians. The extremities of the vertical bars (10^{th}-90^{th} percentile) comprise the eighty percent of the values.

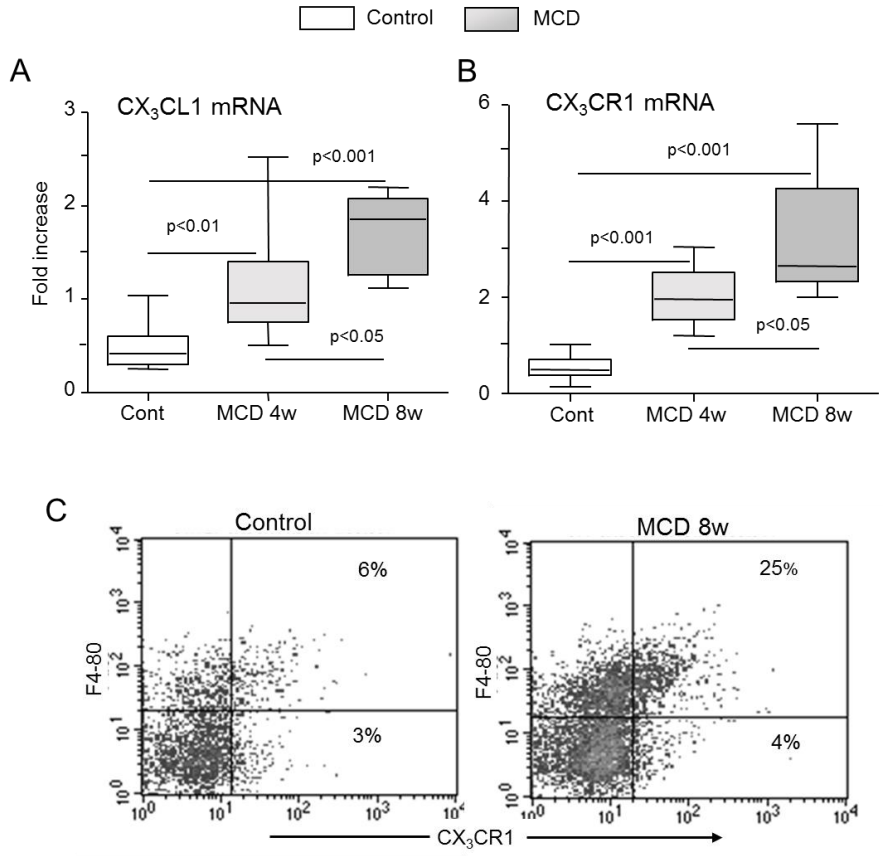

Supplementary Figure 2
The evolution of MCD-induced steatohepatitis is associated with a up-regulation in the hepatic expression of fractalkine signaling.

Mice were fed a methionine-choline deficient (MCD) diet over an 8-week time period.
The expression of fractalkine CX3CL1 (A) and of his receptor CX3CR1 (B) were evaluated by RT-PCR in mRNA extracted from whole liver and isolated macrophages of either control or MCD-fed mice. The values are expressed as fold increase over control values after normalization to the β-actin gene. Data are from 6-8 animals per group; boxes include the values within 25^{th} and 75^{th} percentile, while the horizontal bars represent the medians. The extremities of the vertical bars (10^{th}-90^{th} percentile) comprise the eighty percent of the values. (C) Liver mononucleated cells were analyzed by flow cytometry for the expression of CX_3CR1 in monocyte-derived F4-80+ cells.

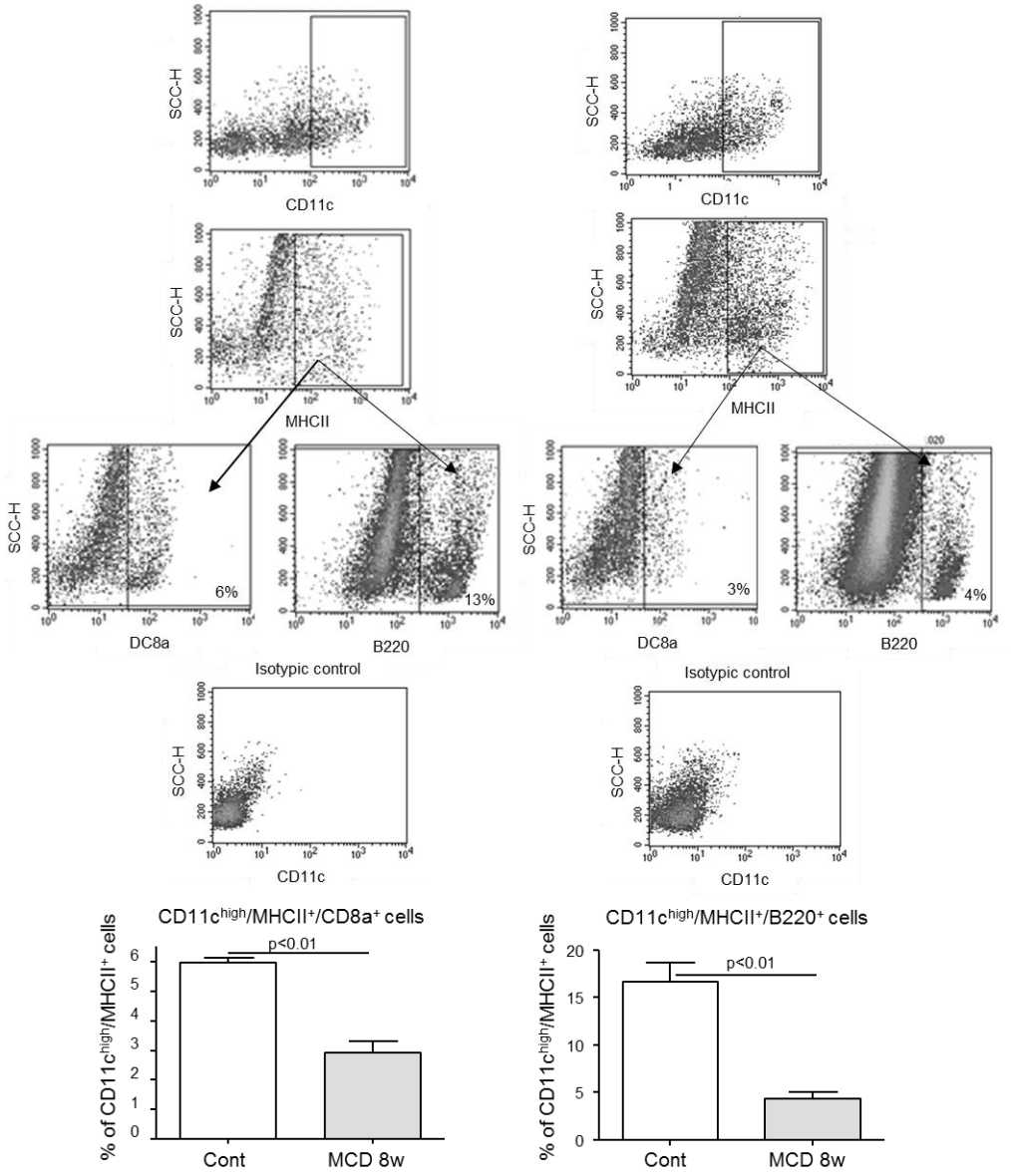

Supplementary Figure 3.

The progression of steatohepatitis is associated with a decrease in the pools of plasmocytoid and lymphocytodid dendritic cells.

Mice were fed a control or a methionine-choline deficient (MCD) diet for 8-weeks and liver mononucleated cells were analyzed by flow cytometry.

$CD11c^{high}/MHCII^{+}$ hepatic dendritic cells were characterized for the expression of plasmocytoid marker B220 and for the lymphocytoid marker CD8a. Quantitative evaluation were from 4 animals per group.

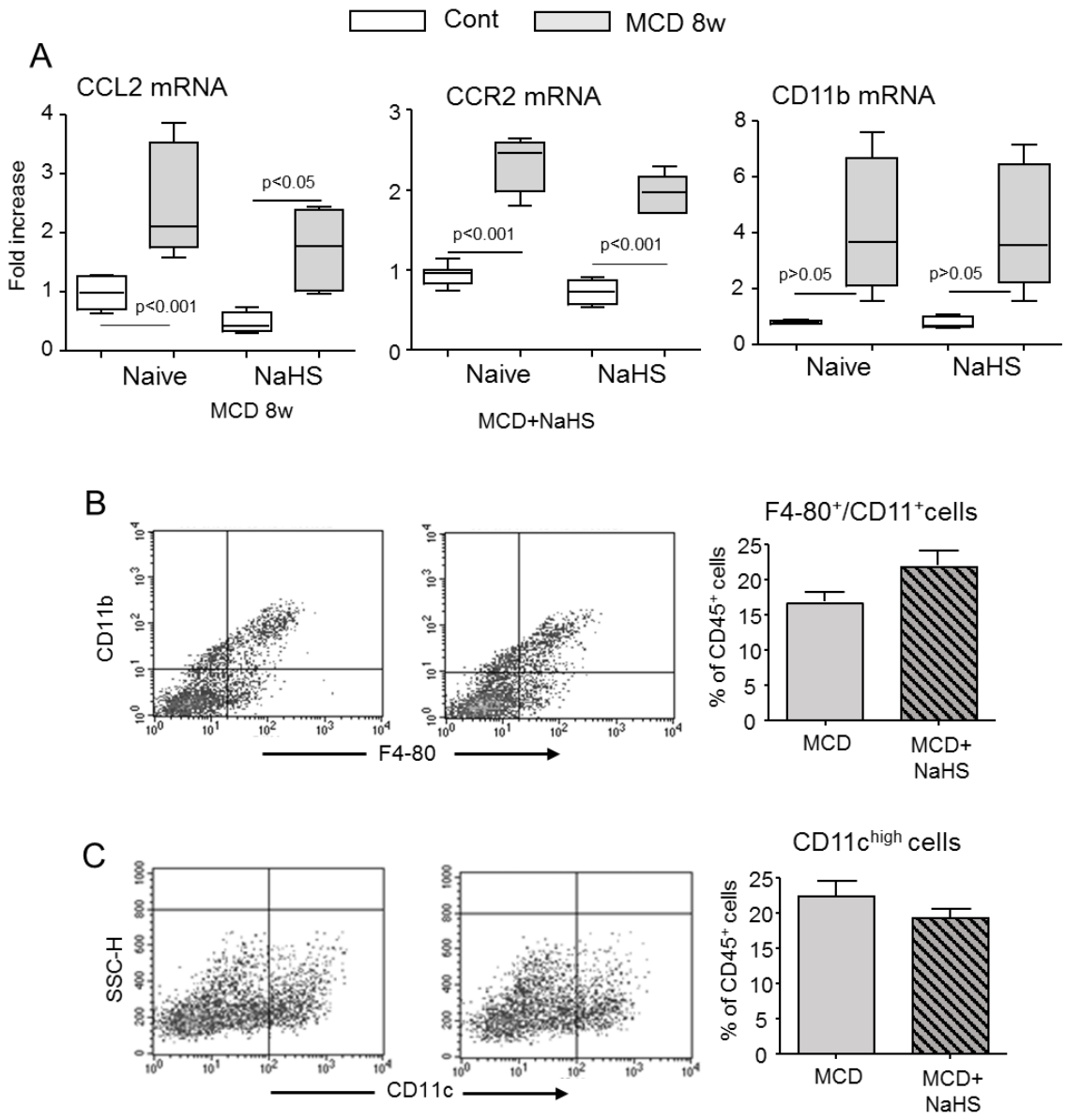

Supplementary Figure 4

The treatment with the H_2S donor NaHS does not affect hepatic macrophage and dendritic cells in mice associated with steatohepatitis.

Mice were fed a methionine-choline deficient (MCD) diet for 8 weeks. NaHS (1mg/kg body wt) was administered to MCD-fed mice starting from the fourth week of treatment.

(A) The hepatic expression of CCL2, CCR2 and CD11b was evaluated by RT-PCR in mRNA extracted from control or MCD-fed mice with or without NaHS supplementation. The values are expressed as fold increase over control values after normalization to the β-actin gene. Data are from 6-9 animals per group; boxes include the values within 25th and 75th percentile, while the horizontal bars represent the medians. The extremities of the vertical bars (10th-90th percentile) comprise the eighty percent of the values.

(B & C) The relative prevalence of F4-80$^+$/CD11b$^+$ macrophages and CD11c^{high} dendritic cells was evaluated by flow cytometry. Data are from 3-4 animals per group.

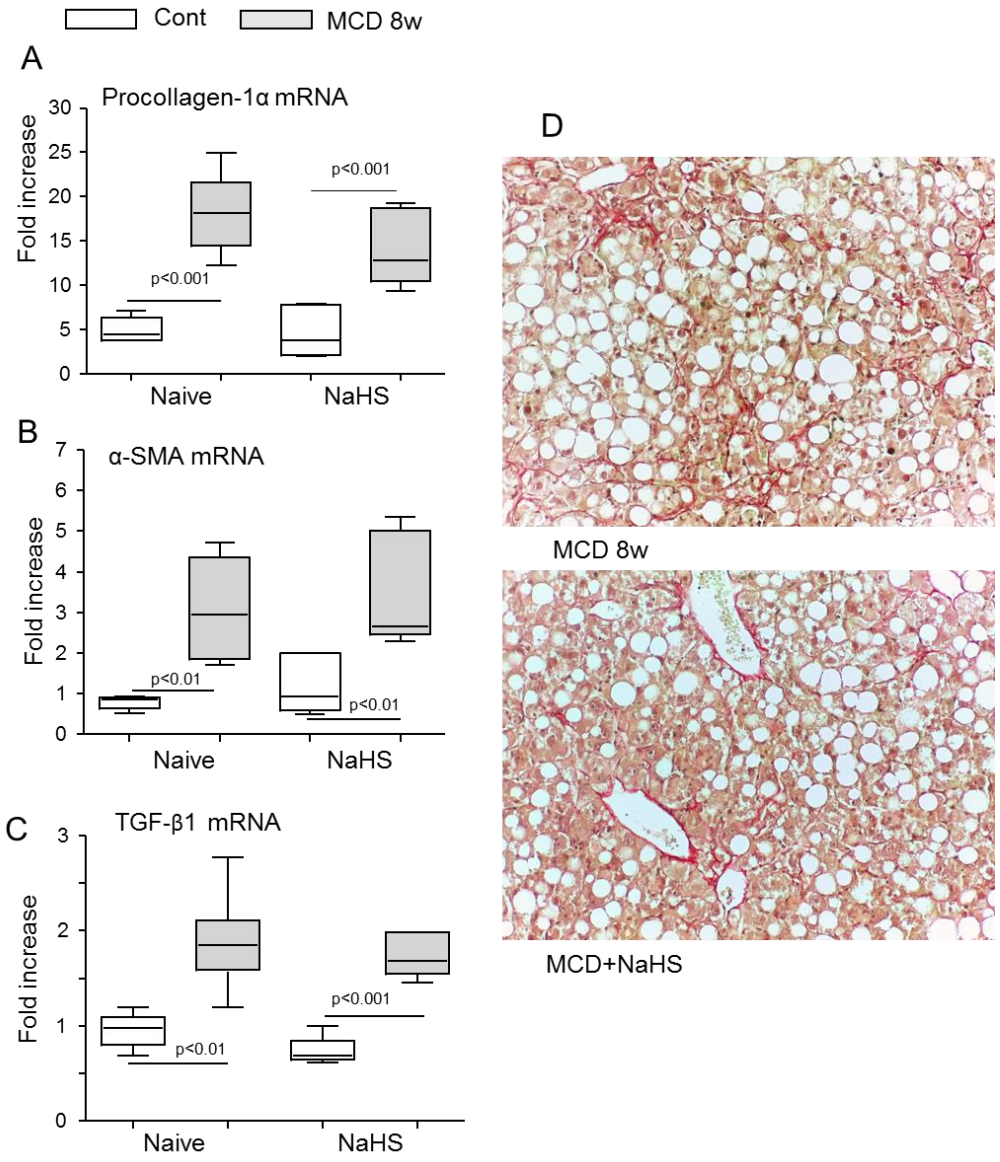

Supplementary Figure 5

The treatment with the H_2S donor NaHS does not affect hepatic fibrosis in mice with advanced steatohepatitis.

Mice were fed a methionine-choline deficient (MCD) diet for 8 weeks. NaHS (1mg/kg body wt) was administered to MCD-fed mice starting from the fourth week of treatment.

(A) The hepatic expression of Procollagen-1 α, TGF-1β and α-smooth muscle actin (α-SMA) was evaluated by RT-PCR in mRNA extracted from control or MCD-fed mice with or without NaHS supplementation. The values are expressed as fold increase over control values after normalization to the β-actin gene. Data are from 6-9 animals per group; boxes include the values within 25th and 75th percentile, while the horizontal bars represent the medians. The extremities of the vertical bars (10th-90th percentile) comprise the eighty percent of the values.

(B) Collagen deposition was evidenced by Picro-Sirius Red (SR) staining of liver sections from MCD-fed animals with or without NaHS supplementation (magnification 200x).

8. Paper 3

Morphological and Functional Changes of Liver Macrophages during the Progression of Nonalcoholic Steatohepatitis (NASH)

Submitted to Liver International (February 2015)

Background and Aims: Hepatic macrophages have an important role in NASH evolution as they represent an important source of pro-inflammatory mediators during the disease evolution and regulate the development of fibrosis. The macrophage expansion in NASH mainly results from liver infiltrating monocytes which differentiates into M1 polarized cells. However, little is known about the functional changes occurring in liver macrophages during the disease progression. In this study we used the methionine-choline deficient (MCD) diet model of NASH to monitor the behaviour of hepatic macrophages.

Results: The hepatic F4/80-positive macrophages increased in parallel with the disease progression. At histology macrophages accumulating in NASH formed small clusters of enlarged cells that contained lipid vesicles positive for the apoptotic cell markers Annexin V likely originating from the phagocytosis apoptotic bodies derived from dying fat-laden hepatocytes. Flow cytometry showed that these enlarged macrophages were $Ly6C^{high}/CD11b^{+}$, suggesting that they might derive from inflammatory monocytes. However, as compared to regular size macrophages the enlarged sub-set was characterized by an enhanced expression of the anti-inflammatory mediators IL-10 and annexin A1. Similar vacuolized macrophages producing annexin A1 were also evident in liver biopsies of NASH patients. In mice with NASH, the accumulation of enlarged $F4/80^{+}$ cells paralleled with a decline of the macrophage M1 activation markers iNOS and IL-12, while the levels of M2 polarization markers arginase-1 and MGL-1 were unchanged.

Conclusions: Altogether, these data indicate that during the progression of NASH liver macrophages that phagocyte apoptotic hepatocytes acquire anti-inflammatory properties and promote the down-modulation of the inflammatory phenotype in the remaining macrophage population.

FAT-LADEN MACROPHAGES MODULATE LOBULAR INFLAMMATION IN NONALCOHOLIC STEATOHEPATITIS (NASH)

Aastha Jindal*[1], Stefania Bruzzì*[1], Salvatore Sutti[1], Irene Locatelli[1], Marco Vacchiano[1], Cristina Bozzola[1], Maurizio Parola[2], Claudia Paternostro[2], Emanuele Albano[1]

[1]Dept. of Health Sciences and Interdisciplinary Research Centre for Autoimmune Diseases, University "Amedeo Avogadro" of East Piedmont, Novara, Italy.

[2]Dept of Clinical and Biological Sciences, University of Turin, Turin, Italy

*These two authors equally contributed to the work

Running title: Fat laden macrophages in NASH.

Word count: Abstract – 241, Whole manuscript - 3436

Figures: 5, References: 30

Corresponding Author:

Prof. Emanuele Albano, Department of Health Science, University "Amedeo Avogadro" of East Piedmont, Via Solaroli 17, 28100 Novara, Italy. Tel. +39 0321 660642 Fax +39 0321 620421; E-mail: emanuele.albano@med.unipmn.it

Abstract

Background & Aims: Nonalcoholic steatohepatitis (NASH) is characterized by extensive hepatic monocyte infiltration and monocyte-derived macrophages have an important role in regulating the disease evolution. However, little is known about the functional changes occurring in liver macrophages during NASH progression. In this study we have investigated phenotypic and functional modifications of hepatic macrophages in experimental NASH.

Methods: NASH was induced by feeding C57BL/6 mice with a methionine-choline deficient (MCD) diet up to 8 weeks.

Results: In mice with steatohepatitis liver F4/80-positive macrophages increased in parallel with the disease progression and formed small clusters of enlarged and vacuolized cells. At immunofluorencesce these cells contained lipid vesicles positive for the apoptotic cell marker Annexin V suggesting the phagocytosis of apoptotic bodies derived from dead fat-laden hepatocytes. Flow cytometry revealed that these enlarged macrophages expressed inflammatory monocyte (CD11b, Ly6C, TNF-α) markers. However, as compared to regular size macrophages the enlarged sub-set was characterized by an enhanced production of the anti-inflammatory mediators IL-10 and annexin A1. Similar vacuolized macrophages producing annexin A1 were also evident in liver biopsies of NASH patients. In mice with NASH, the accumulation of enlarged F4/80^{+} cells paralleled with a decline in the expression of the macrophage M1 activation markers iNOS IL-12 and CXCL10, while the levels of M2 polarization markers arginase-1 and MGL-1 were unchanged.

Conclusions: Altogether, these data indicate that during the progression of NASH fat accumulation within liver macrophages promotes functional changes that can influence hepatic inflammatory responses.

Keywords: Nonalcoholic fatty liver disease, macrophages, annexin A1, liver inflammation.

Introduction

Growing evidence indicates that macrophages are important players in the evolution of hepatic inflammation in NASH. At the onset of the disease Kupffer cell activation in response of lipid accumulation significantly contributes to the production of pro-inflammatory mediators and by releasing chemokines such as CCL1, CCL2, CCL5 which stimulate the liver infiltration by circulating $Ly6C^{high}$ monocytes [1,2]. These latter rapidly differentiates to M1 polarized macrophages further contributing in expanding inflammatory responses [3]. Moreover, macrophage interaction with $CD4^+$ helper T-lymphocytes and NKT cells has an important role in sustaining lobular inflammation during the disease progression [4,5]. Accordingly, Kupffer cell depletion at the onset of NASH or the interference with monocyte recruitment through CCL2/CCR2 signaling prevents hepatic injury and inflammation in experimental models of NASH [6,7]. What is less clear is how liver macrophages behave during the disease progression particularly in relation with the development of fibrosis [8]. Recent studies have pointed out that hepatic macrophages in human NASH, but not in patients with simple steatosis often cluster around lipid droplets forming crown-like aggregates similar to those present in the inflamed visceral adipose tissue of obese patients [9-11]. Furthermore, these macrophages appeared enlarged and contained lipid vesicles resembling foam cells in atherosclerotic plaques [11]. Interestingly, clusters of foamy macrophages are also evident in several mice models of experimental NASH where they are associated with the severity of hepatic fibrosis [12]. These observations prompted us to better characterize the possible origin of foamy macrophages associated with NASH and their significance in relation to the disease evolution.

Material and Methods

Animals and Experimental protocol. Eight weeks old male C57BL/6 mice were purchased from Harlan-Nossan (Corezzana, Italy) and fed for 4 or 8 weeks with either methionine-choline deficient (MCD) or control diets (Laboratorio Dottori Piccioni, Gessate, Italy). The experimental protocols were approved by the University Commission for Animal Care and by the Italian Ministry of Health according to the current law for the use of laboratory animals.

Biochemical analysis. Plasma ALT and liver triglycerides were determined by spectrometric kits supplied by Radim S.p.A. (Pomezia, Italy) and Sigma Diagnostics (Milano, Italy), respectively. Circulating IL-12 was evaluated by a commercial ELISA kit R&D Systems (Abingdon, UK).

Histology and immunohistochemistry.

Liver biopsies from NASH patients were available from the Pathology Unit of the Ospedale Maggiore della Carità of Novara. Liver macrophages were identified in formalin-fixed sections using either anti-mouse F4/80 or anti-human CD68 antibodies (eBioscience, San Diego CA, USA) in combination with peroxidase-linked goat anti-rat IgG or horse-radish peroxidase polymer kit (Biocare Medical, Concord, CA, USA). AnxA1 producing cells were detected using specific antibodies from Zymed Laboratories-Invitrogen (Carlsbad, CA, USA). Hepatic collagen deposition was evidenced by Picro-Sirius Red staining. Activated hepatic stellate cells were identified in formalin-fixed sections using anti-mouse α-smooth muscle actin (α-SMA) polyclonal antibodies (Labvision, Bio-Optica, Milan, Italy) in combination with peroxidase-linked goat anti-rat IgG and horse-radish peroxidase polymer kit (Biocare Medical, Concord, CA, USA). Immunofluorescence analysis were performed in frozen mice liver sections using fluorescin-labelled annexin 5 (Roche Diagnostics, Penzberg, Germany) and Texas Red-labelled goat anti-rat IgG antibodies (Sigma, Milan, Italy).

mRNA extraction and Real time PCR. Liver RNA was retro-transcripted with High Capacity cDNA Reverse Transcription Kit (Applied Biosystems Italia, Monza, Italy). RT-PCR was performed in a Techne TC-312 termalcycler (TecneInc, Burlington NJ, USA) using TaqMan Gene Expression Master Mix and TaqMan Gene Expression probes for mouse TNF-α, IL-1β, IL-12p40, iNOS, arginase-1, MGL-1, and beta-actin (Applied Biosystems Italia, Monza, Italy). All samples were run in duplicate and the relative gene expression was calculated as $2^{-\Delta Ct}$ and expressed as fold increase over control samples.

Isolation and purification of liver macrophages. Liver macrophages were isolated from the livers of either controls or MCD-fed mice by collagenase perfusion according to Froh et al. [13] and purified using biotinylated anti-F4/80 antibodies (eBiosciences, San Diego CA, USA) and streptavidin-coated magnetic beads (Miltenyi Biotec, Germany). Cell purity, as estimated by flow cytometry following immunostaining for CD45 and F4-80, was above 85%. The cells were processed for mRNA extraction using ChargeSwitch® Total RNA Cell Kit (Invitrogen, Frederick, MD, USA).

Isolation of intrahepatic mononucleated cell and flow cytometry analysis. Liver mononucleated cells were isolated from the livers of naive and MCD-fed mice and purified on a density gradient (Lympholyte®-M, Cedarlane Laboratoires Ltd. Burlington, Canada) as described in [14]. Cells were then washed with Hank's medium and incubated 30 min with de-complemented mouse serum to block unspecific immunoglobulin binding. The cells were then stained with fluorochrome-conjugated antibodies for CD45, CD11b, Ly6C, MHCII

(eBiosciences, San Diego CA, USA), F4/80 (Invitrogen, Abingdon, UK) and analyzed with a FACScalibur (Becton Dikinson, Franklin Lakes, NJ, USA) flow cytometer. Intracellular staining for TNF-α, IL-12, and IL-10 was perfomed using specific fluorochrome-conjugated antibodies supplied by (eBiosciences, San Diego CA, USA). AnxA1-producing cells were detected using a polyclonal anti-AnxA1 rabbit antiserum (Millipore, Temecula, CA, USA) and phycoerythrin-conjugated anti-rabbit IgG (Sigma-Aldrich, Milan,Italy).

Data analysis and statistical calculations. Statistical analyses were performed by SPSS statistical software (SPSS Inc. Chicago IL, USA) using one-way ANOVA test with Tukey's correction for multiple comparisons or Kruskal-Wallis test for non-parametric values. Significance was taken at the 5% level. Normality distribution was preliminary assessed by the Kolmogorov-Smirnov test.

Results.

Steatohepatitis in mice receiving the methionine-choline deficient (MCD) diet was characterized by a time dependent worsening of liver histology, triglyceride accumulation and transaminase release that led to appreciable fibrosis after 8 weeks of treatment (Supplementary Fig. 1). In these animals, immunohistochemistry for the monocyte/macrophage marker F4/80 evidenced that the livers of MCD-fed mice showed the diffuse presence of small clusters of enlarged and vacuolized macrophages that were particularly evident after 8 weeks of treatment (Fig. 1). Double staining of frozen sections with anti-F4/80 antibodies and the lipid dye Oil Red O confirmed that the cytoplasmic vacuoles contained lipid droplets (Fig. 1). Furthermore, a fraction of the cytoplasmic vacuoles in F4/80^{+} cells were also stained with the apoptotic cell marker annexin 5 (Fig. 1), suggesting the phagocytosis of apoptotic bodies originating from dying fat-laden hepatocytes. In line with these findings, flow cytometry analysis of hepatic mononuclear cells from controls or MCD-fed mice evidenced a steadily increase in F4/80-positive cells during the progression of NASH (Fig. 2). In parallel, we observed that among F4/80^{+} cells the fraction of enlarged cells, as evidenced by high forward scatter (FSC-H) parameter, also significantly increased in the livers of animals with more advanced disease (Fig. 2). Further characterization of high volume macrophages associated with NASH revealed that these cells had an enhanced expression of leucocyte activation markers CD11b (CD18b) and CD11c (CD18) as well as of Class II Major Histocompatibility Complex (MHCII) (Fig. 2). Furthermore, enlarged F4/80^{+} cells associated with NASH were prevalently Ly6C^{high} indicating their origin from circulating inflammatory monocytes (Fig. 2).

Previous studies have shown that lipid-laden macrophages in NASH had pro- inflammatory features and stained positive for myeloperoxidase and TNF-α [9]. Accordingly, we observed that enlarged F4/80$^+$ cells had an increased TNF-α expression (Supplementary Fig. 2). However, their accumulation during the progression of experimental NASH was associated with complex changes in hepatic inflammatory pattern. In fact, while the liver mRNAs for TNF-α and IL-1β increased steadily with the disease progression, the expression of macrophage M1 activation markers such as inducible NO synthase (iNOS), IL-12p40 sub-unit and CXCL10 peaked in mice receiving the MCD diet for 4 weeks and declined thereafter (Supplementary Fig. 3). In line with these findings, macrophages isolated from the livers of MCD-fed mice at different stages of the disease showed that iNOS and IL-12p40 expression was significantly lower in the cells obtained from mice with advanced NASH as compared to those in the early phase of the disease (Fig. 3). The same pattern was also confirmed by evaluating IL-12-producting F4/80$^+$ cells with flow cytometry as well as by measuring circulating IL-12 levels (Fig. 3). On the other hand, macrophage expression of the M2 polarization markers arginase-1 and galactose-type C-type lectin-1 (MGL-1/CD301) was not affected during NASH progression (Fig. 3).

To get more inside in this phenomenon we measured macrophage production of anti-inflammatory protein such as interleukin-10 (IL-10) and annexin A1 (AnxA1) that modulates hepatic inflammation in NASH [15-17]. Flow cytometry showed that the prevalence of hepatic macrophages producing IL-10 and AnxA1 was increased among F4/80$^+$ cells isolated from 8 weeks MCD-fed mice (Fig. 4). Interestingly, the expression of both these anti-inflammatory mediators was 3-7 folds higher in the enlarged F4/80$^+$ cell sub-set (Fig. 4), while IL-12-producing macrophages did not show appreciable volume-related differences (not shown). This indicated that autocrine/paracrine loops involving AnxA1 and IL-10 released by enlarged lipid-laden macrophages can down-regulate M1-polarized responses. According to previous studies [9-12], enlarged vacuolated macrophage with morphology comparable to those detected in the livers of MCD-fed mice were also detected by CD68 immunostaining of liver biopsies from NASH patients (Fig. 5). These same cells were also selectively stained with anti-AnxA1 antibodies (Fig. 5), confirming that also in human NASH lipid-laden macrophages contribute to AnxA1 production.

Discussion

Small macrophages clusters around lipid vesicles or surrounding fat-containing hepatocytes, commonly referred as lipogranulomas, are often detectable in human NASH [18] as well as in many experimental models of the disease [12]. The macrophages in these clusters are enlarged and have a foamy appearance due to the accumulation of cytoplasmic lipid droplets and cholesterol crystals [11]. These histological features are reminiscent of crown-like structures detectable in adipose tissue of obese subjects who are characterized by macrophage aggregates surrounding dead adipocytes and scavenging cells debris and residual lipids [19]. Although fat-laden macrophages in the crown-like structures have been associated with the evolution of adipose tissue inflammation [20], the actual significance of similar cells in NASH is less well defined.

The recruitment of circulating monocyte through CCL2/CCR2 signaling is considered the main responsible for the expansion of liver macrophage pool in NASH [8,21]. Circulating monocytes are currently differentiated in two sub-sets. The first include inflammatory monocytes characterized as $Ly6C^{high}/CCR2^{+}/CX3CR1^{-}$ in mice or $CD14^{+}/CD16^{-}$ in humans that migrate to tissues in early phase of the response to injury producing pro-inflammatory mediators [22]. The second population, defined as $Ly6C^{-}/CCR2^{-}/CX3CR1^{+}$ in mice or $CD14^{-}/CD16^{+}$ in humans has less characterized functions and it is though to contribute to tissue healing [21,22]. Immunohistochemical studies in human liver biopsies have shown that fat-laden macrophage in NASH express leucocyte activation marker CD11b and CD11c along with TNF-α and myeloperoxidase suggesting pro-inflammatory capability [9,12]. Our present data add on these findings by showing that beside an increased expression of the CD11b, CD11c, enlarged macrophages associated with NASH are prevalently $Ly6C^{high}$, indicating their origin from circulating $Ly6C^{high}/CCR2^{+}$ monocytes. However, in spite showing an up-regulation of TNF-α, these same cells display an increased production of the anti-inflammatory mediators annexin A1 (AnxA1) and IL-10. Interestingly, AnxA1 is also selectively expressed by enlarged vacuolized $CD68^{+}$ macrophages in liver biopsies from NASH patients. AnxA1 is a 37 kDa calcium-phospholipid-binding protein that is produced by myeloid cells in response to glucocorticoids [22]. By interacting with its receptor formyl peptide receptor 2/Lipoxin A_4 receptor (FPR2/ALX) AnxA1 down-regulates the production of pro-inflammatory mediators such eicosanoids, NO and IL-6 and promotes IL-10 production [23,24].

Macrophage phagocytosis of apoptotic bodies is known to be an important mechanism in the termination of acute inflammation as it promotes the release of a variety of mediators involved in reducing phagocyte recruitment/activation and promoting tissue healing [25,26]. We have observed that annexin 5 binds to intracellular lipid vesicles in F4/80^{+} cells, suggesting the phagocytosis of apoptotic fat-laden hepatocytes. Indeed, hepatocyte apoptosis is a common feature in NASH as a result of lipotoxicity and endoplasmic reticulum stress [27,29]. Furthermore, intracellular lipid accumulation in foam cells of atherosclerotic plaques has also been shown to promote macrophage functional changes by stimulating liver X receptors (LXPs) and peroxisome proliferator activated receptors (PPARs) [29]. Thus, is possible that the clearance of apoptotic bodies along with lipid accumulation might lead to partial reprogramming of liver fat-laden macrophages with the co-expression of both pro- and anti-inflammatory mediators. This is line with recent observations showing that following acute liver injury infiltrating Ly6C^{high} macrophages express AnxA1 along with cyclooxygenase-2 [30].

As a result of AnxA1 and IL-10 up-regulation in enlarged lipid-laden macrophages we have observed a down-modulation of liver M1-polarized responses, suggesting that AnxA1 and IL-10 act in an autocrine/paracrine loop affecting pro-inflammatory responses by hepatic macrophages. Accordingly, we have recently reported that the induction of NASH in AnxA1-deficient mice is characterized by enhanced lobular inflammation due to increased macrophage recruitment and the exacerbation of the M1 phenotype [17]. Furthermore, Wan and co-workers [16] have shown that in mice with NAFLD IL-10 secretion promotes the apoptosis of M1-activated macrophage and that this contributes to hamper the severity of lobular inflammation.

In conclusion, our data indicate that during the progression of NASH the accumulation of fat-laden macrophage within liver promotes functional changes that influence hepatic inflammatory responses.

Acknowledgements

This work has been supported by a grant from the Fondazione Cariplo (Milan).

References

1. Tosello-Trampont AC, Landes SG, Nguyen V, Novobrantseva TI, Hahn YS. Kuppfer cells trigger nonalcoholic steatohepatitis development in diet-induced mouse model through tumor necrosis factor-α production. J Biol Chem. 2012;287:40161-40172.

2. Leroux A, Ferrere G, Godie V, Cailleux F, Renoud ML, Gaudin F, et al. Toxic lipids stored by Kupffer cells correlates with their pro-inflammatory phenotype at an early stage of steatohepatitis. J Hepatol. 2012;57:141-149.

3. Maina V, Sutti S, Locatelli I, Vidali M, Mombello C, Bozzola C, et al. Bias in macrophage activation pattern influences non-alcoholic steatohepatitis (NASH) in mice. Clin Sci (Lond) 2012; 122:545-553.

4. Sutti S, Jindal A, Locatelli I, Vacchiano M, Gigliotti L, Bozzola C, et al. Adaptive immune responses triggered by oxidative stress contribute to hepatic inflammation in NASH. Hepatol. 2014;59:886-897.

5. Wehr A, Baeck C, Heymann F, Niemietz PM, Hammerich L, Martin C, et al. Chemokine receptor CXCR6-dependent hepatic NK T Cell accumulation promotes inflammation and liver fibrosis. J Immunol. 2013;190:5226-5236.

6. Baeck C, Wehr A, Karlmark KR, Heymann F, Vucur M, Gassler N, et al. Pharmacological inhibition of the chemokine CCL2 (MCP-1) diminishes liver macrophage infiltration and steatohepatitis in chronic hepatic injury. Gut. 2012;61:416-426.

7. Miura K, Yang L, van Rooijen N, Ohnishi H, Seki E. Hepatic recruitment of macrophages promotes nonalcoholic steatohepatitis through CCR2. Am J Physiol Gastrointest Liver Physiol. 2012;302:G1310-G1321.

8. Tacke F, Zimmermann HW. Macrophage heterogeneity in liver injury and fibrosis. J Hepatol. 2014;60:1090-1096.

9. Rensen SS, Slaats Y, Nijhuis J, Jans A, Bieghs V, Driessen A, Malle E, Greve JW, Buurman WA. Increased hepatic myeloperoxidase activity in obese subjects with nonalcoholic steatohepatitis. Am J Pathol. 2009;175:1473-82.

10. Caballero T, Gila A, Sánchez-Salgado G, Muñoz de Rueda P, León J, Delgado S, Muñoz JA, Caba-Molina M, Carazo A, Ruiz-Extremera A, Salmerón J. Histological and immunohistochemical assessment of liver biopsies in morbidly obese patients. Histol Histopathol. 2012;27:459-66.

11. Ioannou GN, Haigh WG, Thorning D, Savard C. Hepatic cholesterol crystals and crown-like structures distinguish NASH from simple steatosis. J Lipid Res. 2013;54:1326-34.

12. Itoh M, Kato H, Suganami T, Konuma K, Marumoto Y, Terai S, Sakugawa H, Kanai S, Hamaguchi M, Fukaishi T, Aoe S, Akiyoshi K, Komohara Y, Takeya M, Sakaida I, Ogawa Y. Hepatic crown-like structure: a unique histological feature in non-alcoholic

steatohepatitis in mice and humans. PLoS One. 2013;8:e82163. doi: 10.1371/journal.pone.0082163.

13. Froh M, Konno A, Thurman RG. Isolation of Kupffer cells. Currents Protocols in Toxicology 2002;14.4.1-14.4.12.

14. Crispe NI. Isolation of mouse intrahepatic lymphocytes. In: Current Protocols in Immunology.1997;3.21.1-321.8.

15. Wan J, Benkdane M, Teixeira-Clerc F, Bonnafous S, Louvet A, Lafdil F, Pecker F, Tran A, Gual P, Mallat A, Lotersztajn S, Pavoine C. M2 Kupffer cells promote M1 Kupffer cell apoptosis: a protective mechanism against alcoholic and nonalcoholic fatty liver disease. Hepatol. 2014;59:130-42.

16. Moschen AR, Wieser V, Tilg H. Adiponectin: key player in the adipose tissue-liver crosstalk. Curr Med Chem. 2012;19:5467-73.

17. Locatelli I, Sutti S, Jindal A, Vacchiano M, Bozzola C, Reutelingsperger C, et al. Endogenous annexin A1 is a novel protective determinant in nonalcoholic steatohepatitis in mice. Hepatol. 2014;60:531-544.

18. Brunt EM, Pathology of non-alcoholic fatty liver disease. Nat Rev Gastroenterol Hepatol 2010; 7:195-203.

19. Shapiro H, Pecht T, Shaco-Levy R, Harman-Boehm I, Kirshtein B, Kuperman Y, Chen A, Blüher M, Shai I, Rudich A. Adipose tissue foam cells are present in human obesity. J Clin Endocrinol Metab. 2013;98:1173-81.

20. McNelis JC, Olefsky JM. Macrophages, immunity, and metabolic disease. Immunity. 2014 Jul 17;41(1):36-48.

21. Zimmermann HW, Trautwein C, Tacke F. Functional role of monocytes and macrophages for the inflammatory response in acute liver injury. Front Physiol 2012;3:doi: 10.3389/fphys.2012.00056.

22. Murray PJ, Wynn TA. Protective and pathogenetic functions of macrophage subsets. Nat rev Immunol 2011;11:723-737.

23. Perretti M, D'Acquisto F. Annexin A1 and glucocorticoids as effectors of the resolution of inflammation. Nat Rev Immunol. 2009;9:62-70.

24. Cooray SN, Gobbetti T, Montero-Melendez T, McArthur S, Thompson D, Clark AJ, et al. Ligand-specific conformational change of the G-protein-coupled receptor ALX/FPR2 determines pro-resolving functional responses. Proc Natl Acad Sci U S A. 2013;110:18232-18237.

25. Ariel A, Timor O. Hanging in the balance: endogenous anti-inflammatory mechanisms in tissue repair and fibrosis. J Pathol. 2013;229:250-263.

26. Ortega-Gómez A, Perretti M, Soehnlein O. Resolution of inflammation: an integrated view. EMBO Mol Med. 2013;5:661-674.

27. Leamy AK, Egnatchik RA, Young JD. Molecular mechanisms and the role of saturated fatty acids in the progression of non-alcoholic fatty liver disease. Prog Lipid Res 2013;52:165-174. Antioxid Redox Signal 2011;15:505-521.

28. Gentile CL, Frye M, Pagliasotti MJ. Endoplasmic reticulum stress and unfolded protein response in nonalcoholic fatty liver disease

29. Leitinger N, Schulman IG. Phenotypic polarization of macrophages in atherosclerosis. Arterioscler Thromb Vasc Biol 2013;33:1120-1126.

30. Zigmond E, Samia-Grinberg S, Pasmanik-Chor M, Brazowski E, Shibolet O, Halpern Z, et al. Infiltrating monocyte-derived macrophages and resident Kupffer cells display different ontogeny and functions in acute liver injury. J Immunol. 2014;193:344-353.

Figure 1. Morphological changes in liver macrophages during the evolution of steatohepatitis.

Mice were fed methionine-choline supplemented (Cont) or deficient (MCD) diets over an 8-week time period. (Panel A) Hepatic macrophages were evidenced by immunohistochemical staining with anti-F4/80 antibodies (magnification 40x). (Panel B) Double staining of frozen liver sections with the lipid dye Oil Red O (red) and anti-F4/80 antibody (green immunofluorescence; magnification 40x). (Panel C) Co-localization of macrophages F4/80 immunostaining (red) and annexin 5 (green) in frozen liver section from NASH livers. Cell nuclei were courter-stained with DAPI. Images are representative of 3-4 distinct samples.

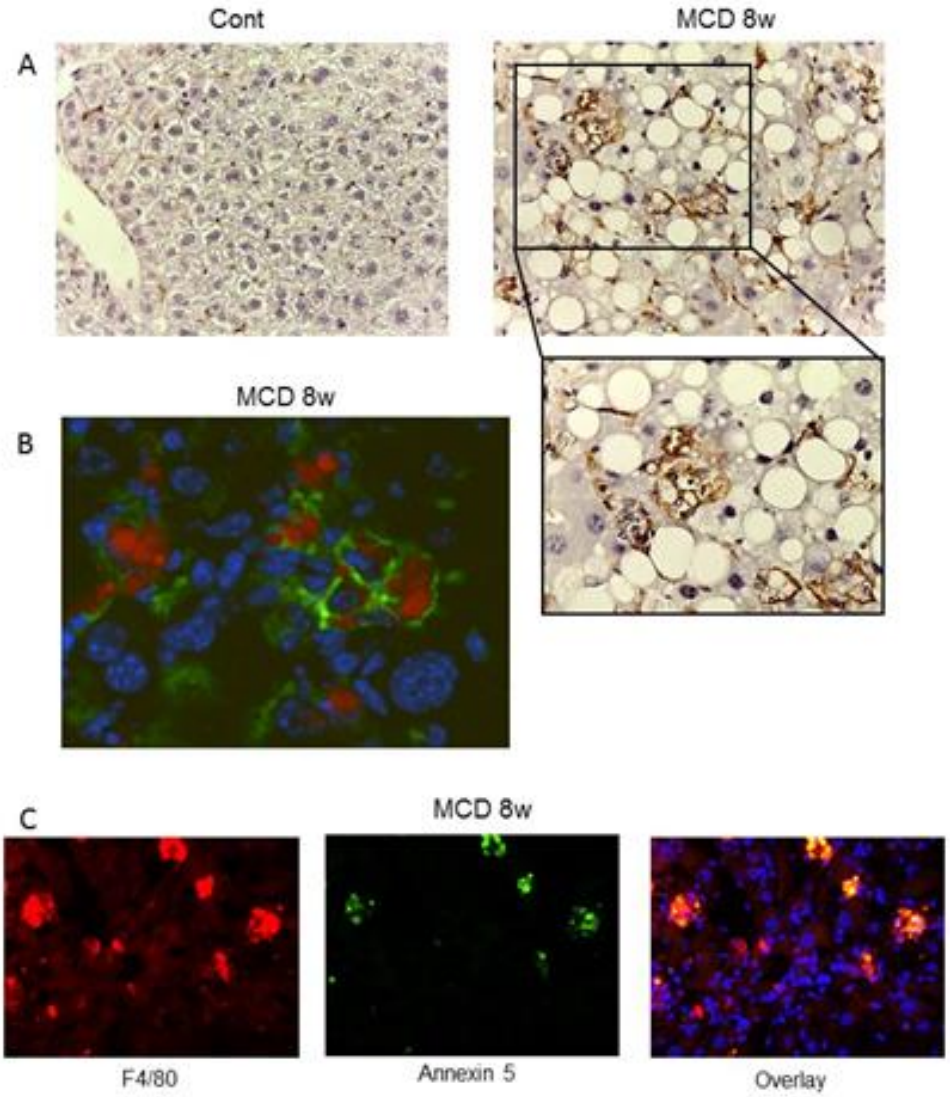

Figure 1

Figure 2: Flow cytometry analysis of hepatic macrophages during the evolution of steatohepatisis.

$CD45^+$ mononucleated cells were isolated from the livers of mice fed methionine-choline supplemented (Cont) or deficient (MCD) diets over an 8-week time period. (Panel A) $F4/80^+$ macrophages were analyzed for cell volume (forward scatter; FSC-H) and the monocyte marker Ly6C distribution. The percent values refers to the number of cells gated as $F4/80^+$. The data were from 3-4 animals per group. (Panel B) expression of leucocyte activation markers CD11b (CD18b), CD11c (CD18) and Class II Major Histocompatibility Complex (MHCII) among regular or enlarged $F4/80^+$ cells. Dotted lines refer to isotypic controls. One experiment representative of three.

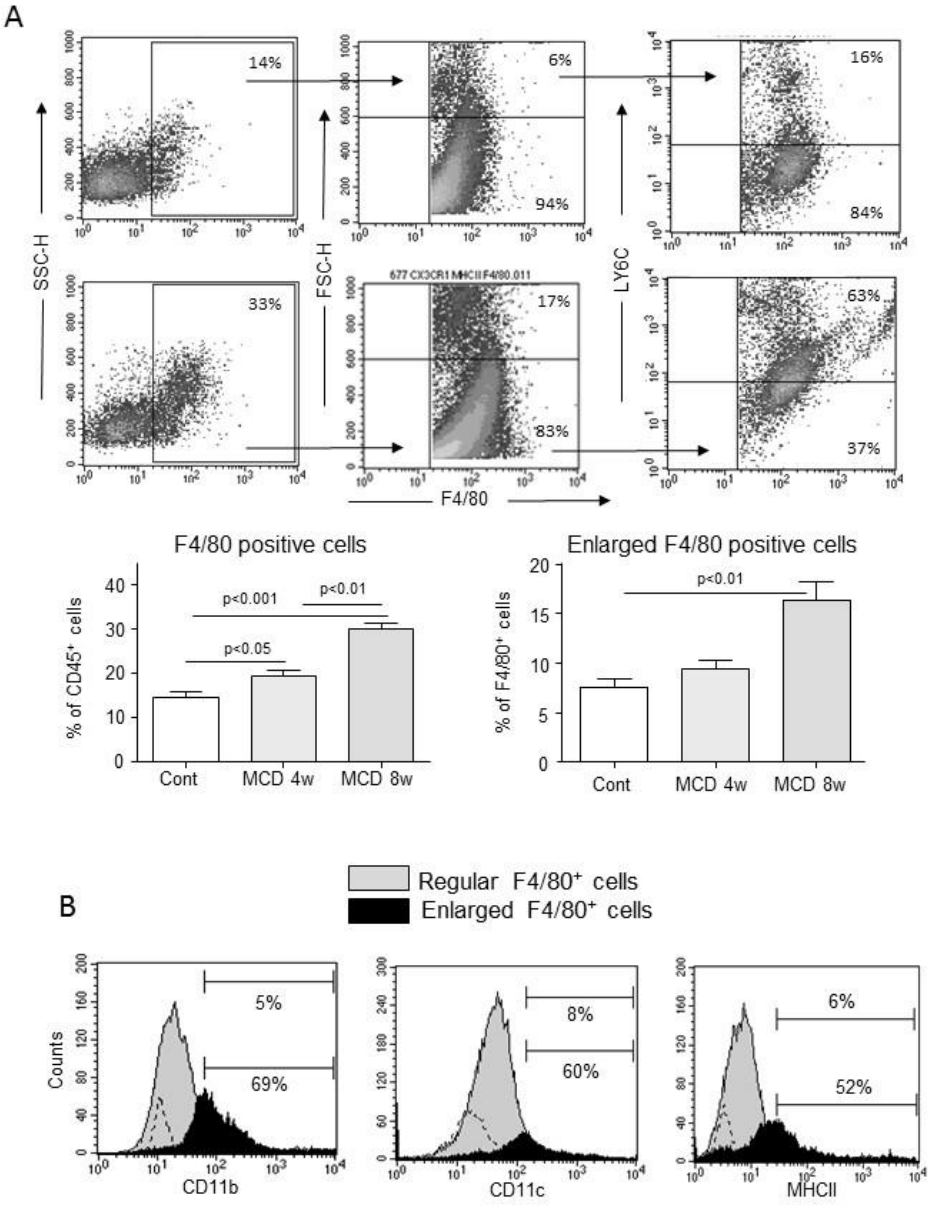

Figure 2

Figure 3. The evolution of steatohepatits is associated with a down-modulation in the M1 activation of liver macrophages.

Mice were fed methionine-choline supplemented (Cont) or deficient (MCD) diets over an 8-week time period. (Panels A-D) Isolated intrahepatic F4/80^{+} macrophages were evaluated for the expression of M1 activation markers inducible NO-synthase (iNOS) and IL-12p40 and of the M2 polarization markers galactose-type C-type lectin-1 (MGL-1) and arginase-1 were evaluated by RT-PCR. The RT-PCR values are expressed as fold increase over control values after normalization to the β-actin gene. The data are from 4 animals per group. (Panel E) Intracellular IL-12 expression was evaluated by flow cytometry in liver CD45^{+}/F4/48^{+} mononucleated cells isolated at different time points. One experiment representative of three. (Panel F) Circulating IL-12 levels were determined control and MCD fed mice by immunoenzymatic assay. The data are from 5-6 animals per group; boxes include the values within 25th and 75th percentile, while the horizontal bars represent the medians. The extremities of the vertical bars (10th-90th percentile) comprise the eighty percent of the values.

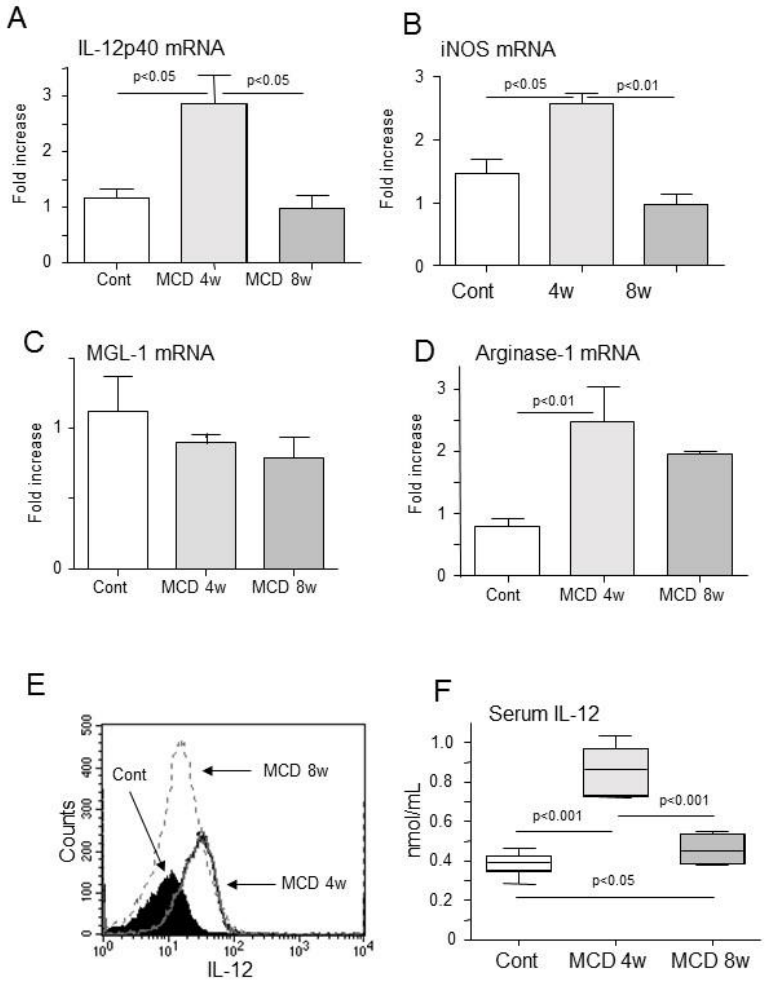

Figure 3

Figure 4: Enlarged macrophages associated with the advanced phases of steatohepatitis shows increased production of anti-inflammatory mediators interleukin-10 (IL-10) and annexin A1 (AnxA1).

$CD45^+$ mononucleated cells were isolated from the livers of mice fed methionine-choline supplemented (Cont) or deficient (MCD) diets over an 8-week time period. (Panel A) Dotted lines refer to isotypic controls. $F4/80^+$ macrophages were analyzed for the production of IL-10 and AnxA1. (Panel B) Expression of IL-10 and AnxA1 among regular or enlarged $F4/80^+$ cells. The percent values refers to the number of cells gated as $F4/80^+$. The data were from 3-4 animals per group.

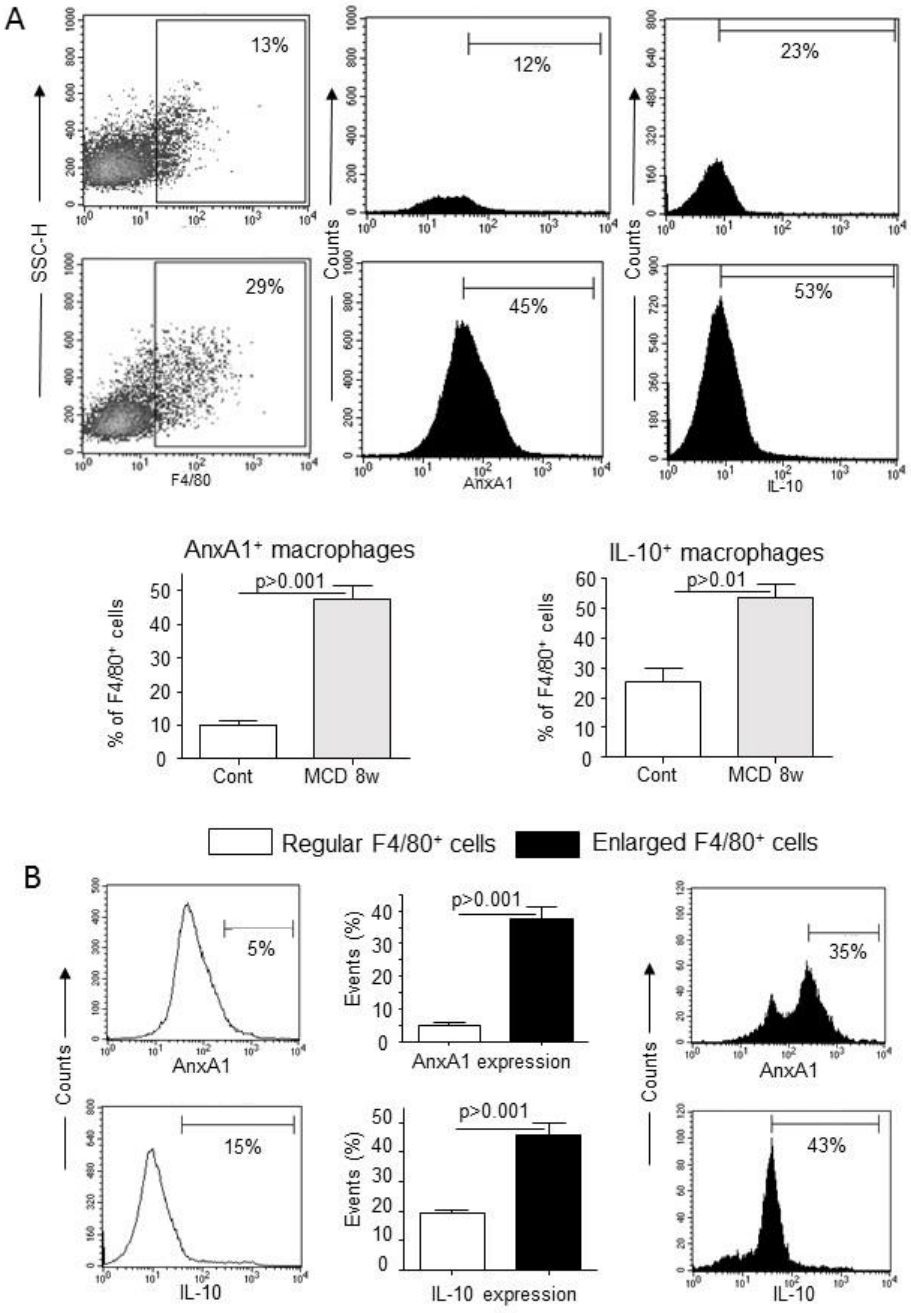

Figure 4

Figure 5: Immunohistochemical detection of enlarged-foamy macrophages in human NASH.

Formalin-fixed sections of liver biopsies from NASH patients were immunostained with anti-human CD68 (Panel A) or anti-AnxA1 (Panel B) antibodies in combination with horse-radish peroxidase polymer kit (magnification 20x).

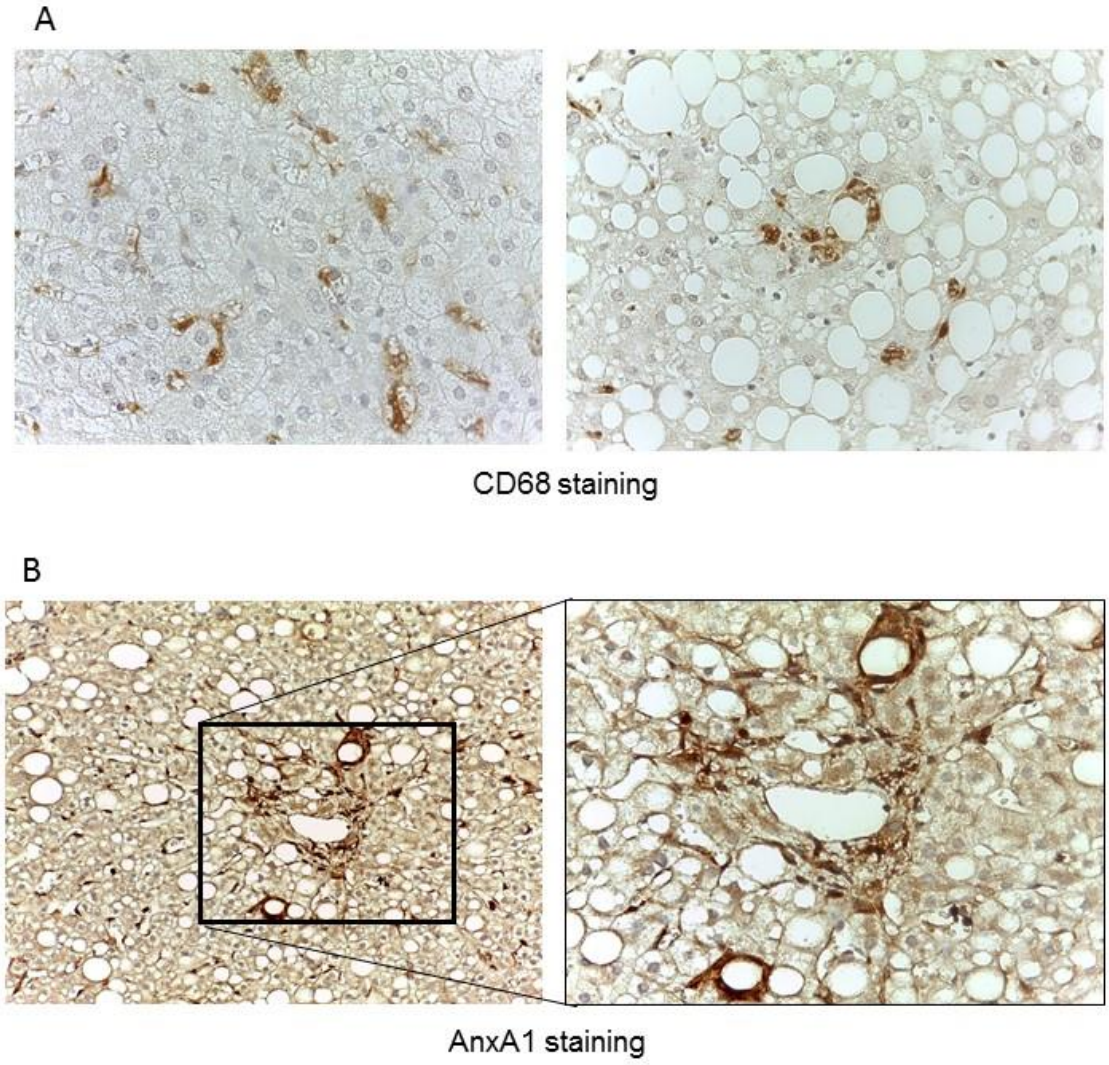

SUPPLEMENTARY MATERIAL

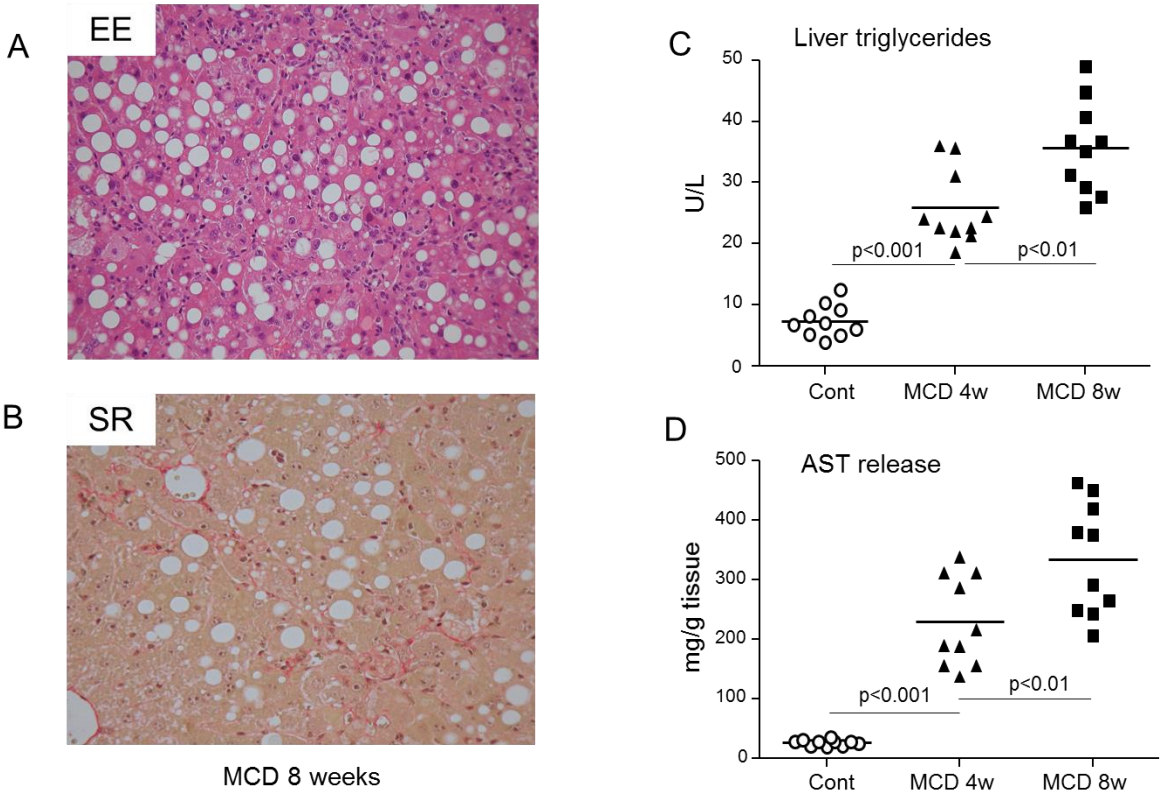

Supplementary Figure 1

Time dependent variations of hepatic injury and fibrogenesis during mice feeding with a methionine/choline deficient (MCD) diet.

Mice were fed methionine-choline supplemented (Cont) or deficient (MCD) diets over an 8-week time period. (Panels A-B) Liver histology was evaluated by hematoxilin/eosin (EE) and collagen Picro-Sirius Red (SR) staining of liver sections (magnification 200x) at the end of the treatment. (Panels C,D) Alanine aminotransferase (ALT) release, and hepatic triglyceride content were determined by enzymatic methods. The values refer to 5-6 animals per group.

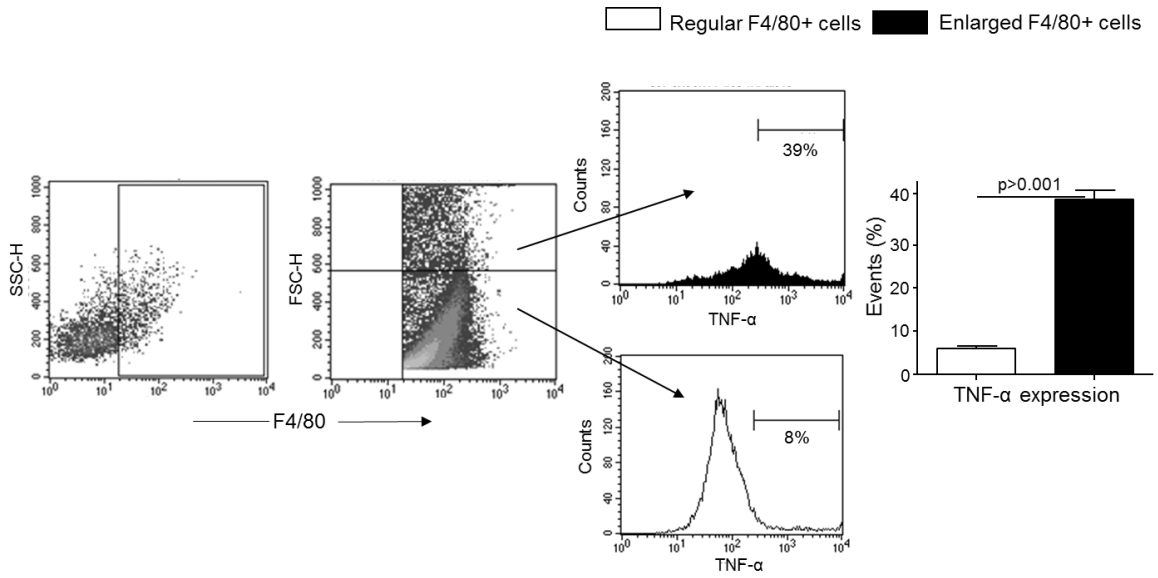

Supplementary Figure 2

Enlarged macrophages associated with the advanced phases of steatohepatitis shows an increased production of TNF-α.

$CD45^+$ mononucleated cells were isolated from the livers of mice fed methionine-choline supplemented (Cont) or deficient (MCD) diets over an 8-week time period. $F4/80^+$ macrophages were analyzed for the production of TNF-α among regular or enlarged cells. The percent values refers to the number of cells gated as $F4/80^+$. The data were from 3-4 animals per group.

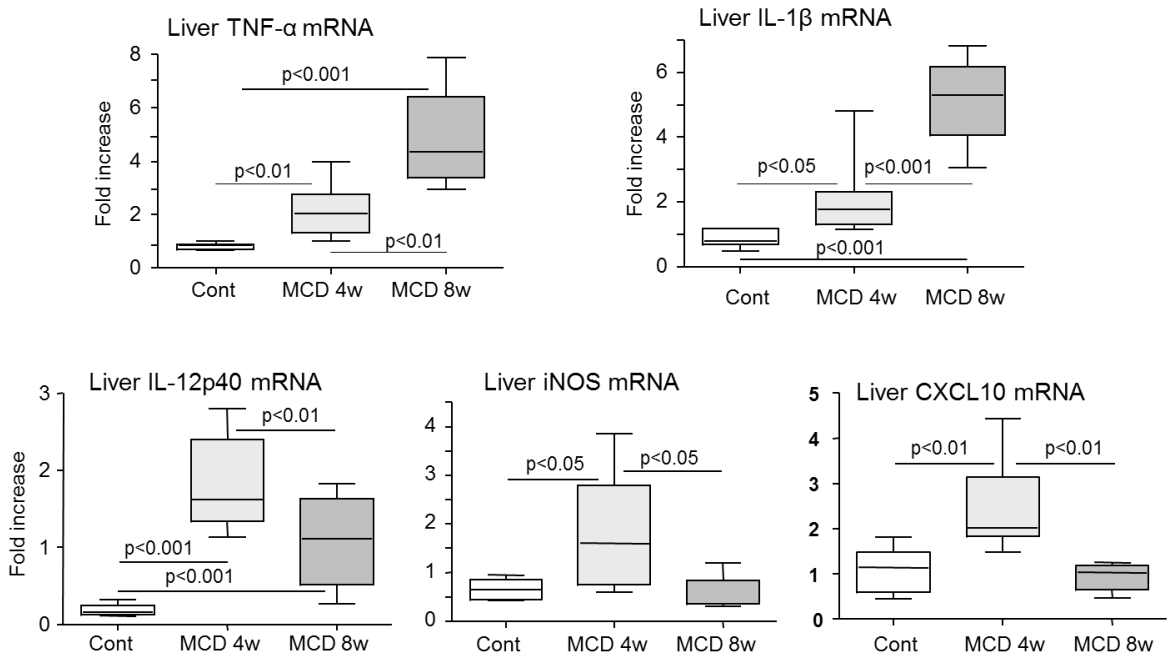

Supplementary Figure 3. The evolution of NASH is associated with a differential modulation of liver inflammatory markers.

Mice were fed methionine-choline supplemented (Cont) or deficient (MCD) diets over an 8-week time period. The hepatic expression of TNF-α, IL-1β, inducible NO-synthase (iNOS) and IL-12p40 and CXCL10 was evaluated by RT-PCR. The RT-PCR values are expressed as fold increase over control values after normalization to the β-actin gene. The data are from 5-6 animals per group; boxes include the values within 25th and 75th percentile, while the horizontal bars represent the medians. The extremities of the vertical bars (10th-90th percentile) comprise the eighty percent of the values.

9. Discussion

One limitation of the studies dealing with NAFLD/NASH pathogenesis relies in the fact that at present there is no universally accepted mouse model for the disease. In my studies I have used an experimental model based on the administration of a methionine choline deficient (MCD) diet model that induces in a rapid (three-four weeks) and reproducible manner steatohepatitis similar to human NASH and evolving to fibrosis within eight-ten weeks of treatment (Larter and Yeh 2008). However, this model lacks obesity and insulin resistance that are hallmarks of the human disease. A wide number of studies have shown that feeding rodents with a high fat diet leads, as in humans, to steatosis combined with subcutaneous and visceral obesity, insulin resistance and adipokine unbalances (Larter and Yeh 2008). However, in this experimental model, liver injury and inflammation are usually modest and fibrosis is very limited (Larter and Yeh 2008). As the aim of my work has been focalized to characterize the functional process connected with hepatic inflammation in NASH the MCD model was better suitable to such purposes in spite of its intrinsic limitations.

Lymphocytes represent along with macrophages the most frequent inflammatory cells in lobular and periportal infiltrates of NASH (Brunt 2010). Although growing evidence points on the importance of adaptive immunity in promoting adipose tissue inflammation in obesity (Sell and other 2012), so far little attention has been paid to the possible involvement of similar mechanisms in NASH. Oxidative stress is one of the features of NAFLD/NASH (Seki and others 2002; Chalasani and others 2004) and in previous studies we have observed that antibodies against lipid peroxidation-derived antigens are detectable in a dietary rat model of NAFLD as well as in patients with NAFLD/NASH (Albano and others 2005; Baumgartener et al 2008, Nobili and others 2010). In rodents, reducing lipid peroxidation by supplementation with the antioxidant N-acetylcysteine (NAC) prevents antibody response and ameliorates hepatic injury (Baumgartener et al 2008). The results presented in paper 1 extend these studies and demonstrate for the first time that, the onset of experimental NASH is characterized by the hepatic recruitment of both $CD4^+$ and $CD8^+$ T-lymphocytes. Both the lymphocyte subsets express CD69 activation marker and $CD4^+$ T-cells show an increased enhanced interferon-γ (IFN-γ) expression indicating that, as in the adipose tissue, adaptive immunity can contribute to hepatic inflammation during the progression of steatohepatitis. Beside lymphocyte recruitment, mice with NASH also show an increase of circulating IgG targeting lipid

peroxidation derived antigens. Interesting the same antigens are also recognized by hepatic T-cells confirming that oxidative stress can promote the activation of both cellular and humoral immunity in NASH. In both experimental and human NASH immune responses against malonyldialdehyde (MDA) derived adducts are predominant and the characterization of the epitopes recognized has revealed the involvement of cyclic methyl-1,4-dihydroxypyridine-3,5-dicarbaldehyde epitopes, also known as malonyldialdehyde-acetaldehyde (MAA) adducts (Albano and others 2005). These adducts originate by the combined interaction of lysine ε–aminogroups with both acetaldehyde and malonyldialdehyde (Thiele and others 2008) and represent important antigens in immune reactions toward lipid peroxidation-derived epitopes associated with alcoholic liver disease (ALD) in both humans and experimental animals (Xu and other 1998; Rolla and others 2000). Moreover, anti-MAA antibodies predict coronary artery disease in atherosclerotic patients (Anderson and others 2014). This latter analogy might have clinical relevance as growing evidence suggest that NAFLD/NASH and atherosclerosis might share common pathogenetic mechanisms and because NASH is associated with an increased rick of atherosclerosis ischemic complications (Biegs and other 2012).

The mechanisms by which hepatic oxidative stress can promote the activation of adaptive immune responses in NASH are still poorly understood. The liver is recognized to have unique immunological properties that modulate systemic tolerance to antigens from the portal circulation (Racanelli and Rehermann 2006; Crispe 2014). Under physiological conditions, Kupffer cells respond to low concentrations of endotoxins by producing interleukin-10 (IL-10) and low levels of pro-inflammatory mediators (TNF-α, ROS and prostanoids) that down-modulate the antigen presentation by dendritic and endothelial cells, thus suppressing T-cell activation (Crispe 2014). Such an effect is lost following liver injury because of macrophage and dendritic cell (DC) activation in response to damage associated molecular patterns (PAMPs) among which oxidized lipids and lipid peroxidation products (Racanelli and Rehermann 2006). On this latter respect, a recent study by Henning and co-workers (2013) has shown that the development of NASH in MCD-fed mice is associated with an early expansion in hepatic mature myeloid dendritic cells, which acquire the capacity to stimulate $CD4^+$ T-cells. Along with these observations, the data presented in paper 2 demonstrate that dendritic cell expansion in NASH involves a sub-set of cells featuring monocyte markers ($F4\text{-}80^{high}/Ly6C^{high}$) that are also characterized by CX_3CR1 expression, while the pools of $CD11c^{high}/MHCII^+/B220^+$ plasmocytoid and $CD11c^{high}/MHCII^+/CD8a^+$ lymphocytoid dendritic cells were significantly decreased. It is known that under inflammatory conditions

infiltrating monocytes can differentiate into a special sub-set of dendritic cells, called monocyte-derived inflammatory dendritic cells (moDCs) (Domininguez and Ardavin 2010). These cells co-express both dendritic and monocyte/macrophage surface markers and show a high production of inflammatory mediators combined to an efficient antigen presenting activity (Domininguez and Ardavin 2010). Thus, we propose that during the evolution of NASH a sub-set of $Ly6C^{high}$ monocytes/macrophages might acquire CX_3CR1 and differentiate to moDCs, which present oxidative stress-derived antigens to B- and $CD4^+$ T-lymphocytes and stimulate B-cell maturation to plasma cells. Moreover, dendritic cells can also cross-prime naïve $CD8^+$ T-lymphocytes promoting cell-mediated responses. Beside dendritic cells, antigen presentation might also involve hepatic stellate cells (Winau and others 2008) and possibly hepatocytes them self, as pro-inflammatory cytokines have been shown to induce the hepatocyte expression of class II major histocompatibility complex (MHC) and co-stimulatory CD80 (B7.1) molecules (Herkel, and others 2003). On the other hand, the metabolic changes leading to NAFLD can also influence the immune system as the development of obesity in mice fed a high fat/carbohydrate lowers regulatory T-cells (Tregs) in the liver (Ma and other 2007). This latter event is particularly important, as Tregs depletions contributes to the development of immune response to oxidative stress-derived antigens in atherosclerosis (George 2008). Furthermore, adipokine unbalances that characterize obesity may also influence immune responses, because adiponectin depresses both B-cell and T-cell activation, while leptin stimulates lymphocyte survival and proliferation (Tilg and Moschen 2006).

Concerning the mechanisms by which adaptive immunity may contribute to sustain hepatic inflammation in NASH our experiments using mice immunized with MDA adducts to stimulate B- and T cells responses (see paper 1) show that, at least in the early phase of the disease, $CD4^+$ T cells play a major role. In particular, the combined use of immunization and $CD4^+$ T-cell depletion with specific antibodies demonstrates that the production of IFN-γ and CD40 ligand (CD154) by Th-1 activated $CD4^+$ T-cells is responsible for stimulating M1 activation of hepatic macrophages. On their turn, by releasing IL-12, ROS and NO macrophages further contributes in promoting lymphocyte functions and oxidative stress. Interestingly, Th-1 activation is also a feature of $CD4^+$ T-cell responses to LDL oxidation antigens in atherosclerotic plaques (Hansson and Libby 2006) and interference with CD40/CD154 dyad reduces adipose tissue inflammation in obese mice (Poggi and others 2011). On the same vein, IFN-γ deficiency attenuates steatohepatitis and hepatic fibrosis in mice feed with a MCD diet (Lou and others 2013). The relevance of these findings in relation

to the human disease is supported by the observation that both paediatric and adult NASH are characterized by an increase in circulating IFN-γ-producing $CD4^+$ T-cells in conjunction with an enhanced liver IFN-γ expression (Inzaugarat and other 2011; Ferreyra Solari and others 2012). Although data in obese mice indicates that B-cell depletion reduces fat inflammation (DeFuria and other 2013), so far little is known about the role in humoral immunity in NASH. In this later respect, our preliminary data indicate that in MCD-fed mice the presence of anti-MDA IgG is associated with IgG deposition within the inflammatory infiltrates suggesting the possibility that these antibodies may contribute to hepatic damage by inducing antibody-dependent cytotoxicity or complement activation that in turn promote macrophage responses. Indeed, Rensen and co-workers (2009) have recently reported that extensive deposition of complement fractions in liver biopsies form NASH patients is associated with increased hepatocyte apoptosis, granulocyte infiltration and higher liver expression of IL-1β, IL-6 and IL-8 mRNAs. Thus, it is possible that humoral responses triggered by lipid peroxidation-derived antigens might have a role in NASH pathogenesis.

As discussed above Th-1 responses appears an important factor in driving hepatic inflammation in NASH by stimulating macrophage M1 responses. However, in paper 3 we report that this inflammatory pattern predominates only during the early phases of NASH, while upon the disease progression the development of fibrosis is associated to with a down-modulation of macrophage M1 activation. In parallel, we have observed that advanced NASH is characterized by an increased prevalence of enlarged fat-laden macrophages often forming small aggregates or crown-like structures around fat droplets. Macrophages with a similar morphology are also evident in liver biopsies from NASH patients (Rensen and others 2009: Ioannou and other 2013; Itoh and others 2013). Immunohystochemical studies in human liver biopsies have shown that these fat-laden macrophage contain cholesterol crystals and express leucocyte activation marker CD11b and CD11c along with TNF-α and myeloperoxidase suggesting pro-inflammatory capability (Rensen and others 2009: Ioannou and other 2013; Itoh and others 2013). Our results confirm the origin of fat-laden macrophages from circulating $Ly6C^{high}/CCR2^+$ inflammatory monocytes. However, in spite showing an up-regulation of TNF-α, these cells also display an increased production of the anti-inflammatory cytokines annexin A1 (AnxA1) and IL-10. This later effect can be particularly relevant in relation to the changes in hepatic inflammatory pattern, as we have previously shown that liver AnxA1 levels are progressively increased during the progression of NASH (Locatelli and others 2014). AnxA1 is a 37 kDa calcium-phospholipid-binding protein that is expressed in

myeloid cells in response to glucocorticoids (Perretti and D'Acquisto 2009). By interacting with its receptor formyl peptide receptor 2/Lipoxin A_4 receptor (FPR2/ALX) AnxA1 promotes IL-10 production and down-regulates macrophage secretion of pro-inflammatory mediators such eicosanoids, NO and IL-6 (Cooray and others 2013). Thus, we propose that the increased release of AnxA1 and IL-10 by enlarged lipid-laden macrophages can act in an autocrine/paracrine loop down-modulating M1-polarized responses in advanced NASH. Accordingly, we have recently reported that the induction of NASH in AnxA1-deficient mice is characterized by enhanced lobular inflammation due to increased macrophage recruitment and the exacerbation of the M1 phenotype (Locatelli and others 2014).

It is noteworthy that, in spite the decline of macrophage M1 responses, hepatic TNF-α production remains sustained even in advanced NASH where it parallels parenchymal injury. The results of paper 2 give a possible explanation for this apparent paradox. As mentioned above, the progression of NASH is in fact associated with hepatic infiltration of CX_3CR1-expressing monocyte-derived inflammatory dendritic cells (moDCs) that are characterized by an increase secretion of TNF-α. In this context, mice treatment with the H_2S donor NaHS selectively interferes with the up-regulation of CX_3CL1/CX_3CR1 dyad associated with the progression of steatohepatitis and blocks the development of TNF-α-producing CX_3CR1^{high} moDCs. This indicates that CX_3CL1/CX_3CR1 signaling might have an important role in the differentiation of inflammatory monocytes to moDCs. Furthermore, the use of NaHS allows defining the contribution of moDCs in sustaining hepatic inflammation during NASH progression. In fact, NaHS treatment prevents further elevation of transaminase release in the animals maintained on the MCD diet, demonstrating that CX_3CR1^{+} moDCs can contribute to the evolution of steatohepatitis not only through the stimulation of immune responses (Henning and others 2013), but also by directly sustaining hepatic TNF-α production. This is in line with the observation that TNF-α-producing dendritic cells sustain hepatic inflammation in other experimental models of liver injury (Connolly and others 2009) as well as during gut inflammation (Rivollier and others 2012).

A further aspect of cell interactions that characterize the progression of NASH involve NKT cells. Indeed, NKT expansion is one of the features of advanced NASH in both humans and rodents, while mice deficient in NKT cells show lower hepatic inflammation and fibrosis than while type littermates (Syn and others 2010; Tajiri and others 2009). We have observed that an increase in hepatic NKT cells is associated with the worsening of steatohepatitis in

immunized MCD-fed mice, as opposed to NKT cell depletion present in similarly treated naïve animals, further supporting the contribution of NKT cells to NASH progression. Changes in the macrophage production of CXCL16, a chemokine specifically involved in NKT cell recruitment along with increased hepatic levels of IL-15 have been proposed to modulate NKT pool in NASH (Kremer and others 2010; Wehr and others 2013). We have observed that IL-15 is selectively up-regulated in immunized MCD-fed mice concomitantly with stimulation in NKT cell recruitment, while $CD4^+$ T cell ablation significantly lowered the intrahepatic IL-15 mRNA. This suggests that Th-1 responses might promote the expansion of hepatic NKT cell pool through IL-15 up-regulation, which, in turn, can participate to the evolution of NASH. At present, the mechanisms by which NKT cells contribute to liver injury in NASH are still poorly understood. Syn and co-workers (2012) have proposed that osteopontin (OPN) generated by NKT cells can contribute to fibrosis in NASH. An up-regulation in liver OPN is evident in either humans and rodents with advanced NASH (Syn and others 2011; Syn and others 2012; Locatelli and other 2013), while OPN-deficient mice are protected against steatohepatitis and fibrosis induced by feeding the MCD diet (Sahai and others 2007; Syn and others 2011). In our hands, hepatic OPN content is specifically increased in MCD-fed immunized mice in concomitance with NKT cell recruitment and OPN-expressing NKT cells are evident in the livers of these animals. Thus, OPN might account for the stimulation in collagen deposition that is evident in these animals as OPN has been has been shown to directly stimulate collagen synthesis by hepatic stellate cells (HSCs) (Urtasum and others 2012) and to promote ductular reaction (Wang and other 2014).

10. Conclusions

The data presented indicate that immune responses triggered by oxidative stress-derived antigens can contribute to the progression of experimental NASH by promoting the Th-1 activation of $CD4^+$ T-lymphocytes that, in turn stimulates macrophage M1 responses and liver NKT cell recruitment. These data along with the observations in humans support the possible contribution of adaptive immunity in the mechanisms leading to NAFLD evolution.

Nonetheless, NAFLD progression to fibrosis is a complex process that involves multiple interactions between inflammatory cells. In particular, we have observed that macrophages progressively increase their number during NASH progression and change their phenotype and morphology. This associates with the down-modulation of M1 activation and the emergence of inflammatory dendritic cells that sustain inflammation during the advanced stage of the disease and likely promotes further expansion of adaptive immune responses. Altogether, these results represent a good starting point to investigate in more detail how the interactions between innate and adaptive immunity accounts for the inter-individual variability in the evolution of NAFLD/NASH. Furthermore, the results obtained with sulphide donor open the possibility to test these compounds as possible novel treatments to control NASH evolution.

11. References

Abdelmegeed MA, Banerjee A, Yoo SH, Jang S, Gonzalez FJ, Song BJ. 2012. Critical role of cytochrome P450 2E1 (CYP2E1) in the development of high fat-induced non-alcoholic steatohepatitis. J Hepatol 57(4):860-6.

Adams LA, Angulo P, Lindor KD. 2005. Nonalcoholic fatty liver disease. CMAJ 172(7):899-905.

Albano E, Mottaran E, Vidali M, Reale E, Saksena S, Occhino D, Burt AD, Day CP. Immune response toward lipid peroxidation products as a predictor of the progression of non-alcoholic fatty liver disease (NAFLD) to advanced fibrosis. Gut 2005;54:987-993.

Alexander B. 1998. The role of nitric oxide in hepatic metabolism. Nutrition 14(4):376-90.

Ali R, Cusi K. 2009. New diagnostic and treatment approaches in non-alcoholic fatty liver disease (NAFLD). Ann Med 41(4):265-78.

Alkhouri N, McCullough AJ. 2012. Noninvasive Diagnosis of NASH and Liver Fibrosis Within the Spectrum of NAFLD. Gastroenterol Hepatol (N Y) 8(10):661-8.

Anderson DR, Duryee MJ, Shurmur SW, Um JY, Bussey WD, Hunter CD, Garvin RP, Sayles HR, Mikuls TR, Klassen LW, Thiele GM. Unique antibody responses to malondialdehyde-acetaldehyde (MAA)-protein adducts predict coronary artery disease. PLoS One. 2014;9:e107440. doi: 10.1371/journal.pone.0107440.

Armutcu F, Akyol S, Ucar F, Erdogan S, Akyol O. 2013. Markers in nonalcoholic steatohepatitis. Adv Clin Chem 61:67-125.

Baeck C, Wehr A, Karlmark KR, Heymann F, Vucur M, Gassler N, Huss S, Klussmann S, Eulberg D, Luedde T, Trautwein C, Tacke F. 2012. Pharmacological inhibition of the chemokine CCL2 (MCP-1) diminishes liver macrophage infiltration and steatohepatitis in chronic hepatic injury. Gut 61(3):416-26.

Bahrami H, Daryani NE, Mirmomen S, Kamangar F, Haghpanah B, Djalili M. 2003. Clinical and histological features of nonalcoholic steatohepatitis in Iranian patients. BMC Gastroenterol 3:27.

Bambha K, Belt P, Abraham M, Wilson LA, Pabst M, Ferrell L, Unalp-Arida A, Bass N, Nonalcoholic Steatohepatitis Clinical Research Network Research G. 2012. Ethnicity and nonalcoholic fatty liver disease. Hepatology 55(3):769-80.

Basaranoglu M, Basaranoglu G, Senturk H. 2013. From fatty liver to fibrosis: a tale of "second hit". World J Gastroenterol 19(8):1158-65.

Baskol G, Baskol M, Kocer D. 2007. Oxidative stress and antioxidant defenses in serum of patients with non-alcoholic steatohepatitis. Clin Biochem 40(11):776-80.

Baumgardner JN et al. N-acetylcysteine attenuates progression of liver pathology in a rat model of non-alcoholic steatohepatitis. J Nutr 2008;138:1872-1879.

Begriche K, Igoudjil A, Pessayre D, Fromenty B. 2006. Mitochondrial dysfunction in NASH: causes, consequences and possible means to prevent it. Mitochondrion 6(1):1-28.

Bellentani S, Scaglioni F, Marino M, Bedogni G. 2010. Epidemiology of non-alcoholic fatty liver disease. Dig Dis 28(1):155-61.

Berres ML, Koenen RR, Rueland A, Zaldivar MM, Heinrichs D, Sahin H, et al. Antagonism of the chemokine CCL5 ameliorates experimental liver fibrosis in mice. J Clin Invest. 2010;120:4129-4140.

Bhala N, Jouness RI, Bugianesi E. 2013. Epidemiology and natural history of patients with NAFLD. Curr Pharm Des 19(29):5169-76.

Bieghs V, Rensen PC, Hofker MH, Shiri-Sverdlov R. NASH and atherosclerosis are two aspects of a shared disease: central role for macrophages. Atherosclerosis. 2012;220:287-93.

Brunt EM, Kleiner DE, Wilson LA, Belt P, Neuschwander-Tetri BA, Network NCR. 2011. Nonalcoholic fatty liver disease (NAFLD) activity score and the histopathologic diagnosis in NAFLD: distinct clinicopathologic meanings. Hepatology 53(3):810-20.

Brunt EM, Ramrakhiani S, Cordes BG, Neuschwander-Tetri BA, Janney CG, Bacon BR, Di Bisceglie AM. 2003. Concurrence of histologic features of steatohepatitis with other forms of chronic liver disease. Mod Pathol 16(1):49-56.

Brunt EM. Pathology of nonalcoholic fatty liver disease. Nat Rev Gastroenterol Hepatol 2010;7:195-203.

Bugianesi E, Moscatiello S, Ciaravella MF, Marchesini G. 2010. Insulin resistance in nonalcoholic fatty liver disease. Curr Pharm Des 16(17):1941-51.

Burt AD, Mutton A, Day CP. 1998. Diagnosis and interpretation of steatosis and steatohepatitis. Semin Diagn Pathol 15(4):246-58.

Cao J, Dai DL, Yao L, Yu HH, Ning B, Zhang Q, Chen J, Cheng WH, Shen W, Yang ZX. 2012. Saturated fatty acid induction of endoplasmic reticulum stress and apoptosis in human liver cells via the PERK/ATF4/CHOP signaling pathway. Mol Cell Biochem 364(1-2):115-29.

Capeau J. 2008. Insulin resistance and steatosis in humans. Diabetes Metab 34(6 Pt 2):649-57.

Carulli L, Canedi I, Rondinella S, Lombardini S, Ganazzi D, Fargion S, De Palma M, Lonardo A, Ricchi M, Bertolotti M, Carulli N, Loria P. 2009. Genetic polymorphisms in non-alcoholic fatty liver disease: interleukin-6-174G/C polymorphism is associated with non-alcoholic steatohepatitis. Dig Liver Dis 41(11):823-8.

Chalasani N, Deeg MA, Crabb DW. 2004. Systemic levels of lipid peroxidation and its metabolic and dietary correlates in patients with nonalcoholic steatohepatitis. Am J Gastroenterol 99(8):1497-502.

Charlton M, Krishnan A, Viker K, Sanderson S, Cazanave S, McConico A, Masuoko H, Gores G. 2011. Fast food diet mouse: novel small animal model of NASH with ballooning, progressive fibrosis, and high physiological fidelity to the human condition. Am J Physiol Gastrointest Liver Physiol 301(5):G825-34.

Chitturi S, Abeygunasekera S, Farrell GC, Holmes-Walker J, Hui JM, Fung C, Karim R, Lin R, Samarasinghe D, Liddle C, Weltman M, George J. 2002. NASH and insulin resistance: Insulin hypersecretion and specific association with the insulin resistance syndrome. Hepatology 35(2):373-9.

Choudhury J, Sanyal AJ. 2004. Insulin resistance and the pathogenesis of nonalcoholic fatty liver disease. Clin Liver Dis 8(3):575-94, ix.

Choudhury J, Sanyal AJ. 2005. Insulin resistance in NASH. Front Biosci 10:1520-33.

Connolly MK, Bedrosian AS, Mallen-St Clair J, et al. In liver fibrosis, dendritic cells govern hepatic inflammation in mice via TNF-alpha. J Clin Invest. 2009;119:3213-3225.

Cooray SN, Gobbetti T, Montero-Melendez T, McArthur S, Thompson D, Clark AJ, et al. Ligand-specific conformational change of the G-protein-coupled receptor ALX/FPR2 determines pro-resolving functional responses. Proc Natl Acad Sci U S A. 2013;110:18232-18237

Cotrim HP, De Freitas LA, Freitas C, Braga L, Sousa R, Carvalho F, Parana R, Santos-Jesus R, Andrade Z. 2004. Clinical and histopathological features of NASH in workers exposed to chemicals with or without associated metabolic conditions. Liver Int 24(2):131-5.

Crispe IN. Immune Tolerance in Liver Disease. Hepatol 2014; doi: 10.1002/hep.27254

Cusi K. 2009. Role of insulin resistance and lipotoxicity in non-alcoholic steatohepatitis. Clin Liver Dis 13(4):545-63.

Day CP, James OF. 1998. Steatohepatitis: a tale of two "hits"? Gastroenterology 114(4):842-5.

Day CP. 2006. From fat to inflammation. Gastroenterology 130(1):207-10.

DeFuria J, Belkina AC, Jagannathan-Bogdan M, Snyder-Cappione J, Carr JD, Nersesova YR, Markham D, et al. B cells promote inflammation in obesity and type 2 diabetes through regulation of T-cell function and an inflammatory cytokine profile. Proc Natl Acad Sci U S A. 2013;110:5133-5138.

Domininguez PM, Ardavin C. Differentiation and function of mouse monocyte-derived dendritic cells in steady state and inflammation. Immunol Rev. 2010;234:90-104.

Ducluzeau PH, Boursier J, Bertrais S, Dubois S, Gauthier A, Rohmer V, Gagnadoux F, Leftheriotis G, Cales P, Andriantsitohaina R, Roullier V, Aube C. 2013. MRI measurement of liver fat content predicts the metabolic syndrome. Diabetes Metab 39(4):314-21.

Duwaerts CC, Maher JJ. 2014. Mechanisms of Liver Injury in Non-Alcoholic Steatohepatitis. Curr Hepatol Rep 13(2):119-129.

Exley MA, Koziel MJ. (2004) To be or not to be NKT: natural killer T cells in the liver. Hepatology. 40, 1033-40.

Fang DL, Wan Y, Shen W, Cao J, Sun ZX, Yu HH, Zhang Q, Cheng WH, Chen J, Ning B. 2013. Endoplasmic reticulum stress leads to lipid accumulation through upregulation of SREBP-1c in normal hepatic and hepatoma cells. Mol Cell Biochem 381(1-2):127-37.

Ferreyra Solari NE, Inzaugarat ME, Baz P, De Matteo E, Lezama C, Galoppo M, Galoppo C, Chernavsky AC. (2012) The role of innate cells is coupled to a Th1-polarized immune response in paediatric nonalcoholic steatohepatitis. J Clin Immunol. 32, 611-21.

Ferreyra Solari NE, Inzaugarat ME, Baz P, De Matteo E, Lezama C, Galoppo M, Galoppo C. The role of innate cells is coupled to a Th1-polarized immune response in pediatric nonalcoholic steatohepatitis. J Clin Immunol. 2012;32:611-621.

Friedman SL. Mechanism of hepatic fibrogenesis. Gastroenterol. 2008;134:1655-1669.

Galastri S, Zamara E, Milani S, Novo E, Provenzano A, Delogu W, Vizzutti F, Sutti S, Locatelli I, Navari N, Vivoli E, Caligiuri A, Pinzani M, Albano E, Parola M, Marra F. 2012. Lack of CC chemokine ligand 2 differentially affects inflammation and fibrosis according to the genetic background in a murine model of steatohepatitis. Clin Sci (Lond) 123(7):459-71.

Gambino R, Musso G, Cassader M. 2011. Redox balance in the pathogenesis of nonalcoholic fatty liver disease: mechanisms and therapeutic opportunities. Antioxid Redox Signal 15(5):1325-65.

Gao B, Jeong WI, Tian Z. (2008) Liver: an organ with predominant innate immunity. Hepatology. 47, 729-36.

Gao B, Radaeva S. (2013) Natural killer and natural killer T cells in liver fibrosis. Biochim Biophys Acta. 1832, 1061-9.

Geissmann F, Cameron TO, Sidobre S, Manlongat N, Kronenberg M, Briskin MJ, Dustin ML, Littman DR. 2005. Intravascular immune surveillance by CXCR6+ NKT cells patrolling liver sinusoids. PLoS Biol 3(4):e113.

George, J. Mechanisms of Disease: the evolving role of regulatory T cells in atherosclerosis. Nat Clin Pract Cardiovascular Med 2008;5:531-540.

Gramlich T, Kleiner DE, McCullough AJ, Matteoni CA, Boparai N, Younossi ZM. 2004. Pathologic features associated with fibrosis in nonalcoholic fatty liver disease. Hum Pathol 35(2):196-9.

Hansson GK, Libby P. The immune response in atherosclerosis: a double-edged sword. Nature Rev Immunol 2006;6:508-519.

Harbrecht BG, Nweze I, Smith JW, Zhang B. 2012. Insulin inhibits hepatocyte iNOS expression induced by cytokines by an Akt-dependent mechanism. Am J Physiol Gastrointest Liver Physiol 302(1):G116-22.

Hashimoto E, Taniai M, Tokushige K. 2013. Characteristics and diagnosis of NAFLD/NASH. J Gastroenterol Hepatol 28 Suppl 4:64-70.

Haukeland JW, Damas JK, Konopski Z, Loberg EM, Haaland T, Goverud I, Torjesen PA, Birkeland K, Bjoro K, Aukrust P. 2006. Systemic inflammation in nonalcoholic fatty liver disease is characterized by elevated levels of CCL2. J Hepatol 44(6):1167-74.

Henkel A, Green RM. 2013. The unfolded protein response in fatty liver disease. Semin Liver Dis 33(4):321-9.

Henning JR, Graffeo CS, Rehman A, Fallon NC, Zambirinis CP, Ochi A, et al. Dendritic cells limit fibroinflammatory injury in nonalcoholic steatohepatitis in mice. Hepatol. 2013;58:589-602.

Herkel, J. Jagemann B, Wiegard C, Lazaro JF, Lueth S, Kanzler S, Blessing M, Schmitt E, Lohse AW. MCH class II-expressing hepatocytes function as antigen presenting cells and activate specific CD4 T lymphocytes. Hepatol. 2003;37:1079-1085.

Hui JM, Hodge A, Farrell GC, Kench JG, Kriketos A, George J. 2004. Beyond insulin resistance in NASH: TNF-alpha or adiponectin? Hepatology 40(1):46-54.

Ikura Y, Ohsawa M, Suekane T, Fukushima H, Itabe H, Jomura H, Nishiguchi S, Inoue T, Naruko T, Ehara S, Kawada N, Arakawa T, Ueda M. 2006. Localization of oxidized

phosphatidylcholine in nonalcoholic fatty liver disease: impact on disease progression. Hepatology 43(3):506-14.

Inzaugarat ME, Ferreyra Solari NE, Billordo LA, Abecasis R, Gadano AC, Chernavsky AC. (2011) Altered phenotype and functionality of circulating immune cells characterize adult patients with nonalcoholic steatohepatitis. J Clin Immunol. 31, 1120-30.

Inzaugarat ME, Ferreyra Solari NE, Billordo LA, Abecasis R, Gadano AC, Cherñavsky AC. Altered phenotype and functionality of circulating immune cells characterize adult patients with nonalcoholic steatohepatitis. J Clin Immunol. 2011;31:1120-1130.

Ioannou GN, Haigh WG, Thorning D, Savard C. Hepatic cholesterol crystals and crown-like structures distinguish NASH from simple steatosis. J Lipid Res. 2013;54:1326-34.

Itoh M, Kato H, Suganami T, Konuma K, Marumoto Y, Terai S, Sakugawa H, Kanai S, Hamaguchi M, Fukaishi T, Aoe S, Akiyoshi K, Komohara Y, Takeya M, Sakaida I, Ogawa Y. Hepatic crown-like structure: a unique histological feature in non-alcoholic steatohepatitis in mice and humans. PLoS One. 2013;8:e82163. doi: 10.1371/journal.pone.0082163.

Kallwitz ER, Guzman G, TenCate V, Vitello J, Layden-Almer J, Berkes J, Patel R, Layden TJ, Cotler SJ. 2009. The histologic spectrum of liver disease in African-American, non-Hispanic white, and Hispanic obesity surgery patients. Am J Gastroenterol 104(1):64-9.

Kang K, Reilly SM, Karabacak V, Gangl MR, Fitzgerald K, Hatano B, Lee CH. 2008. Adipocyte-derived Th2 cytokines and myeloid PPARdelta regulate macrophage polarization and insulin sensitivity. Cell Metab 7(6):485-95.

Kapoor A, Sanyal AJ. 2009. Endoplasmic reticulum stress and the unfolded protein response. Clin Liver Dis 13(4):581-90.

Kremer M, Thomas E, Milton RJ, Perry AW, van Rooijen N, Wheeler MD, Zacks S, Fried M , Rippe RA, Hines IN. (2010) Kupffer cell and interleukin-12-dependent loss of natural killer T cells in hepatosteatosis. Hepatology 51, 130-41.

Kremer M, Thomas E, Milton RJ, Perry AW, van Rooijen N, Wheeler MD, Zacks S, et al. Kupffer cell and interleukin-12-dependent loss of natural killer T cells in hepatosteatosis. Hepatol. 2010;51,130-141.

Larter CZ Yeh MM. Animal model of NASH: getting both pathology and metabolic contest right J Gastroenterol Hepatol 2008;23:1635-1648.

Lee JS, Zheng Z, Mendez R, Ha SW, Xie Y, Zhang K. 2012. Pharmacologic ER stress induces non-alcoholic steatohepatitis in an animal model. Toxicol Lett 211(1):29-38.

Leroux A, Ferrere G, Godie V, Cailleux F, Renoud ML, Gaudin F, et al. Toxic lipids stored by Kupffer cells correlates with their pro-inflammatory phenotype at an early stage of steatohepatitis. J Hepatol. 2012;57:141-149.

Li CP, Li JH, He SY, Li P, Zhong XL. 2014. Roles of Fas/Fasl, Bcl-2/Bax, and Caspase-8 in rat nonalcoholic fatty liver disease pathogenesis. Genet Mol Res 13(2):3991-9.

Li Z, Soloski MJ, Diehl AM. (2005) Dietary factors alter hepatic innate immune system in mice with nonalcoholic fatty liver disease. Hepatology. 42, 880-5.

Lieber CS. 2004. CYP2E1: from ASH to NASH. Hepatol Res 28(1):1-11.

Locatelli I, Sutti S, Jindal A, Vacchiano M, Bozzola C, Reutelingsperger C, et al. Endogenous annexin A1 is a novel protective determinant in nonalcoholic steatohepatitis in mice. Hepatol. 2014;60:531-544.

Locatelli I, Sutti S, Vacchiano M, Bozzola C, Albano E. NF-kB1 deficiency stimulates the progression of nonalcoholic steatohepatitis (NASH) in mice by promoting NKT-mediated responses. Clin Sci (Lond). 2013;124:279-287.

Lomonaco R, Ortiz-Lopez C, Orsak B, Finch J, Webb A, Bril F, Louden C, Tio F, Cusi K. 2011. Role of ethnicity in overweight and obese patients with nonalcoholic steatohepatitis. Hepatology 54(3):837-45.

Lonardo A, Loria P. 2002. Apolipoprotein synthesis in nonalcoholic steatohepatitis. Hepatology 36(2):514-5; author reply 515.

Lou XY, Takara T, Kawai K, Fujino M, Sugiyama T, Tsuneyama K, Tsukada K, Nakac S, Zhong L, Li XK. IFN-γ deficiency attenuates hapatic inflammation and fibrosis in a steatohepatitis model induced by a methionine-and choline-deficient high fat diet. Am J Physiol Gastroinstest Liver Physiol 2013;305:G891-G899.

Ma X et al A high fat diet and regulatory T cells influence the susceptibility to endotoxin-induced liver injury. Hepatol 2007;46:1519-1529.

Maina V, Sutti S, Locatelli I, Vidali M, Mombello C, Bozzola C, et al. Bias in macrophage activation pattern influences non-alcoholic steatohepatitis (NASH) in mice. Clin Sci (Lond) 2012; 122:545-553.

Malhi H, Bronk SF, Werneburg NW, Gores GJ. 2006. Free fatty acids induce JNK-dependent hepatocyte lipoapoptosis. J Biol Chem 281(17):12093-101.

Malhi H, Kaufman RJ. 2011. Endoplasmic reticulum stress in liver disease. J Hepatol 54(4):795-809.

Marra F, Aleffi S, Bertolani C, Petrai I, Vizzutti F. 2005. Adipokines and liver fibrosis. Eur Rev Med Pharmacol Sci 9(5):279-84.

Meng F, Wang K, Aoyama T, Grivennikov SI, Paik Y, Scholten D, COng M, Iwaisako K, Liu X, Zhang M, Osterreicher CH, Stickel F, Ley K, Brenner DA, Kisseleva T. (2012) Interleukin-17 signalling in inflammatory, Kupffer cells, and hepatic stellate cells exacerbats liver fibrosis in mice. Gastroenterology. 143, 765-76.

Merriman RB, Aouizerat BE, Bass NM. 2006. Genetic influences in nonalcoholic fatty liver disease. J Clin Gastroenterol 40 Suppl 1:S30-3.

Mirza MS. 2011. Obesity, Visceral Fat, and NAFLD: Querying the Role of Adipokines in the Progression of Nonalcoholic Fatty Liver Disease. ISRN Gastroenterol 2011:592404.

Miura K, Yang L, van Rooijen N, Ohnishi H, Seki E. 2012. Hepatic recruitment of macrophages promotes nonalcoholic steatohepatitis through CCR2. Am J Physiol Gastrointest Liver Physiol 302(11):G1310-21.

Murray PJ, Wynn TA. 2011. Protective and pathogenic functions of macrophage subsets. Nat Rev Immunol 11(11):723-37.

Musso G, Gambino R, Durazzo M, Biroli G, Carello M, Faga E, Pacini G, De Michieli F, Rabbione L, Premoli A, Cassader M, Pagano G. 2005. Adipokines in NASH: postprandial lipid metabolism as a link between adiponectin and liver disease. Hepatology 42(5):1175-83.

Neuschwander-Tetri BA, Cadwell SH. Nonalcoholic steatohepatitis: summary of an AASLD single topic conference. Hepatol 2003;37:1202-1219.

Nobili V, Parola M, Alisi A, Marra F, Piemonte F, Mombello C, Sutti S, Povero D, Maina V, Novo E, Albano E. Oxidative stress parameters in paediatric non-alcoholic fatty liver disease. Int J Molec Med 2010;26:471-476.

Novo E, Parola M. Redox mechanisms in hepatic chronic wound healing and fibrogenesis. Fibrogen. Tissue Rep. 2008; 1:5 (doi:10.1186/1755-1536-1-5).

Orlik B, Handzlik G, Olszanecka-Glinianowicz M. 2010. [The role of adipokines and insulin resistance in the pathogenesis of nonalcoholic fatty liver disease]. Postepy Hig Med Dosw (Online) 64:212-9.

Osteopontin induces ductular reaction contributing to liver fibrosis. Gut. 2014;63:1805-18.

Ou J, Carlos TM, Watkins SC, Saavedra JE, Keefer LK, Kim YM, Harbrecht BG, Billiar TR. 1997. Differential effects of nonselective nitric oxide synthase (NOS) and selective

inducible NOS inhibition on hepatic necrosis, apoptosis, ICAM-1 expression, and neutrophil accumulation during endotoxemia. Nitric Oxide 1(5):404-16.

Pacana T, Sanyal AJ. 2012. Vitamin E and nonalcoholic fatty liver disease. Curr Opin Clin Nutr Metab Care 15(6):641-8.

Pagliassotti MJ. 2012. Endoplasmic reticulum stress in nonalcoholic fatty liver disease. Annu Rev Nutr 32:17-33.

Panasiuk A, Dzieciol J, Panasiuk B, Prokopowicz D. 2006. Expression of p53, Bax and Bcl-2 proteins in hepatocytes in non-alcoholic fatty liver disease. World J Gastroenterol 12(38):6198-202.

Perretti M, D'Acquisto F. Annexin A1 and glucocorticoids as effectors of the resolution of inflammation. Nat Rev Immunol. 2009;9:62-70.

Pinto MA, Marchevsky RS, Pelajo-Machado M, Santiago MA, Pissurno JW, Franca MS, Baptista ML, Gouvea AS, Santana AA, Bertho AL, Schatzmayr HG, Gaspar AM, Kubelka CF. 2000. Inducible nitric oxide synthase (iNOS) expression in liver and splenic T lymphocyte rise are associated with liver histological damage during experimental hepatitis A virus (HAV) infection in Callithrix jacchus. Exp Toxicol Pathol 52(1):3-10.

Poggi M, Engel D, Christ A, Beckers L, Wijnands E, Boon L, Driessen A, et al. CD40L deficiency ameliorates adipose tissue inflammation and metabolic manifestations of obesity in mice. Arterioscler Thromb Vasc Biol. 2011;31:2251-2260.

Polyzos SA, Kountouras J, Papatheodorou A, Katsiki E, Patsiaoura K, Zafeiriadou E, Papadopoulou E, Zavos C, Terpos E. 2013. Adipocytokines and cytokeratin-18 in patients with nonalcoholic fatty liver disease: Introduction of CHA index. Ann Hepatol 12(5):749-57.

Postic C, Girard J. 2008. Contribution of de novo fatty acid synthesis to hepatic steatosis and insulin resistance: lessons from genetically engineered mice. J Clin Invest 118(3):829-38.

Racanelli V, Rehermann B. The liver as an immunological organ. Hepatol. 2006; 43:S54- S62.

Rensen SS, Bieghs V, Xanthoulea S, Arfianti E, Bakker JA, Shiri-Sverdlov R, Hofker MH, Greve JW, Buurman WA. 2012. Neutrophil-derived myeloperoxidase aggravates non-alcoholic steatohepatitis in low-density lipoprotein receptor-deficient mice. PLoS One 7(12):e52411.

Rensen SS, Slaats Y, Driessen A, Peutz-Kootstra CJ, Nijhuis J, Steffensen R et al. Activation of complement system in human non-alcoholic fatty liver disease. Hepatol 2009;50:1809-1817.

Rensen SS, Slaats Y, Nijhuis J, Jans A, Bieghs V, Driessen A, Malle E, Greve JW, Buurman WA. Increased hepatic myeloperoxidase activity in obese subjects with nonalcoholic steatohepatitis. Am J Pathol. 2009;175:1473-82.

Rinella ME, Loomba R, Caldwell SH, Kowdley K, Charlton M, Tetri B, Harrison SA. 2014. Controversies in the Diagnosis and Management of NAFLD and NASH. Gastroenterol Hepatol (N Y) 10(4):219-27.

Rivollier A, He J, Kole A, Valatas V, Kelsall BL. Inflammation switches the differentiation program of Ly6Chigh monocytes from anti-inflammatory macrophages to inflammatory dendritic cells in the colon. J Exp Med. 2012;209:139-155.

Rocha R, Cotrim HP, Carvalho FM, Siqueira AC, Braga H, Freitas LA. 2005. Body mass index and waist circumference in non-alcoholic fatty liver disease. J Hum Nutr Diet 18(5):365-70.

Rolla R, Vay D, Mottaran E, Parodi M, Traverso N, Aricó S, Sartori M, Bellomo G, Klassen LW, Thiele GM, Tuma DJ, Albano E. Detection of circulating antibodies against malondialdehyde-acetaldehyde adducts in patients with alcohol-induced liver disease. Hepatology. 2000;31:878-84.

Sahai A, Malladi P, Melin-Aldana H, Green RM, Whitington PF. Upregulation of osteopontin expression is involved in the development of nonalcoholic steatohepatitis in a dietary murine model. Am. J. Physiol. Gastrointest. Liver Physiol. 2004;287:G264-G273.

Seino K, Taniguchi M. (2005) Functionally distinct NKT cell subsets and subtypes. J Exp Med. 202, 1623-6.

Seki S, Kitada T, Yamada T, Sakaguchi H, Nakatani K, Wakasa K. 2002. In situ detection of lipid peroxidation and oxidative DNA damage in non-alcoholic fatty liver diseases. J Hepatol 37(1):56-62.

Sell H, Habich C, Eckel J. Adaptive immunity in obesity and insulin resistance. Nat Rev Endocrinol 2012;8:709-716.

Sheth SG, Gordon FD, Chopra S. 1997. Nonalcoholic steatohepatitis. Ann Intern Med 126(2):137-45.

Sica A, Mantovani A. 2012. Macrophage plasticity and polarization: in vivo veritas. J Clin Invest 122(3):787-95.

Sreekumar R, Rosado B, Rasmussen D, Charlton M. 2003. Hepatic gene expression in histologically progressive nonalcoholic steatohepatitis. Hepatology 38(1):244-51.

Swain MG. 2010. Natural killer T cells within the liver: conductors of the hepatic immune orchestra. Dig Dis 28(1):7-13.

Syn WK, Agdobola KM, Swiderska M, Michelotti GA, Liaskou E, Pang H, Xie G, Philips G, Chan IS, Karaca GF, Pereira Tde A, Chen Y, Mi Z, Kuo PC, Choi SS, Guy CD, Abdelmalek MF, Diehl AM. (2012) NKT-associated hedgehog and osteopontin drive fibrogenesis in non-alcoholic fatty liver disease. Gut. 61, 1323-9.

Syn WK, Choi SS, Liaskou E, Karaca GF, Agboola KM, Oo YH, Mi Z, et al. Osteopontin is induced by hedgehog pathway activation and promotes fibrosis progression in nonalcoholic steatohepatitis. Hepatol. 2011;53:106-115.

Syn WK, Oo YH, Pereira TA, Karaca GF, Jung Y, Omenetti A, Witek RP, Choi SS, Guy CD, Fearing CM, Teaberry V, Pereira FE, Adams DH, Diehl AM. (2010) Accumulation of natural killer T cells in progressive nonalcoholic fatty liver disease. Hepatology. 51, 1998-2007.

Syn WK, Oo YH, Pereira TA, Karaca GF, Jung Y, Omenetti A, Witek RP, et al. Accumulation of natural killer T cells in progressive non-alcoholic fatty liver disease. Hepatol. 2010;51:1998-2007.

Tajiri K, Shimizu Y, Tsuneyama K, Sugiyama T. (2009) Role of liver-infiltrating CD3+CD56+ natural killer T cells in the pathogenesis of nonalcoholic fatty liver disease. Eur J Gastroenterol Hepatol. 21, 673-80.

Tajiri K, Shimizu Y, Tsuneyama K, Sugiyama T. Role of liver-infiltrating CD3+CD56+ natural killer T cells in the pathogenesis of nonalcoholic fatty liver disease. Eur J Gastroenterol. Hepatol. 2009;21:673-680.

Takei Y, Sato N. 2006. [Adipokine interrelationship with the liver]. Nihon Rinsho 64(6):1083-7.

Tang Y, Bian Z, Zhao L, Liu Y, Liang S, Wang Q, Han X, Peng Y, Chen X, Shen L, Qiu D, Li Z, Ma X. (2011) Inteleukin-17 exacerbates hepatic steatosis and inflammation in non-alcoholic fatty liver disease. Clin Exp Immunol. 166, 281-90.

Thiele GM, Klassen LW, Tuma DJ. Formation and immunological properties of aldehyde-derived protein adducts following alcohol consumption. Methods Mol Biol. 2008;447:235-57.

Tilg H & Moschen AR Adipokines: mediators linking adipose tissue, inflammation and immunity. Nat Rev Immunol 2006;6:4772-83.

Tilg H, Mochen AR. Evolution of inflammation in non-alcoholic fatty liver disease: the multiple parallel hits hypothesis. Hepatol 2010;52:1836-1846.

Tosello-Trampont AC, Landes SG, Nguyen V, Novobrantseva TI, Hahn YS. 2012. Kuppfer cells trigger nonalcoholic steatohepatitis development in diet-induced mouse model through tumor necrosis factor-alpha production. J Biol Chem 287(48):40161-72.

Tosello-Trampont AC, Landes SG, Nguyen V, Novobrantseva TI, Hahn YS. Kuppfer cells trigger nonalcoholic steatohepatitis development in diet-induced mouse model through tumor necrosis factor-α production. J Biol Chem. 2012;287:40161-40172.

Uede T. (2011) Osteopontin, intrinsic tissue regulator of intractable inflammatory diseases. Pathol Int. 61, 265-80.

Vuppalanchi R, Chalasani N. 2009. Nonalcoholic fatty liver disease and nonalcoholic steatohepatitis: Selected practical issues in their evaluation and management. Hepatology 49(1):306-17.

Wang J, Brymora J, George J. Role of adipokines in liver injury and fibrosis. Exp. Rev. Gastroenterol. Hepatol. 2008;2:47-57.

Wang X, Lopategi A, Ge X, Lu Y, Kitamura N, Urtasun R, Leung TM, Fiel MI, Nieto N.

Wehr A, Baeck C, Heymann F, Niemietz PM, Hammerich L, Martin C, et al. Chemokine receptor CXCR6-dependent hepatic NK T Cell accumulation promotes inflammation and liver fibrosis. J Immunol. 2013;190:5226-5236.

Wehr A, Baeck C, Heymann F, Niemietz PM, Hammerich L, Martin C, et al. Chemokine receptor CXCR6-dependent hepatic NK T Cell accumulation promotes inflammation and liver fibrosis. J Immunol. 2013;190:5226-5236.

Williamson RM, Price JF, Glancy S, Perry E, Nee LD, Hayes PC, Frier BM, Van Look LA, Johnston GI, Reynolds RM, Strachan MW, Edinburgh Type 2 Diabetes Study I. 2011. Prevalence of and risk factors for hepatic steatosis and nonalcoholic Fatty liver disease in people with type 2 diabetes: the Edinburgh Type 2 Diabetes Study. Diabetes Care 34(5):1139-44.

Winau F, Quack C, Darmoise A, Kaufmann SH. Starring stellate cells in liver immunology. Cur Opin Immunol 2008;20:68-74.

Wong VW. 2013. Nonalcoholic fatty liver disease in Asia: a story of growth. J Gastroenterol Hepatol 28(1):18-23.

Xu D, Thiele GM, Beckenhauer JL, Klassen LW, Sorrell MF, Tuma DJ. Detection of circulating antibodies to malondialdehyde-acetaldehyde adducts in ethanol-fed rats. Gastroenterology. 1998;115:686-92.

Yang L, Jhaveri R, Huang J, Qi Y, Diehl AM. (2007) Endoplasmic reticulum stress, hepatocyte CD1d and NKT cell abnormalities in murine livers. Lab Invest. 87, 927-37.

Yki-Jarvinen H. 2014. Non-alcoholic fatty liver disease as a cause and a consequence of metabolic syndrome. Lancet Diabetes Endocrinol.

Yoshiike N, Lwin H. 2005. Epidemiological aspects of obesity and NASH/NAFLD in Japan. Hepatol Res 33(2):77-82.

Younossi ZM, Stepanova M, Negro F, Hallaji S, Younossi Y, Lam B, Srishord M. 2012. Nonalcoholic fatty liver disease in lean individuals in the United States. Medicine (Baltimore) 91(6):319-27.

Yu J, Shen J, Sun TT, Zhang X, Wong N. 2013. Obesity, insulin resistance, NASH and hepatocellular carcinoma. Semin Cancer Biol 23(6 Pt B):483-91.

Zelber-Sagi S, Ratziu V, Oren R. 2011. Nutrition and physical activity in NAFLD: an overview of the epidemiological evidence. World J Gastroenterol 17(29):3377-89.

Zhang C, Chen X, Zhu RM, Zhang Y, Yu T, Wang H, Zhao H, Zhao M, Ji YL, Chen YH, Meng XH, Wei W, Xu DX. 2012a. Endoplasmic reticulum stress is involved in hepatic SREBP-1c activation and lipid accumulation in fructose-fed mice. Toxicol Lett 212(3):229-40.

Zhang Y, Xue R, Zhang Z, Yang X, Shi H. 2012b. Palmitic and linoleic acids induce ER stress and apoptosis in hepatoma cells. Lipids Health Dis 11:1.

Zheng Z, Zhang C, Zhang K. 2011. Measurement of ER stress response and inflammation in the mouse model of nonalcoholic fatty liver disease. Methods Enzymol 489:329-48.